MICROTUBULE DYNAMICS DURING EARLY NEURAL DIFFERENTIATION OF P19 EMBRYONAL CARCINOMA CELLS

by

Sarang V. Kulkarni

A thesis submitted
to the School of Graduate Studies and Research,
University of Ottawa,
in partial fulfillment of the requirements
for the degree of
Master of Science
in the
Department of Biology

ISBN 0-315-85801-X

Canada

UNIVERSITÉ D'OTTAWA
UNIVERSITY OF OTTAWA

I hereby declare that I am the sole author of this thesis.

I authorize the University of Ottawa to lend this thesis to other institutions or individuals for the purpose of scholarly research.

Sarang V. Kulkarni

I further authorize the University of Ottawa to reproduce this thesis by photocopying or by other means, in total or in part, at the request of other institutions or individuals for the purpose of scholarly research.

Sarang V. Kulkarni

I dedicate this thesis to my family and to

my dearest Savitri.

ACKNOWLEDGEMENTS

I would like to extend my gratitude to many friends that I have had the pleasure of making acquaintances during the course of this study. I extend my appreciation to my advisory committee members, Dr. Michael W. McBurney, Dr. Peter J. Anderson and Dr. Natalie Chaly for guidance throughout the research. I wish to thank Dr. Micheline Paulin-Levasseur for many helpful discussions throughout the course of this study and for providing the french translation of the abstract in this thesis.

I also thank Dr. Gianni Piperno for supplying the antibody to acetylated tubulin, Dr. Lester Binder for supplying the antibodies to MAP 1A, MAP 2 and tau, and Dr. Anthony Frankfurter for his kind gift of the anti-ß-III tubulin antibody. I am deeply indebted to Dr. David Coll for setting up the video microscopy imaging system and for writing customized image processing programs used in this study. I thank Mrs. Judy Little for maintaining general laboratory supplies and Mrs. Beatrice Valentine for excellent technical guidance in microscopy.

The preparation of this manuscript has been possible by the financial support of my parents for providing the necessary funds to purchase a computer. The continual love, support and understanding of my family is affectionately acknowledged.

Lastly, I wish to extend my thanks to my supervisor Dr. David Brown for providing me guidance and the opportunity to do research.

TABLE OF CONTENTS

LIST OF TABLES AND FIGURES

TABLES

FIGURES

ABBREVIATIONS

ACET	:	acetylated tubulin
α-MEM	:	alpha minimal essential media
BSA	:	bovine serum albumin
B-Tb	:	biotin-tubulin
DMSO	:	dimethylsulfoxide
DNA	:	deoxyribonucleic acid
DTAF	:	dichlorotriazinyl amino fluorescein
EC	:	embryonal carcinoma
EDTA	:	ethylene diamine tetra-acetic acid
EGTA	:	ethylene glycol bis (ß-aminoethylether) N,N,N',N'-tetra-acetic acid
FBS	:	fetal bovine serum
FRAP	:	fluorescence recovery after photobleaching
GDP	:	guanosine diphosphate
GLU	:	detyrosinated tubulin
GTP	:	guanosine triphosphate
HEPES	:	(n-2-hydroxyethylpiperazine-N'-2-ethane sulfonic acid)
IF(s)	:	intermediate filament(s)
IgG	:	immunoglobulin class G
MAB	:	microtubule assembly buffer
MAP(s)	:	microtubule-associated protein(s)
$MgCl_2$	:	magnesium chloride
MIJ	:	microinjection
MT(s)	:	microtubule(s)
NaCl	:	sodium chloride
Na_2HPO_4	:	di-sodium hydrogen orthophosphate (dibasic)
$NaPO_4$	:	sodium phosphate
PBS	:	phosphate buffered saline
PC-Tubulin	:	phosphocellulose-purified tubulin
PC 12	:	pheochromocytoma 12
PEM	:	PIPES, EGTA and $MgCl_2$ buffer
PHEM	:	(same as PEM buffer, but with HEPES)
PIPES	:	piperazine N,N'-bis(2-ethane sulfonic acid)
RA	:	retinoic acid
SDS	:	sodium dodecyl sulfate
SDS-PAGE	:	sodium dodecyl sulfate-polyacrylamide gel electrophoresis
SIT	:	silicon intensified target
TYR	:	tyrosinated tubulin

ABSTRACT

Altered microtubule (MT) stability prior to neurite extension was examined in P19 embryonal carcinoma cells induced to differentiate along the neural pathway by retinoic acid. In undifferentiated P19 cells few acetylated MTs were detected by immunofluorescence staining and these were resistant to disassembly by colchicine at 1 μg/mL for 45 minutes. Twenty-four hours after neural induction there was an increase in the number of acetylated MTs and in the number of MTs that were resistant to colchicine treatment. This suggested that the MT array in undifferentiated cells is initially dynamic and becomes less dynamic during early neural differentiation prior to morphogenesis. Quantitative immunoblotting showed no change in the levels of total tubulin, but a two-fold increase in the relative level of acetylated tubulin was detected. MT turnover in P19 cells was then examined directly by microinjecting biotin-conjugated bovine brain tubulin. Computer-aided silicon intensified target camera (SIT) imaging of biotin-tubulin incorporation into the MT array showed that by 30 minutes, 92.4 $\pm$ 3.02% of total MTs turned over in undifferentiated cells. In contrast, in the retinoic acid-induced cells 52.8 $\pm$ 19.37% of the MT array turned over in 30 minutes. In conclusion, there are changes in colchicine stability and in tubulin acetylation that are correlated with changes in MT dynamics occurring prior to neurite outgrowth.

RÉSUMÉ

Nous avons étudié la stabilité des microtubules (MTs) pendant la phase initiale de différentiation, antérieure à las formation des neurites, dans les cellules de carcinome embryonnaire P19 induites par l'acide rétinoïque. Par immunofluorescence, nous avons pu démontrer: 1) qu'un petit nombre de MTs sont acétylés dans les cellules P19 non différenciées et que ceux-xi résistent à l'action dépolymérisante de la colchicine (1μg/ml pendant 45 minutes); et 2) que le nombre de MTs acétylés de meme que le nombre de MTs résistant à la colchicine augmentent dans ces cellules après 24 heures de traitement avec l'acide rétinoïque. Ces observations suggéraient que le système microtubulaire des cellules non différenciées est au départ dynamique et que, tot durant la différentiation et avant meme l'apparition de neurites, ce systeme devient moins dynamique. L'analyse quantitative par immunoblotting n'a révélé aucun changement dans le contenu total de tubuline, mais a montré que le contenu relatif en tubuline acétylée est augmenté de 200%. Nous avons ensuite procedé à l'étude de la dynamique des MTs dans les cellules P19 en microinjectant de la tubuline isolée a partir de cerveaux de boeuf et préalablement conjuguée à la biotine. Par microscopie assistée d'un système vidéo, nous avons observé que, 30 minutes après la microinjection, 92.4 $\pm$ 3.02% des MTs avaient incorporé la tubuline marquée sur toute leur longueur dans les cellules non différenciées comparativement a seulement 52.8 $\pm$ 19.37% dans les cellules induites par l'acide rétinoïque. Ces résultats nous amènent à conclure qu'il y a corrélation entre les changements dans le niveau de la résistance à la colchicine et de l'acétylation de la tubuline et les changements dans la dynamique des MTs durant la phase initiale d'induction qui précède la formation de neurites.

INTRODUCTION

Microtubules (MTs), a component of the cytoskeleton, play an active role in establishing cell polarity, in cell division and in cell differentiation. Early biochemical studies have shown that these polymers are composed of α- and ß-tubulin subunit proteins that associate to form a heterodimer. These dimers then polymerize to form 13 protofilaments arranged side-by-side that close to yield the 24 nm diameter hollow cylinder of the MT (Dustin, 1986).

Weisenberg (1972) was the first investigator who reproduced in vitro conditions that promoted MT assembly from brain extracts. Since then, MT assembly buffer components have been optimized and it has been found that MT assembly required the presence of GTP and the absence of calcium. Biochemical studies have shown that the tubulin heterodimer has two GTP binding sites: one is non-exchangeable on the α subunit and the second is exchangeable on the ß subunit (Avila, 1989).

Despite their structural similarity, MTs show a great deal of heterogeneity in composition. The α- and ß-tubulins are encoded by a multigene family. Lewis et al., (1985) have found six α-tubulin genes in mouse that encode five distinct α-tubulin isotypic polypeptides. Cleveland's group have identified seven ß-tubulin genes in chicken that encode seven distinct ß-tubulin polypeptides (Sullivan et al., 1985; Monteiro and Cleveland, 1988).

Another process that introduces heterogeneity in MTs is post-translational modification. Four post-translational modifications of tubulin have been reported; a) cyclic tyrosination/detyrosination of α-tubulin (Barra et al., 1973; Thompson, 1982), b)

acetylation of α-tubulin (L'Hernault and Rosenbaum, 1985a), c) phosphorylation of ß-tubulin (Gard and Kirschner, 1985) and more recently, d) polyglutamylation of α-tubulin (Eddé et al., 1990) and of ß-tubulin (Lee et al., 1990a). The biological implications of these modifications of tubulin are still not fully understood. One possible function is that post-translational modifications of tubulin may contribute to generate the stability of MTs. Stable MTs are abundant in a variety of cell systems, including specialized cells such as neurons (Lim et al., 1990a).

Other factors such as tubulin isotype sorting (Joshi and Cleveland, 1989), microtubule-associated proteins (MAPs) (Matus, 1988, 1990), and possibly crosslinking to an intermediate filament (IF) network (Klymkowsky et al., 1989; Shaw and Hou, 1990) have been suggested to be directly or indirectly involved in conferring stability to MTs. This introduction, however, will focus on the role of post-translational modifications of tubulin and MT dynamics that relate to MT stability.

I. POST-TRANSLATIONAL MODIFICATIONS

A) Tyrosination/Detyrosination

Most α-tubulins are initially synthesized with a C-terminal tyrosine (Villasante et al., 1986). Of the 4 α-tubulin genes that are expressed in mouse brain, only the **Mα4** does not encode a tyrosine at its C-terminus (Gu et al., 1988). However, the **Mα4** tubulin gene product has been shown to be retyrosinated post-translationally (Cambray-Deakin and Burgoyne, 1990). The removal of the terminal tyrosine in most α-tubulins, exposing a penultimate glutamic acid, is mediated by a specific enzyme called the tubulin carboxypeptidase (Kumar and Flavin, 1981). This detyrosinated α-tubulin then serves as a substrate for the readdition of tyrosine by the enzyme, tubulin tyrosine ligase (Murofushi, 1980). Thus depending on the amino acid present at the C-terminus, the α-tubulins and the MTs in which they are found are referred to as tyrosinated or detyrosinated. I will now refer to these as TYR or GLU, depending on their C-terminal amino acid residues.

In vitro evidence suggests that the preferential substrates for the enzymes tubulin carboxypeptidase and tubulin tyrosine ligase are polymeric tubulin and monomeric tubulin, respectively (Arce et al., 1978; Arce and Barra, 1985). This is also supported by in vivo evidence from studies of established cell lines (Gundersen et al., 1984, 1987; Gundersen and Bulinski, 1986) and of chick erythrocytes (Beltramo et al., 1989). Antibodies that were generated to TYR tubulin (Wehland et al, 1983) and GI U tubulin (Gundersen et al, 1984) were utilized to identify and localize the distribution of these post-translationally modified forms of MTs by immunofluorescence microscopy in many

cell systems. However, some of these post-translationally modified forms of MTs are not found in all cell types. For example, no GLU MTs were detected in HeLa cells (Bulinski et al.,1988).

B) Acetylation

The acetylation of tubulin occurs on the ϵ-amino group of lysine 40 on the α-subunit. This post-translational modification was identified in studies of flagellar assembly and regeneration in Chlamydomonas (L'Hernault and Rosenbaum, 1983, 1985a,b). The acetylation and deacetylation are mediated by tubulin acetyltransferase and tubulin deacetylase, respectively (Maruta et al., 1986). In vitro experiments on the kinetics of tubulin acetylation/deacetylation have shown that the tubulin acetyltransferase is associated with MTs and that this enzyme acts preferentially on polymerized tubulin, while tubulin deacetylase acts on monomeric tubulin (Maruta et al., 1986). In Chlamydomonas, tubulin deacetylase exists in soluble form in the cytoplasm and is not found to be associated with flagellar MTs. Kinetic studies of α-tubulin acetylation/deacetylation in vivo, in cultured rat sympathetic neurons, have shown that acetylation is not coupled to polymerization of MTs, but that deacetylation is tightly coupled to depolymerization (Black et al., 1989).

An antibody to acetylated α-tubulin (Piperno and Fuller, 1985) has been used to localize different populations of acetylated MTs (ACET MTs) both in tissue culture cells and in tissues. For example, it has been shown that there is an increase in the levels of ACET tubulin during early development and particularly during neurulation (Schatten,

et al., 1988; Chu and Klymkowsky, 1989). The presence of ACET MTs, especially in brain (See Fig.4B) is often correlated with MT stability (Cambray-Deakin and Burgoyne, 1987).

C) Phosphorylation

The phosphorylation of ß-tubulin was first detected during serum deprivation-induced differentiation of mouse N115 neuroblastoma cells (Gard and Kirschner, 1985). Later studies have shown that only the neuron-specific isoform of ß-tubulin (Class III ß-tubulin) was phosphorylated (Serrano et al., 1987; Ludueña et al., 1988). The site of phosphorylation of bovine Class III ß-tubulin was localized to tyrosine-437 or serine-444 using tandem mass spectrometry (Alexander et al., 1990).

When undifferentiated and differentiated N115 cells were treated with taxol, a drug that stimulates MT assembly, an increase in the level of phosphorylation of ß-tubulin was observed. In contrast, when such cells were treated with drugs that promoted disassembly of MTs, a rapid dephosphorylation was detected. These results suggested that phosphorylation occurred preferentially on polymeric tubulin (Gard and Kirschner, 1985).

D) Polyglutamylation

This post-translational modification of tubulin was first shown to occur on the α-tubulin subunit (Eddé et al., 1990). The successive addition of glutamyl residues to the α-tubulin polypeptide at the extreme C-terminus results in the formation of acidic variants of tubulin. In a later study, it was shown that much of the heterogeneity of neuronal α-tubulins is due to polyglutamylation and not acetylation (Eddé et al., 1991).

Recently, Alexander et al., (1990, 1991) have shown by tandem mass spectrometry that the neuron-specific Class III ß-tubulin from rat brain is also polyglutamylated in the C-terminus at position glutamate 438. The length of the polyglutamylated side chain also was shown to be developmentally regulated. The site of polyglutamylation overlaps the MAP binding region of tubulin (Maccioni et al., 1988). It has been proposed that acidification of tubulin by polyglutamylation, in part, may enhance MAP binding (Lee et al., 1990a,b) thereby generating stable MT arrays for nerve cell maturation.

Post-translational Modifications and Microtubule Stability

In various established cell lines it was found that in interphase, the TYR MT distribution was virtually indistinguishable from the one visualized with general anti-tubulin antibodies. These general anti-tubulin antibodies recognize all tubulin isoforms irrespective of their post-translational modifications. TYR MTs extended from the centrosome, toward the edge of the cell periphery. In marked contrast, the GLU MT and

the ACET MT populations had much more restricted distributions. These MTs had a sinuous morphology and rarely extended to the cell periphery (Gundersen et al., 1984; Schulze et al., 1987). Studies of drug-induced and cold-induced depolymerization of MTs in established cell lines have shown that MTs persisting after such treatments showed immunoreactivity only to the anti-GLU antibody (Gundersen et al., 1987; Khawaja, et al., 1988) and/or to the anti-ACET antibody (Piperno et al., 1987; Bulinski et al., 1988).

These observations suggested that at least drug-stable and cold-stable MTs tend to be post-translationally modified. This suggestion was tested by measuring the turnover of TYR, GLU, and ACET MTs directly in vivo by microinjecting biotinylated- or rhodamine-labelled tubulin (Kreis, 1987; Webster et al., 1987a,b; Webster and Borisy, 1989). The results showed that the TYR MT array turned over to a significant extent by 5 minutes and completely within 1 hour of microinjection. The GLU MT array however, turned over with a half-time of 1 hour or more. The ACET MT population turned over with dynamics similar to that of the GLU MT array. These results showed there was a good correlation between post-translational modification and MT stability.

However, it was directly shown that post-translational modification by detyrosination of α-tubulin is not the cause of MT stability. Webster et al., (1990) have experimentally induced the formation of a GLU MT array from a predominantly TYR MT array in Swiss 3T3 fibroblasts by microinjecting antibodies to tubulin tyrosine ligase. This resulted in an inhibition of the enzyme and retyrosination of α-tubulin. The stability of these MTs were then directly assayed by reinjecting the same cells with labelled

tubulin and measuring MT turnover by either hapten-mediated immunocytochemistry or fluorescence recovery after photobleaching (FRAP). The results showed that experimentally induced GLU MTs were turning over at a rate similar to TYR MTs. This suggested that detyrosination was a consequence of MT stability and that some other mechanism(s) was (were) responsible for generating stable MTs.

II. MODELS FOR MICROTUBULE DYNAMICS

Several models have been proposed to explain the mechanism of MT turnover. These include uniform exchange (Inoue and Ritter, 1975), treadmilling (Margolis and Wilson, 1978; Hotani and Horio, 1988), GTP Cap/ Lateral Cap model (Bayley, 1990; Bayley et al., 1989, 1990), and dynamic instability (Kirschner and Mitchison, 1986).

Uniform Exchange

This model (illustrated in Fig. 1) states that tubulin subunit exchange occurs along the entire length of the MT with no apparent growth polarity (Inoue and Ritter, 1975).

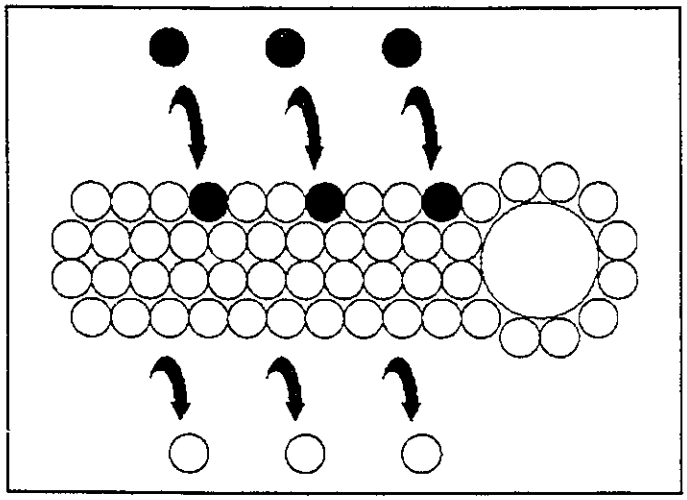

Fig. 1: Uniform Exchange Model

Currently, there is no experimental evidence that supports this model. In vitro MT assembly experiments using isolated ciliary or flagellar axonemes as stable nucleating "seeds" show that there is in fact growth polarity on the exposed ends of axonemal MTs (Allen and Borisy, 1974).

Treadmilling

This model (illustrated in Fig. 2) states that at steady state, there is a net addition of tubulin subunits on to the "plus" end of a MT and a net loss from the minus end while the polymer mass remains constant (Margolis and Wilson, 1978; Hotani and Horio, 1988).

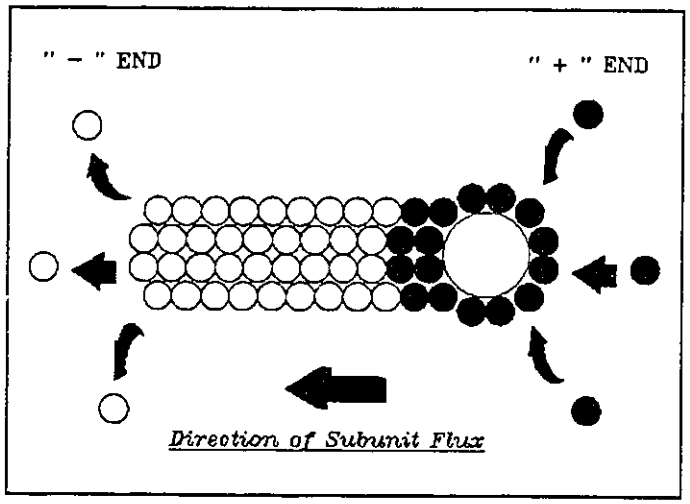

Fig. 2: Treadmilling Model

Treadmilling was only observed after MTs had been stabilized by MAPs. MTs polymerized from phosphocellulose-purified tubulin (PC-Tubulin) exhibited dynamic instability (see below).

GTP Cap and Dynamic Instability

The most widely accepted model, the dynamic instability model, was proposed by Mitchison and Kirschner (1984a,b). Their in vitro experiments have shown that MTs deviated from the predicted behaviour of equilibrium polymerization of linear polymers.

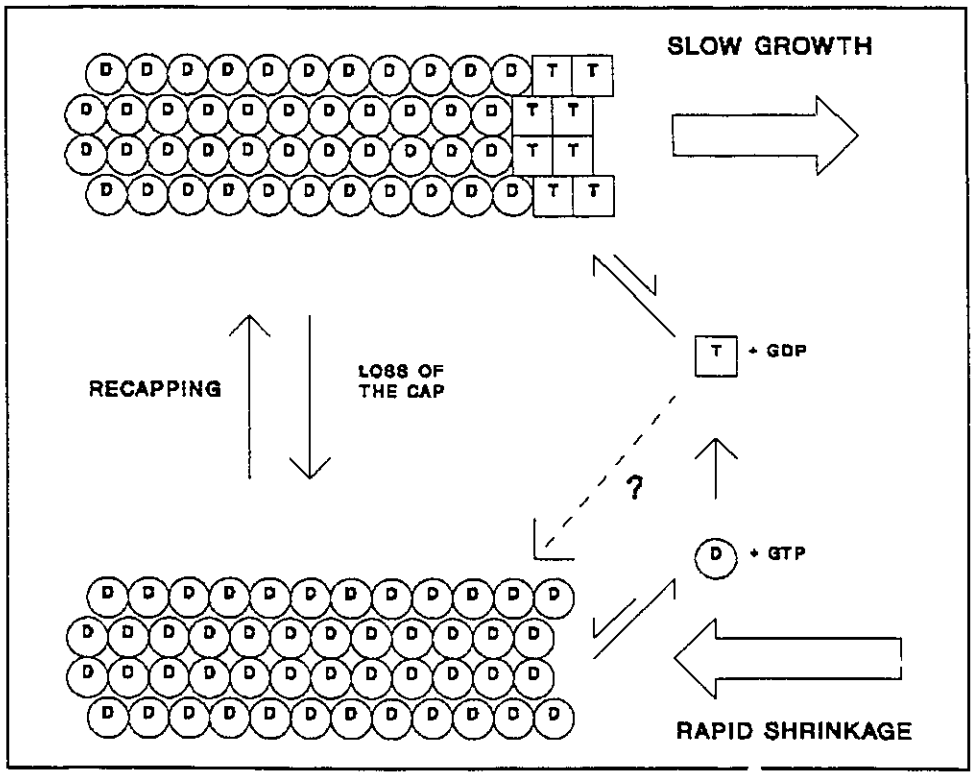

Fig. 3: GTP Cap Model for Dynamic Instability. [From: Kirschner and Mitchison (1986)].

The most consistent deviation was the fluctuation in length of individual MTs at steady state. Thus it was suggested that two populations, a growing and a shrinking MT population, existed that interconverted infrequently, an hypothesis that was originally proposed by Hill and Chen (1984). The complication of GTP hydrolysis being separate from polymerization (Carlier and Pantaloni, 1981) and the observed deviations of MT lengths at steady state led to the formulation of a GTP cap model for dynamic instability (Kirschner and Mitchison, 1986). The GTP cap model is illustrated in Figure 3.

Briefly, if GTP-bound tubulin subunits ("T" inside open squares) are at the MT ends, the MT is said to be stable and will continue to grow slowly. If on the other hand GDP-bound tubulin subunits ("D" inside open circles) are exposed at the ends of the polymers, MTs will depolymerize rapidly. The interconversions between these two phases would be rare. At steady state where the total polymer mass is constant, the slow growing population of MTs would comprise the majority while the rapid depolymerizing population of MTs would be a minority.

Lateral Cap Model

The lateral cap model proposed by Bayley et al., (1989, 1990) is a complex mathematical formulation based on the observed behaviour of MT assembly in vitro. Briefly, Bayley and coworkers have utilized the basic GTP cap model and modified it to account for dynamic instability. The main principle of the lateral cap model is that when tubulin subunits add onto the ends of growing MTs, there is a coupled hydrolysis of GTP to GDP of the nucleotide bound to the previous terminal tubulin. This means that the

GTP cap would be limited only to the terminal layer of the MT and that it would be sufficient to stabilize them for the growing phase.

III. MICROTUBULE DYNAMICS IN VIVO

To carry out such a wide variety functions, MTs have to be differentially dynamic. For example, MTs are very dynamic when cells are undergoing mitosis (Mitchison, 1989) but turn over very slowly when they establish stable neuronal morphologies (Okabe and Hirokawa, 1988, 1990; Lim et al., 1989, 1990).

A technique that has been frequently used to assay MT dynamics in vivo is the introduction of labelled tubulin into cells by microinjection and then detection of its extent of incorporation into the preexisting MT array by immunocytochemical procedures (Soltys and Borisy, 1985; Schulze and Kirschner, 1986, 1987; Sammak et al., 1987; Schulze et al., 1987; Okabe and Hirokawa, 1988; Sammak and Borisy, 1988; Geuens et al., 1989).

Such microinjection experiments have shown that labelled tubulin subunits were incorporated at the "plus" end in existing MTs and that new fully labelled segments were seen to emanate from the centrosome. Also two populations of MTs were detected that differed in their turnover rates: a) a dynamic population of MTs that turned over with $t_{1/2}$ of five to ten minutes and b) a stable population that had a $t_{1/2}$ turnover time exceeding one hour (Schulze and Kirschner, 1986, 1987). These types of techniques have been used to examine MT dynamics in nerve cells.

MT Dynamics in Nerve Cells

The neuronal cytoskeleton is a highly ordered and complex structure primarily consisting of MTs, neurofilaments and actin microfilaments. MTs and neurofilaments are aligned in a longitudinal parallel arrangement and actin microfilaments are arranged either as parallel bundles or in a meshwork. Morphologically, neurons are multipolar cells having one or more dendrites that often branch and an axon. (See Fig. 4A for the extensive arborization of Purkinje cell dendrites). The cytoskeleton in these cells is intimately involved in forming axons and dendrites, intracellular transport, synaptic transmission and development (see review by Riederer, 1990).

Using the "Hook Decoration Method" developed by Heidemann and Euteneuer (1982) it has been demonstrated that the polarity of MTs within dendrites differs from axons (Baas et al., 1988). Dendritic MTs were shown to have nonuniform polarity while axonal MTs had uniform polarity, i.e., the "plus" ends of axonal MTs are oriented away from the cell body while the "minus" ends are directed towards the cell body. Figure 4 shows the compartmentalization of specific cytoskeletal proteins in neurons to either dendrites or axons. The basis for this compartmentalization has been proposed to involve the polarity of MTs within the dendrites and axons and the transport of specific mRNAs for local synthesis of specific cytoskeletal proteins (see reviews by Black and Baas, 1989 and Ginzburg, 1991).

Fig. 4: **Immunofluorescent Staining of ß-III tubulin (A), Acetylated Microtubules (B), MAP 2 (C) and Neurofilament 160 kD Protein (D) in Paraffin Sections of Methacarn-fixed Adult Mouse Cerebellum.** Note the compartmentalization of MAP 2 in Purkinje cell dendrites and cell bodies and the neurofilament 160 kD protein in cell bodies and axons of the white matter. Bars in (A) = 25 μm, in (B,C) = 50 μm and in (D) = 100 μm.

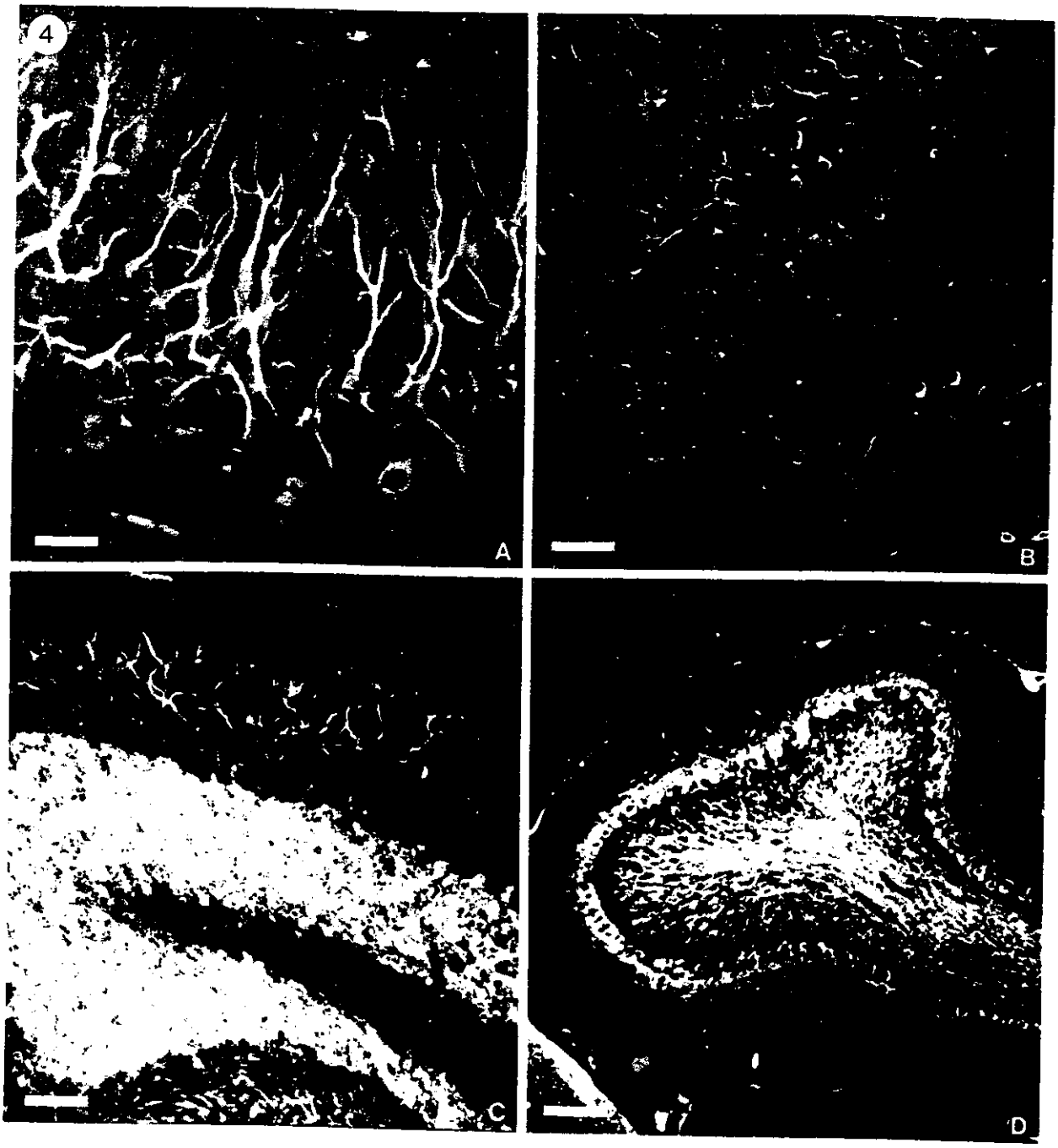
4
A
B
C
D

Earlier studies using quick-freeze, deep-etch techniques have revealed a rather static image of the neuronal cytoskeleton (Hirokawa, 1982). The molecular mechanisms that are involved in assembling this elaborate network are largely unknown. In particular, the role of MTs in establishing stable neuronal morphologies has received much attention in this past decade.

Microinjecting haptenized tubulin into nerve cells has recently yielded some novel features of MT dynamics. Okabe and Hirokawa (1988) were the first to show that existing MTs within neurites of pheochromocytoma 12 (PC12) cells incorporated biotin-tubulin subunits at their distal ends and that this occurred throughout the length of the neurite. No labelled MT segments within the neurite were seen to emanate from the centrosome.

MT assembly is a requirement for neurite elongation. This property has been tested in NB2a/d1 neuroblastoma cells (Shea and Beermann, 1990; Shea et al., 1990), PC 12 cells (Keith, 1990) and primary cell cultures of chick sensory neurons (Baas and Heidemann, 1986). It has been proposed that stable MTs that resist drug-induced and cold-induced depolymerization may serve to act as nucleating "seeds" for further MT assembly within neuritic processes (Heidemann et al., 1984; Baas and Heidemann, 1986).

Recently, it was shown by Baas and Black (1990) that along the entire length within axonal processes of rat sympathetic neurons, there exist "labile" and "stable" domains of individual MTs. Using immunogold electron microscopy procedures, it was shown that the stable domains were enriched in GLU tubulin and that the labile domains were enriched in TYR tubulin. These stable detyrosinated domains and labile tyrosinated

domains were directed proximally and distally, respectively, from the cell body.

This has led to the suggestion that not only do the stable domains act as MT nucleating structures, but also that their continual presence would regulate MT dynamics locally within the axon and that this may be a means for the transport of tubulin during active axonal elongation (Bass and Black, 1990). That is, the stable portion of the MT network would remain stationary while the labile portion would be transported distally.

Two independent groups have made a similar suggestion using different nerve cell culture systems (Lim et al., 1989, 1990; Okabe and Hirokawa, 1990). Both groups have microinjected fluorescently-labelled tubulin into nerve cells and have used the FRAP technique to quantify MT turnover. They observed that, after photobleaching a portion of the neurite shaft, the recovery of fluorescence corresponded to a $t_{1/2}$ of 1 to 2 hours for neuronal MTs. No distal movement of the bleached zone was observed indicating that the MT component of the neuritic cytoskeleton was stationary and that transport of tubulin was not due to polymer translocation. Rather, tubulin transport was mediated by local assembly into and disassembly from neuritic MTs while moving distally from the cell body in soluble form.

In contrast to the evidence presented by Okabe and Hirokawa (1990) and Lim et al., (1990), Reinsch et al., (1991) have shown that neurite elongation is in fact due to polymer translocation. Early Xenopus embryos were microinjected with caged-fluorescein tubulin. The caged-fluorescein tubulin probe used in this study became fluorescent only after photoactivation with 360nm light. Microinjected Xenopus embryos were allowed to develop until neural tubes were formed. This also ensured that the

labelled tubulin was incorporated uniformly in existing MT arrays in the cells of the developing embryo. The neural tubes were then explanted and maintained in culture. After photoactivating a small region along the axonal shaft, real-time low light level video microscopy revealed that the photoactivated zone of fluorescence moved distally at a rate similar to axonal elongation. After extracting the soluble tubulin from these explanted cells the photoactivated zone of fluorescence still persisted, thereby indicating that the observed distal movement was due to polymer translocation.

It still remains to be established how MTs generate neurites. Currently there have been no studies that have examined MT dynamics in nerve cells prior to neurogenesis.

THE EMBRYONAL CARCINOMA (EC) CELL SYSTEM

The multipotent embryonal carcinoma (EC) cell line, P19S18, (McBurney and Rogers, 1982) is a useful system to examine MT dynamics during early neural differentiation. These cells can be maintained in an uncommitted state and induced to differentiate into a restricted spectrum of cell types by the application of certain concentrations of retinoic acid (RA) or dimethylsulfoxide (DMSO). For example, these EC cells can be induced to differentiate into glial cells and neurons by the addition of 1μM RA (Jones-Villeneuve et al., 1982; Edwards and McBurney, 1983), or into muscle cells by the addition of DMSO (Rudnicki et al., 1990). In cells induced to differentiate along the neural developmental pathway it should be possible to examine MT dynamics during the earliest period of differentiation.

Previous studies have used PC 12 cells and primary cultures of neurons to examine the role of MTs in establishing cell polarity. Such studies were not able to examine MT dynamics during the earliest stages of differentiation because these cells were already committed to the neuronal pathway. For instance, the PC 12 cell line expressed the neuron-specific ß-III tubulin isotype (Asai and Remlona, 1989) and tau protein (Joshi and Cleveland, 1989). This is significant because tau protein has been shown to alter the dynamic properties of MTs in vivo (Drubin and Kirschner, 1986). In the P19 EC cell system, tau protein is not expressed until day 6 after neural induction with RA (Falconer et al., 1989a).

The expression of cytoskeletal proteins during early developmental stages of RA-induced neural differentiation of P19 EC cells has been documented by Falconer et al.,

(1989a, 1989b) and the incorporation of these proteins into stable MT arrays has been depicted as occurring in 3 Stages. In the undifferentiated state, most MTs in EC cells were not acetylated and were disassembled by colchicine. MAP 1B was also detected in undifferentiated EC cells.

At Stage 1, 24 hours following neural induction with 1 μM RA, prior to neuritogenesis, there was an increase in the number of ACET MTs in the majority of the population. In a subpopulation of these cells, MTs were observed to be resistant to depolymerization by colchicine and were acetylated. In a minor population, a colchicine-stable MT bundle was detected that was also acetylated. Using specific polyclonal antibodies to ß-tubulin isotypes (Lopata and Cleveland, 1987) it was shown by immunofluorescence microscopy that following neural induction of EC cells at Stage 1, there was an increase in the level of the major brain ß-tubulin isotype II (ß-II) (Falconer and Brown, 1989, 1990; Echeverri et al., 1990). This Class II isotype was preferentially enriched in colchicine-stable MT arrays. A similar increase was also noted in the nerve growth factor-induced differentiation of PC 12 cells (Joshi and Cleveland, 1989) and in developing brain (Lewis et al., 1985).

At Stage 2, the first sign of neurite extension was evident. MTs within these neurites were thought to be stabilized by two other cytoskeletal elements i.e., vimentin and juvenile MAP 2 (Falconer et al., 1989b). Quantitative immunoblotting showed there was a preferential inclusion of the Class II ß-tubulin isotype and a preferential exclusion of the neuron-specific Class III ß-tubulin isotype from colchicine-stable MT arrays (Falconer, et al., submitted). At this stage in differentiation the culture seemed to be segregated into two populations: one that expressed Class III ß-tubulin and the other that did not.

At Stage 3, neurite specialization was accompanied by the appearance of juvenile tau protein, high molecular weight MAP 2 and neurofilament polypeptides. The limitation of the P19 EC cell system is that not all cells develop into either neurons or glial cells. Due to the heterogeneity of the culture, quantitative analyses are difficult to interpret.

The observations of the changes in MT stability and the appearance of ACET MTs at Stage 1 have led to the hypothesis that the MT array in undifferentiated P19 EC cells is initially dynamic and becomes less dynamic in a subpopulation of cells prior to morphogenesis. The objective of this thesis is to experimentally test this hypothesis. I have directly examined MT dynamics during early RA-induced neural differentiation by purifying tubulin from beef brain, labelling it with an N-hydroxysuccinimide ester of biotin, and then microinjecting it into EC cells to quantify MT turnover. This strategy, developed by Schulze and Kirschner (1986), has been used to examine interphase MT dynamics in several established cell lines.

The significance of the work presented in this thesis is that it may provide critical information regarding the alteration in MT dynamics prior to neurogenesis. The generation of stable MT arrays and their role in neurite elongation at later stages in neuronal differentiation has been well documented in a variety of primary cell culture systems. In this thesis I report changes in colchicine stability and in tubulin acetylation that correlate with changes in MT dynamics occurring prior to morphogenesis of RA-induced P19 EC cells. I also present a model for the generation of stable MTs during early neural commitment of P19 EC cells.

MATERIALS AND METHODS

I. Cell Cultures

The P19 EC cell line obtained from Dr. M. McBurney (McBurney and Rogers, 1982) was maintained at 37°C and 5% CO_2 in α-MEM (Flow Laboratories; Mississauga, Ont.) supplemented with 10% heat-inactivated fetal bovine serum (FBS)(Gibco; Burlington, Ont.). Cells were passaged every 48 hours using 0.25% trypsin (Sigma; St. Louis, MO) and 1mM EDTA (Sigma) in calcium- and magnesium-free PBS. For neural induction, 5 X 10^4 to 10^5 cells in a volume of 2.5 mL were seeded onto glass coverslips, in a 35mm tissue culture dish, in α-MEM plus 10% FBS. After 24 hours, the medium was replaced with α-MEM plus 2% FBS (differentiation medium) and 10^{-6}M retinoic acid (Sigma). (Stock RA at 10^{-2}M in ethanol was typically stored at -80°C and diluted to 10^{-4}M in α-MEM for use in differentiation experiments.) For longer differentiating cultures, the differentiation medium was replaced every 48 hours after neural induction. For some experiments, colchicine (Sigma) was added to the cell cultures at a final concentration of 1μg/mL for 45 minutes to promote depolymerization of the MT array. After this treatment, the cells were then fixed and processed for immunofluorescence microscopy.

Pt K2 cells (rat kangaroo epithelial cells)(American Type Culture Collection (ATCC) *cat. #CCL56*; Rockville, MD) and L6E9 cells (undifferentiated rat myoblasts; ATCC *cat. #CRL1458*) also were maintained at 37°C and 5% CO_2 in α-MEM plus 10% FBS. These cells were passaged in the same way as described above for EC cells and were only used to learn the microinjection technique.

II. Immunofluorescence Staining

For immunofluorescence microscopy, the cells were fixed as follows: coverslips were rinsed briefly in PBS, then simultaneously fixed and extracted with 3.7% formalin (BDH Chemicals; Toronto, Ont.), 0.25% glutaraldehyde (J.B. EM Services; Dorval, Que.) and 0.5% Triton X-100 (Pierce; Rockford, IL) in PEM buffer [80mM PIPES (Sigma), 1mM EGTA (Sigma), 1mM $MgCl_2$ (Fisher; Toronto, Ont.), pH 6.8] for 8 minutes. Coverslips were then rinsed 3 times with PBS, post-fixed with 95% ethanol at -20°C for 5 minutes and then finally rinsed with PBS as before.

EC cells were then double-labelled for total tubulin using the rat monoclonal antibody YOL 1/34 (Dimension Laboratories, Mississauga, Ont; Kilmartin et al., 1982) at a 1:200 dilution in PBS, and for ACET MTs using the mouse monoclonal antibody to acetylated tubulin (clone 6-11B-1; Piperno and Fuller, 1985) at a 1:20 dilution for 45 minutes. The coverslips were then rinsed in PBS and then double-stained for 45 minutes using a mixture of Texas Red-conjugated donkey anti-rat IgG (cross absorbed to mouse; Jackson Research, Westgrove, PA) and DTAF (dichlorotriazinyl amino fluorescein)-conjugated donkey anti-mouse IgG (cross absorbed to rat; Jackson Research) antibodies at 1:80 and 1:100 dilution in PBS, respectively. The cells were then stained for DNA with Hoechst 33258 (1μg/mL of PBS)(Calbiochem; LaJolla, CA) at 1:5000 dilution in PBS for one minute followed by rinses in PBS as described before. The coverslips were then mounted in p-phenylene-diamine (Sigma) to retard bleaching. Samples were viewed on a Zeiss Universal microscope or a Zeiss Axiophot microscope, both equipped with epifluorescence optics and photographed with Ilford XP-1 400 ASA film.

III. Quantitative Immunoblotting

(A) Preparation of Cell Extracts

Three types of cell extracts were prepared for gel electrophoresis to quantify the amount of total cellular tubulin, total polymerized tubulin and tubulin in colchicine-stable MTs. Uncommitted EC cells or one day RA-treated cells were cultured in 100mm tissue culture dishes to prepare cell extracts. To prepare whole cell protein extracts the cells were first washed with 37°C PBS briefly, twice with 37°C PEM buffer (80 mM PIPES, 5 mM EGTA, 1 mM $MgCl_2$, pH 6.8) and then solubilized with 1mL of 0.5% SDS in 25mM Na_2HPO_4 and 0.4M NaCl, pH 7.2 (lysis buffer).

To prepare total polymerized tubulin extracts, the cells were washed as described above and then extracted for 3 minutes in 2mL of 0.1% Triton X-100 in PEM buffer. This extraction removes soluble tubulin and other proteins leaving behind an insoluble cytoskeletal array (Solomon, 1986). The remaining insoluble component was solubilized in the lysis buffer.

To prepare tubulin from the colchicine stable MT population, uncommitted EC cells and one day RA-induced cells were pretreated with 1μg/mL colchicine for 45 minutes at 37°C. This treatment would depolymerize the colchicine-labile MT population. Following treatment with colchicine, the cells were extracted and solubilized as described above. All solubilized cell extracts were scraped using a rubber policeman and pipetted into eppendorf tubes and then sonicated for one minute to reduce the viscosity for DNA measurements. All extracts were then stored at -20°C. After thawing samples, protein estimation was done using the bicinchonic acid assay (Sigma) with

bovine serum albumin as the standard.

(B) DNA Measurements

The amount of DNA in the cell extracts was quantified utilizing the procedure of Brunk et al. (1979) as modified by Labarca and Paigen (1980).

The principle of this technique is to quantify the amount of DNA in cell extracts using a fluorescence-based assay. Hoechst 33258 was initially dissolved at 1mg/mL in distilled water (1000X stock) and then diluted to 1ug/mL in a DNA buffer (0.05M $NaPO_4$, 2.0 M NaCl, 5 X 10^{-3} EDTA, pH 7.4) for fluorescence measurements. Calf thymus DNA (Type 1 from Sigma) was used as a standard and was initially made to 2mg/mL in distilled water (100X stock) and then diluted to 20ug/mL. Fluorescence measurements were made using the Turner 430 Spectrofluorometer.

The procedure was as follows: Fluorescence of the Hoechst dye in DNA buffer (2mL volume) was first determined. To this, increasing amounts of the EC cell extracts (typically 10uL increments) were added sequentially, and fluorescence measurements were made after each addition. When a sufficient number of measurements was obtained, increasing amounts (10uL increments) of the calf thymus DNA standard at 20ug/mL were added to the same tube and fluorescence measurements were also made after each addition. Finally, the values were plotted on a graph and the slope of fluorescence enhancement for an EC cell extract was compared with the slope for the DNA standard. After calculating this ratio, this value was multiplied by the known DNA standard concentration (20ug/mL) to give the DNA concentration in the various EC cell extracts.

This procedure is sensitive because problems of fluorescence quenching due to cellular components or buffers are compensated for by including an internal DNA standard for each unknown sample (Labarca and Paigen, 1980).

(C) Electrophoresis and Immunoblotting

Samples of whole cell proteins, MT polymer extracts and colchicine-stable MT polymer extracts from undifferentiated and one day neurally-induced EC cells were electrophoresed on a 7.5% SDS polyacrylamide gel at a constant voltage of 200 volts, using the Bio-Rad mini-gel apparatus. The amount of protein electrophoresed from each sample were normalized per μg DNA. This was done to detect any changes in tubulin levels per some constant cell number. Phosphocellulose-purified tubulin (PC-Tubulin) dilutions were included in every experiment for internal standards. Following electrophoresis the proteins were electrophoretically transferred to a nitrocellulose membrane for 1 hour at a constant voltage of 100 volts with a cooling unit. The membranes were transiently stained with 0.2% (w/v) Ponceau Red (Sigma) in 3% trichloroacetic acid, blotted dry and the lanes of protein samples were pencilled in around their entire perimeter. After the membranes were destained in PBS, they were blocked in 1% (w/v) powdered skim milk in PBS for 2 hours and then mounted on a Miniblotter 28 (Immunetics; Cambridge, MA). Each sample was then probed with the mouse monoclonal anti-ß-tubulin antibody DM1B (Amersham; Oakville, Ont.) at a dilution of 1:10,000 and with the mouse monoclonal anti-acetylated tubulin antibody 6-11B-1 at a dilution of 1:10 in PBS for one hour. The DM1B antibody was chosen to detect total

tubulin because it recognizes a conserved epitope at the C-terminal portion, spanning residues 416-431 (de la Vina et al., 1988; Lee et al., 1990a), of all avian and mammalian ß-tubulins. After the blots were rinsed extensively with PBS, they were incubated with ^{125}I-goat-anti-mouse antibody (specific activity: 4.23μCi/μg; NEN Research Products; Mississauga, Ont.) at 0.4μCi/mL for 15 hours. They were then rinsed in 0.3% Tween-20 in PBS, 3 times for 30 minutes each. The blots were then exposed to X-ray film (KOKAK X-OMAT) using a Quanta-III intensifying screen (Picker) at -70°C for 9 hours. The X-ray film was developed in GBX developer for 4 minutes and fixed for 3 minutes followed by a final water rinse.

The resulting autoradiogram was then scanned using an LKB Ultroscan XL laser densitometer that determined the area under the curve corresponding to the density of the ^{125}I-conjugated secondary antibody binding. Each sample was scanned 5 times at 400μm intervals to determine the density of the band and the mean values were obtained for each sample. A tubulin standard curve was generated from PC-Tubulin dilutions by computing the area under the curve by densitometry. Values within the linear range were used to determine the amount of tubulin present in each type of cell extract by extrapolating these values from the tubulin standard curve. The resulting data was then normalized per μg of DNA. Relative ACET tubulin levels (as expressed by the computed area under the curve) were also normalized per μg of DNA. The TWO-WAY Analysis of variance test and the multiple comparisons TUKEY test (Zar, 1984) were done to determine if the mean tubulin values from each type of extract were significantly different from each other and if they were different during early neural differentiation of P19 EC cells.

IV. Purification of Tubulin

MT protein was purified from beef brain by two cycles of assembly/disassembly by a modification of the procedure of Weingarten et al., (1975).

Two beef brains, purchased from Earl Thomas Slaughterhouse (Nepean, Ont.), were weighed and then homogenized in a pre-cooled waring blender in MT assembly buffer (MAB) [100mM PIPES, 1mM EGTA, 1mM $MgCl_2$, 4M glycerol (BDH), pH 6.4] for 45 seconds at top speed. The homogenate was distributed in four plastic bottles and centrifuged using a GSA rotor at 10 krpm (16,300 g) at 4°C for 5 minutes in a Sorval RC-5C preparative centrifuge. Pellets were discarded and the supernatant was transferred to 50 mL polycarbonate tubes and centrifuged at 18 krpm (39,100 g) for 30 minutes at 4°C in a Sorval SS-34 rotor. The supernatant (S1) fraction was saved, GTP (Sigma) was added to 1.8mM (1mg/mL) and incubated at 35°C for 30 minutes to promote MT assembly. Assembled MTs from the S1 fraction were then centrifuged at 18 krpm for 30 minutes at 35°C. Pellets were resuspended in approximately 15% of the S1 volume in cold MAB and homogenized on ice for 30 minutes using a glass to glass homogenizer to depolymerize MTs. The cold homogenate was then centrifuged at 4°C for 30 minutes at 18 krpm and the supernatant was designated as the S2 fraction. To this, GTP was added to 1.8mM and MTs were assembled at 35°C for 30 minutes and centrifuged at 18 krpm as before. The warm supernatants were discarded and the pellets were resuspended in 10% of the S2 volume using cold MAB. After solubilization on ice for 30 minutes using the glass homogenizer, the homogenate was centrifuged at 4°C for 30 minutes at 18 krpm and the resulting supernatant was re-centrifuged for 20 minutes. The final

supernatant, designated the S3 fraction, was aliquoted in 1mL fractions into eppendorf tubes and frozen at -80°C.

Tubulin was further purified from MAPs by phosphocellulose chromatography at 4°C according to Mitchison and Kirschner (1984a). Prior to chromatography the S3 fraction was cycled one more time as before and the pellet was resuspended in 1 to 2mL of 100mM Pipes buffer (100mM PIPES, 1mM EGTA, 1mM $MgCl_2$, pH 6.4). Typically, 1mg of MT protein was loaded per mL of bed volume. Protein was eluted at a rate of 1mL per minute. MAPs were eluted from the column using 0.55M NaCl in 100mM Pipes buffer.

The peak flow-through fractions were pooled and then dialysed at 4°C overnight against a buffer consisting of 8M glycerol, 100mM PIPES, 1mM EGTA, 1mM $MgCl_2$, pH 6.4. After dialysis, tubulin was stored at -80°C in 1mL fractions. MAP fractions were dialysed against the same 8M glycerol/Pipes buffer and then stored at -80°C.

All samples were subjected to SDS-PAGE and stained with Coomassie Blue (Bio-Rad; Richmond, CA). The MAP fraction also was immunoblotted using mouse monoclonal antibodies against various MAPs including: anti-MAP 1A (clone 1WM-4C8), anti-MAP 1B (clone G10; Calvert and Anderton, 1985), anti-MAP 2 (clone AP-18; Tucker et al., 1988), and anti-tau (clone tau1; Binder et al., 1985). The anti-MAP 1A antibody was obtained from Dr. L.I. Binder and its characterization has not been published. All anti-MAP antibodies were used at 1:1000 dilution in PBS. The immunoblot was then incubated with biotinylated goat anti-mouse IgG secondary antibodies (Amersham) and streptavidin-horseradish peroxidase (Amersham). The

reaction was developed using 4-chloronaphthol (Bio-Rad).

V. Biotinylation of Tubulin

PC-Tubulin was biotinylated essentially according to the procedure of Kristofferson et al., (1986) but with many modifications.

22.8mg of PC-Tubulin was biotinylated. PC-Tubulin, stored at -80°C, in 8M glycerol/Pipes buffer (8M glycerol, 100mM PIPES, 1mM EGTA, 1mm $MgCl_2$, pH 6.4), was thawed and brought to assembly buffer conditions by diluting it 1:1 with 60 mM Pipes buffer (60mM PIPES, 1mM EGTA, 1mM $MgCl_2$, pH 6.4). Assembly was initiated at a tubulin concentration of 3mg/mL at 37°C by adding 2mM GTP and 10mM $MgCl_2$. During the assembly, 10mg of N-Hydroxysuccinimidobiotin (Sigma) was dissolved in 100μL DMSO (Pierce) and set aside at room temperature. 50% sucrose solutions were then made by dissolving 20g sucrose (BDH) in 40mL of Pipes Buffer. 200mg of sodium glutamate (BDH) was dissolved in 20mL of the 50% sucrose cushion solution. An additional 100mg of sodium glutamate was weighed and set aside for quenching the biotinylation reaction. 4.5mL of the glutamate sucrose solution were pipetted into each of four Beckman 50Ti rotor bottles. The tubes and caps were balanced and placed in a Beckman 50Ti rotor pre-equilibrated at 37°C.

After 30 minutes of MT assembly, 61μL of the biotin solution was added to the assembly mixture, vortexed lightly to ensure even mixing and then returned to the 37°C water bath for a further 15 minutes (timed with a stopwatch). The addition of 61μL of the biotin solution in this step yields a labelling stoichiometry of approximately 2.5 to 3

biotin molecules per tubulin dimer (Mitchison and Kirschner, 1985). During the biotinylation, biotin-labelled MTs were vortexed gently every 3-5 minutes. After 15 minutes, 100mg of sodium glutamate was added and then immediately vortexed to dissolve the solid. The addition of sodium glutamate quenches the biotinylation reaction. The assembly mixture must appear turbid at this point to ensure that MT assembly has occurred.

At 37°C, 2.5mL of biotin-labelled MTs were pipetted onto each of the four glutamate/sucrose cushions, balanced, placed into the 50Ti rotor and centrifuged at 49 krpm (216,000 g) at 35°C for 2 hours in a Beckman L8M ultracentrifuge. The warm supernatants were carefully aspirated and saved for protein determination. The four MT pellets were resuspended in a total volume of 1mL of cold 80mM Pipes buffer (80mM PIPES, 1mM EGTA, 1mM $MgCl_2$, pH 6.4). The pellets were homogenized on ice using a teflon glass homogenizer and GTP was added to 1mM and left on ice for 20 minutes. The homogenate was distributed in 500μL eppendorf tubes and placed in a chilled 50mL polycarbonate tube. Then this tube was partially filled with cold Pipes buffer until the level reached the neck of the eppendorf tubes that contained the biotinylated tubulin (B-Tb). A balance tube was made and the samples were centrifuged in a Sorval RC-5C preparative centrifuge at 20 krpm (48,000 g) in a SS-34 rotor at 4°C for 30 minutes. The cold pellets were saved for protein determinations.

To the supernatant, 500μL of a solution consisting of 6 volumes glycerol to 1 volume 0.56M PIPES, 196mM $MgCl_2$, 7mM EGTA at pH 6.4 was added to bring the components to assembly buffer conditions. GTP was added to 1mM and B-Tb was

assembled at 37°C for 30 minutes. During this second assembly step, 5.5mL of the sucrose solution (no glutamate this time) was pipetted into each of two 50Ti rotor bottles, balanced and then placed in a 37°C incubator to equilibrate.

At the end of incubation the assembly mixture must appear turbid, to ensure that B-Tb has assembled into MTs. An equal volume of the assembled Biotin-MTs were loaded onto each of the sucrose cushions at 37°C and then centrifuged using a 50Ti rotor at 49 krpm, 35°C for 2 hours. The warm supernatants were carefully aspirated and saved for protein determinations. One MT pellet was resuspended in the 100mM Pipes buffer at pH 6.4 and the other pellet was resuspended in a microinjection (MIJ) buffer [50mM potassium glutamate (BDH), 1mM $MgCl_2$, pH 6.8]. Both pellets were homogenized separately on ice for 20 minutes and clarified by centrifugation at 20 krpm in the SS-34 rotor as before for 20 minutes. The cold pellets (CP2) were saved for protein estimation. B-Tb in the Pipes buffer was aliquoted in 20μL portions in eppendorf tubes and B-Tb in MIJ buffer was dispensed in 10μL fractions. All fractions were then frozen in liquid nitrogen and then stored at -80°C.

B-Tb was electrophoresed, transferred to a nitrocellulose membrane, and detected by incubating the membrane with streptavidin-conjugated horseradish peroxidase and developing with 4-chloronaphthol.

VI. MT Assembly off Purified Axonemes

(A) Axoneme Isolation

Axonemes were isolated from Tetrahymena (purchased from Ward's Biology, Mississauga) according to Brown, D.L. (unpublished procedures). Tetrahymena were grown in sterile PPY medium [125μM ferric citrate (BDH), 50μM calcium chloride dihydrate (Baker; Toronto, Ont.), 1mM magnesium sulfate (Fisher), 0.5mM potassium dihydrogen orthophosphate (BDH), 83.3mM D-glucose (BDH), 7.5g/L yeast extract (Difco) and 7.5g/L proteose peptone (Difco)] and passaged every 4 to 5 days.

For deciliation, 400mL of cells were pipetted into 50mL polycarbonate tubes and pelleted at 3 krpm (1000 g) in a Sorval SS-34 rotor at room temperature for 10 minutes. The culture media supernatant was discarded and the cell pellets were gently resuspended in a total volume of 10mL cold MAB (see recipe in Tubulin Purification) on ice. The cell suspensions were pooled, swirled and triturated very gently with a pasteur pipette. When the cells were immersed in MAB, they shrunk and in the process, shed their cilia. The progress of deciliation was monitored by Differential Interference Microscopy (Nomarski) at 2 minute intervals. The deciliation was usually 70 to 90% complete by about 6 minutes on ice. Cells were pelleted in a polycarbonate tube at 4 krpm for 10 minutes at 4°C. The supernatant was recentrifuged at 10 krpm (12,100 g), at 4°C for 25 minutes to pellet the cilia. The supernatant was discarded and the cilia were demembranated by resuspension in 2 mL cold distilled water (dH_2O), plus 0.4mL 10mM Tris (Sigma)(pH 8.3) and 1.6mL 1% Triton X-100 (in 1mM Tris, pH 8.3). The suspension was triturated vigorously with a pasteur pipette and left on ice. After 15

minutes, 20mL of cold 1mM Tris (pH 8.3) was added and the axonemes were pelleted at 12 krpm for 30 minutes. The supernatant was discarded and the axonemes were resuspended in 0.8 to 1.0mL of cold MAB. The suspension was then sheared 3 to 4 times using a 22-gauge needle. Axonemes were then aliquoted and stored at -20°C until further use. Axonemes stored in this manner are stable for at least a month.

(B) In vitro Assembly Experiments

The assembly competence of B-Tb was assessed by growth off axonemes as per Mitchison and Kirschner (1984b) and Kristofferson et al., (1986) but B-Tb was detected by immunogold procedures and visualized by electron microscopy.

Initially, 10μL of axonemes were placed onto each parlodion-coated 400 mesh nickel grid (J.B. EM Services Inc.) and allowed to adhere for 10 minutes. Parafilm was placed onto a heating block adjusted to 37°C. B-Tb was mixed with unmodified PC-Tubulin at 1:9, 1:4, and at 1:1 ratios. Controls included only B-Tb and only PC-Tubulin. To each assembly mixture, GTP was added to 2mM (from a 200mM stock) and the $MgCl_2$ was brought to 2.5mM. All assemblies were initiated at a tubulin concentration of 1.3mg/mL. Each assembly mixture was pipetted onto the parafilm, on the heating block, and the EM grids were placed directly on top of them, axoneme-side-down. The objective was to polymerize tubulin onto axonemes, directly on the EM grid. Adjacent to each of the assembly reactions, 100μL of 1% glutaraldehyde in 100mM Pipes buffer (pH 6.4) was pipetted to terminate the assembly after 10 minutes. Following glutaraldehyde fixation for 5 minutes, each grid was rinsed briefly with filtered PBS

supplemented with 0.01% Triton X-100 and 2mM sodium azide (PBS-T) and extensively rinsed with filtered dH_2O.

Each grid was then incubated at room temperature with rabbit anti-biotin antibody (ENZO Diagnostics, Inc; New York, NY) at 1:50 dilution in filtered antibody buffer (2mM sodium azide, 1% BSA in PBS) for 1 hour. At the end of incubation, each grid was rinsed briefly with PBS-T as before, and extensively with filtered dH_2O. The grids were then incubated at room temperature with 10nm colloidal gold-conjugated goat anti-rabbit IgG (Sigma) at a dilution of 1:50 in antibody buffer for 3 hours. Following incubation, each grid was extensively rinsed as before, and then stained with 1% uranyl acetate $_{(aq)}$(J.B. EM Services). Samples were examined with a Phillips 201C Electron Microscope and photographed on Kodak EM film, grade SO163.

(C) Length Measurements and Data Analysis

MT lengths were measured using a Zeiss IBAS Interactive Image Analyzer. The mean MT lengths of each B-Tb: PC-Tubulin assembly mixture, were obtained and the resulting data was subjected to the One Way Analysis of Variance Test and the statistical parametric Tukey Test procedure according to Zar (1984). The former test determines if the mean lengths are statistically different from each other and the latter test determines their group structure (Zar, 1984).

VII. Microinjection Technique

(A) Microinjection of Pt K2 Cells

Pt K2 cells were used to learn the MIJ technique, because of their larger cytoplasmic volume in comparison to EC cells. These cells are well spread, attached and are relatively easy to microinject. Micropipettes (World Precision Instruments; New Haven, CT) were pulled on a Kopf Vertical Pipette Puller (David Kopf Instruments; Tujunga, California), to a tip diameter less than 2 micrometers. Cells, grown on coverslips in tissue culture dishes, were placed on a Zeiss IM inverted microscope stage equipped with a heating element to maintain them at 37°C. For microinjection, 20mM HEPES was added to the culture medium to buffer any pH changes. Protein samples to be injected were centrifuged in a Eppendorf minifuge at 4°C and 14 krpm for 20 minutes prior to injection. Pulled micropipettes were back-loaded with 0.5μL of sample with a Hamilton syringe. The needles were then inserted into the capillary holder and mounted at an angle of approximately 45° on the micromanipulator. Injections were performed using the Eppendorf microinjector 5242 (West Germany) with an attached nitrogen tank as a source of pressure. Successful injections were noted by a swelling of the cell and a marked change in contrast of the cytoplasm. Pt K2 cells can be easily microinjected with a success rate greater than 90%, without causing cell lysis or changing the overall cell morphology. To determine if the integrity of the MT network in such cells was disrupted, the anti-tubulin antibody 5A6 (Aitchison and Brown, 1986) was microinjected into Pt K2 cells. Two to three minutes after microinjection the cells were simultaneously fixed and extracted using the procedure outlined in Section II [Immunofluorescence

Staining]. The coverslips were subsequently incubated with an FITC-conjugated goat anti-mouse antibody (Cappell Labs) at a 1:100 dilution in PBS. The 5A6 antibody has been previously shown not to depolymerize MTs when it is microinjected in Pt K2 cells (Jones-Villeneuve, unpublished observations).

(B) Microinjection of EC Cells

The same technique was utilized to microinject EC cells. Since EC cells have very little cytoplasm compared to Pt K2 cells, lower injection pressures and an angle of 60° for microinjection had to be used. In spite of these modifications EC cells lysed upon the entry of the micropipette. To overcome this difficulty, EC cells were grown on 0.1% gelatin-coated coverslips to improve their attachment to the substrate. Although these modifications have increased the likelihood for successful injections of EC cells, the technique is still very difficult to accomplish. The success rate varies from 10 to 20%.

VIII. Microinjection of B-Tb into L6E9 and EC Cells

The rat myoblast L6E9 cell line, which like the Ptk2 cells is relatively easy to microinject, was used to detect the assembly competence of B-Tb in vivo.

B-Tb, at a concentration of 2.39mg/mL, was microinjected into the cells and, at various times after injection, they were fixed and processed for immunofluorescence. The cells were pre-extracted with 0.5% Triton X-100 in PHEM buffer (same as PEM buffer but supplemented with 25mM HEPES and pH 6.94) for 90 seconds. This extraction solution was aspirated and the cells were then fixed with the same simultaneous

extraction/fixation solution and post-fixed with 95% ethanol as described earlier [see II, Immunofluorescence Staining].

Prior to staining with antibodies, all coverslips were incubated for 45 minutes in PBS + 0.1% Triton X-100 (Schulze and Kirschner, 1986). Detection of B-Tb incorporation and the total MT array in these cells was accomplished by the successive incubation with the following antibodies, all diluted in PBS + 0.1% Triton X-100: rabbit IgG anti-biotin (ENZO) at 1:100 dilution, biotin-conjugated-goat IgG anti-rabbit IgG (Vector Labs) at 1:100 dilution, Texas Red-conjugated streptavidin (Amersham) at 1:50 dilution, mouse IgG anti-α-tubulin (clone 5A6, Aitchison and Brown, 1986) at 1:10,000 dilution, and finally DTAF-conjugated Donkey IgG anti-mouse (cross absorbed to rabbit, Jackson Laboratories) at 1:200 dilution. All antibody incubations were for 30 minutes followed by rinses in PBS + 0.1% Triton X-100 3 times for 5 minutes each. Prior to mounting in p-phenylamine diamine, the coverslips were rinsed with PBS alone.

After determining its assembly competence in L6E9 cells, B-Tb was microinjected into EC cells at 2.39mg/mL. The extent of MT turnover for uncommitted and one day neurally-induced EC cells was determined in samples fixed 10 and 30 minutes after injection. Detection of the total MT array and the incorporation of B-Tb into the endogenous array were as described above. A MT was defined as having turned over if the biotin signal was uniformly distributed over the entire length of the polymer (Schulze and Kirschner, 1986 and see Fig. 5).

To analyze MT turnover the entire MT array must be visualized. Since EC cells are not flat, the total MT array and the Biotin-MT array were reconstructed using

Fig. 5: **Model for Microtubule Turnover.** Biotin-tubulin (B-Tb) is microinjected into a cell (a) and at various times after injection, it is fixed and processed for immunofluores cence. The extent of incorporation of B-Tb (red lines) into the endogenous microtubule array (blue lines) is then analyzed at different times (b and c) after microinjection. (CM = Cell Membrane; N = nucleus). Inset, (d), phase contrast micrograph showing the microinjection of P19 EC cells. Bar = 30 μm.

MODEL FOR MICROTUBULE TURNOVER

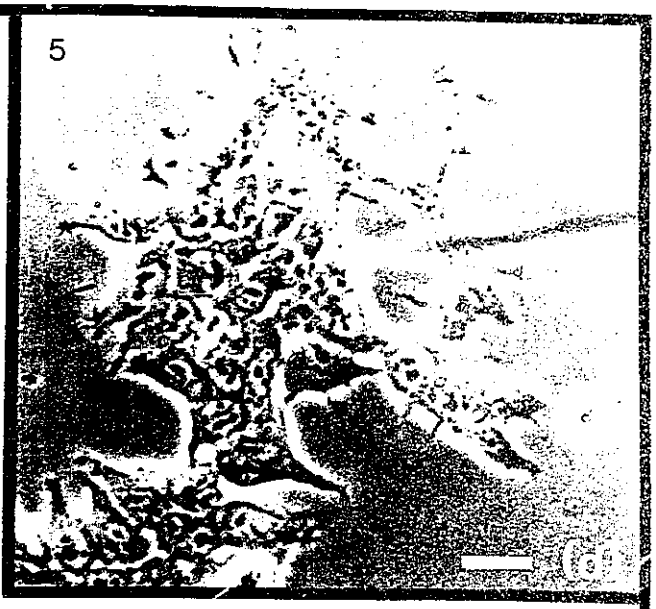

computer-aided video microscopy and digital image processing. (See below).

IX. Video Microscopy and Digital Image Processing

Low light intensity video microscopy and digital image processing were used to record immunofluorescence images of MTs in microinjected EC cells. This allowed the recording of multiple optical sections of the same cell without photobleaching.

(A) Video Microscopy

The components of the video microscopy system used in this study were the following: a Zeiss Photomicroscope III equipped with epifluorescence optics and a Xenon burner, a silicon-intensified target (SIT) camera (DAGE-MTI Inc.; Michigan City, IN.), a SONY video monitor (Japan), an AKRAN 386 computer equipped with CORECO frame grabber boards (Coreco Inc.; Ville St-Laurent, Quebec) and Image Processing software from Media Cybernetics (Silverspring, MD.). Additional customized programs for image processing, designed by Dr. David Coll (Carleton University), were also used.

The video imaging system was set up as follows: fluorescent images of MTs in EC cells were projected onto the SIT camera from the attached photomicroscope. The video monitor was also attached between the SIT camera and the host computer. A pointing device, a mouse, was installed to facilitate tracings of MTs.

Fluorescent images of MTs were viewed using the Plan 100/N.A. 1.3 objective lens, at selected focal planes in EC cells. To prevent saturation of the fluorescent images projected onto the SIT camera, neutral density filters (Nos. 0.5 and 0.12) were placed

in front of the excitation filter on the photomicroscope. Images were then displayed on the video monitor, digitized by the frame grabber, averaged to increase the signal to noise ratio, and stored for further image processing. The averaging program is recursive, i.e., it takes the weighted average of the last 32 video frames after terminating the integration program. Phase contrast images of EC cells were also projected onto the SIT camera, and averaged as described above.

(B) Image Enhancement and MT Tracing

The Run Contrast program distributes the total number of pixels in an area of interest equally over a selected range of grey levels. The Deconvolution program uses a high-pass filter such that the resultant image is slightly "deblurred". This high-pass filter increases the noise, but reduces the "spreading" of information in the digital image. Both programs were used in succession (in any order) to improve the quality of the image, but only deconvolution was used prior to tracing of MTs. In some instances, only averaged images were used for MT tracings.

In the IMAGEPRO directory, numerous programs were used for image analysis and image enhancement. Background fluorescence was eliminated by initially measuring the grey levels of the background and the area(s) of interest. The measured grey level of the background was then subtracted from the entire image. If higher grey levels were subtracted, a loss of information would have resulted. The DR. HALO program, also found in the IMAGEPRO directory, was used for tracing MTs. For such tracings, a processed digital image of the first focal plane was projected onto the video monitor.

Using the DR. HALO program, individual MTs were traced with the aid of the pointing device. After performing the appropriate mathematical manipulations, only the tracing was selectively retrieved from this combined image. This was achieved by first subtracting the highest grey level of the original image from the combined image and then multiplying by the appropriate constant. This ensured that only the tracing of the MT network was projected onto the video monitor. The cartoon was then stored on the hard drive. The first tracing was then mathematically added onto the processed digital image of the second focal plane. The tracing of the MT network was then resumed using the DR. HALO program.

For microinjection experiments, this technique was repeated until the entire MT network and the incorporation of B-Tb into the MT array, at every focal plane in an EC cell was traced.

(C) Photography

All digital phase contrast and fluorescent images were photographed on Ilford XP1-400 ASA film, directly from the video monitor using a PENTAX SF10 super focus camera with a TAMRON macrolens. The camera, mounted on a tripod, was placed at a distance of 77 centimetres away from the video monitor. In the dark, photographs were taken with the camera previously set on automatic aperture/exposure (A/E) mode. The shutter speeds used for photographing video images were either 1 or 0.5 seconds.

RESULTS

I. EC Cell System

A) Immunofluorescence Studies

Immunofluorescence staining of the MT array in undifferentiated EC cells is illustrated in Fig. 6. Anti-tubulin staining with the YOL 1/34 antibody (Fig. 6B,H) reveals a simple centrosome-based MT array. Anti-acetylated tubulin staining with the 6-11B-1 antibody (Fig. 6C,I) shows that few MTs at this stage are acetylated. The 6-11B-1 antibody was used to detect acetylated MTs (ACET MTs) as an indicator of MT stability. When EC cells are treated with colchicine at 1 μg/mL for 45 minutes, most MTs depolymerize (Fig. 6E,K). The few MTs that do persist after colchicine treatment are acetylated (Fig. 6F,L).

Twenty-four hours after neural induction with 1 μM RA, no overall change in cell morphology is apparent (compare Fig. 6A,G and Fig. 7A,G,J), but there appears to be more MT assembly in neurally-induced EC cells (Fig. 7B,H,K) and most MTs are acetylated (Fig. 7C,I,L). In a restricted population of cells, the MT array is organized into bundles (Fig. 7K,L) which are also acetylated. When these cells are treated with colchicine at this early stage of neural differentiation, most MTs are depolymerized in a majority of the population. In a subpopulation of cells (Fig. 7E,N,Q) colchicine-stable MTs are present and in some cells those MTs are organized into bundles (Fig. 7E,Q). Anti-acetylated tubulin staining of MTs in these cells shows that almost all of the colchicine-stable MTs are acetylated (Fig. 7F,O,R).

Fig. 6: **Microtubule Arrays in Undifferentiated P19 Cells.** Phase contrast (A,D,G,J), total tubulin stained with YOL 1/34 antibody (B,E,H,K), and acetylated tubulin stained with 6-11B-1 antibody (C,F,I,L). Control untreated cells (A-C,G-I) have a centrosome-based microtubule array with few acetylated microtubules. A majority of the colchicine-treated cells (D-F,J-L) have no polymerized microtubules (arrows) and in a minority of the cells only a few acetylated microtubules persist (arrowheads). Bar (A-F) = 30μm and Bar (G-L) = 10μm.

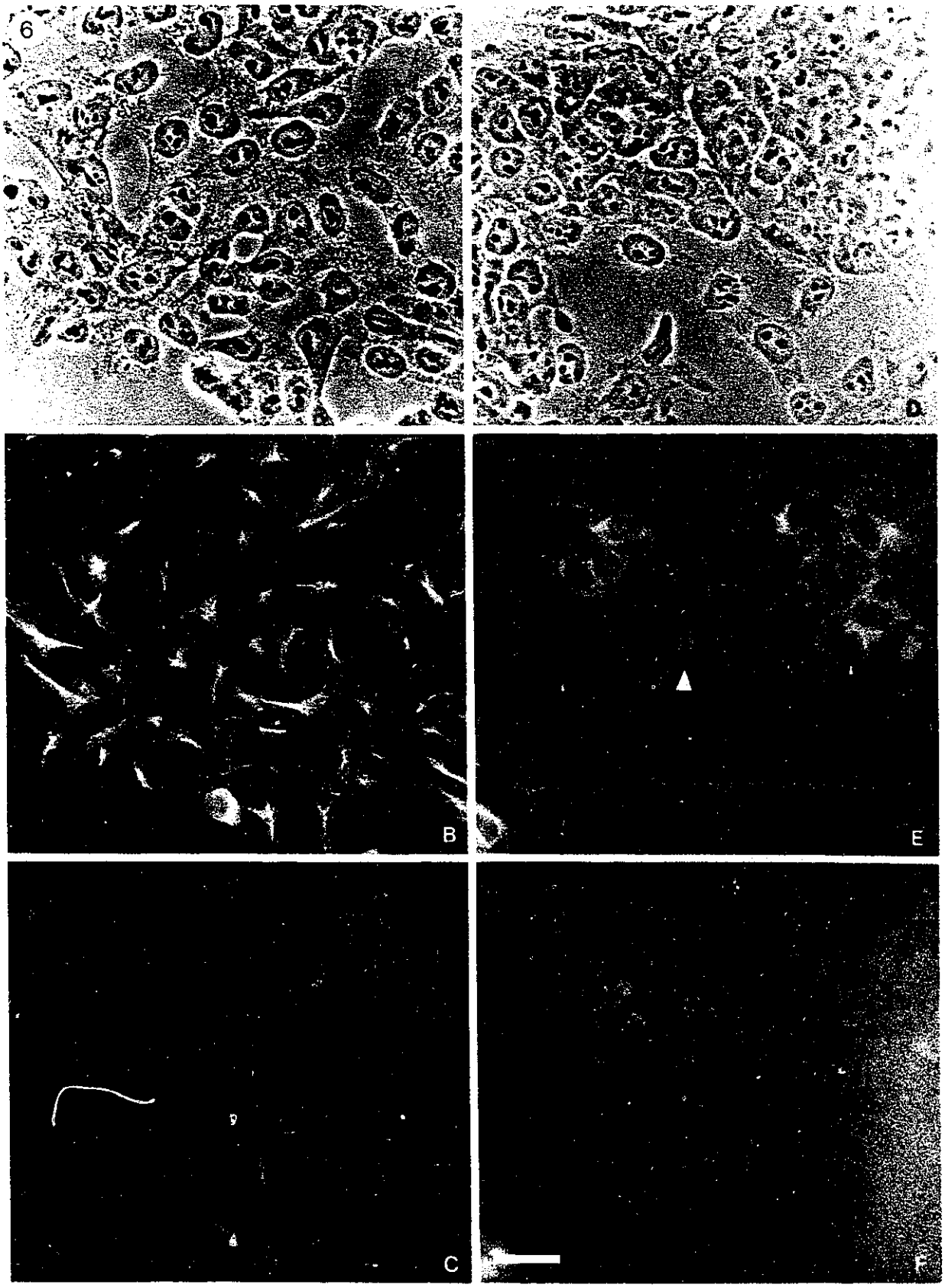
6
B
C
D
E
F

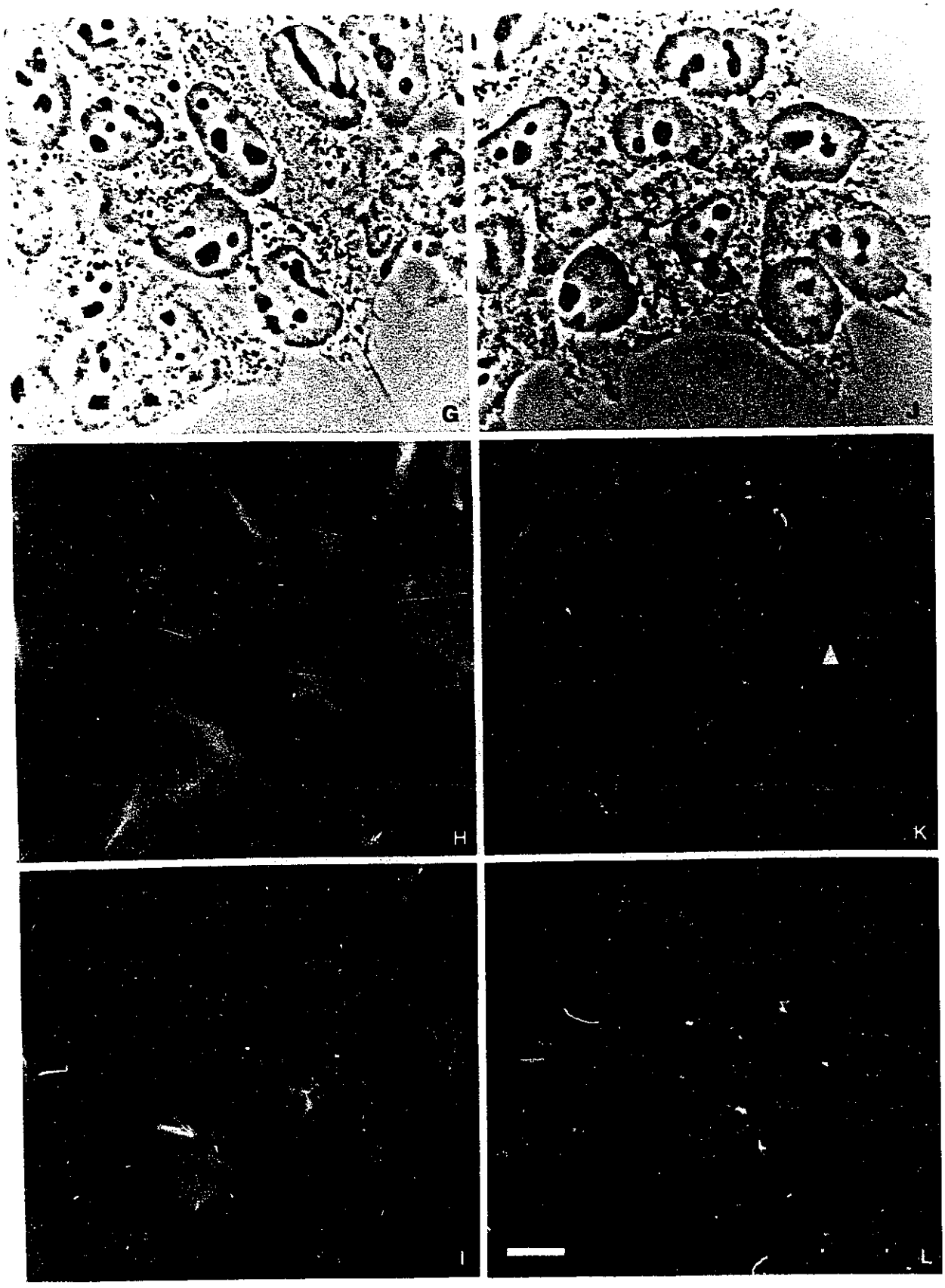
G
J
H
K
I
L

Fig. 7: **Microtubule Arrays in One Day Neurally-Induced P19 Cells.** Phase contrast (A,D,G,J,M,P), total tubulin stained with YOL 1/34 antibody (B,E,H,K,N,Q), and acetylated tubulin stained with 6-11B-1 antibody (C,F,I,L,O,R) showing cell morphology and microtubule arrays. After neural induction, there is still no change in overall cell morphology and many cells have microtubule arrays similar to undifferentiated cells (A-C,G-L). A subpopulation of cells has MT arrays that are organized into bundles (arrows in B,C,K,L). After colchicine treatment (D-F,M-R) only some cells have stable microtubule arrays that are acetylated (arrows in F,O,R), while many do not have microtubules (arrowheads in E,Q). Bar (A-F) = 30 μm and Bar (G-R) = 10 μm.

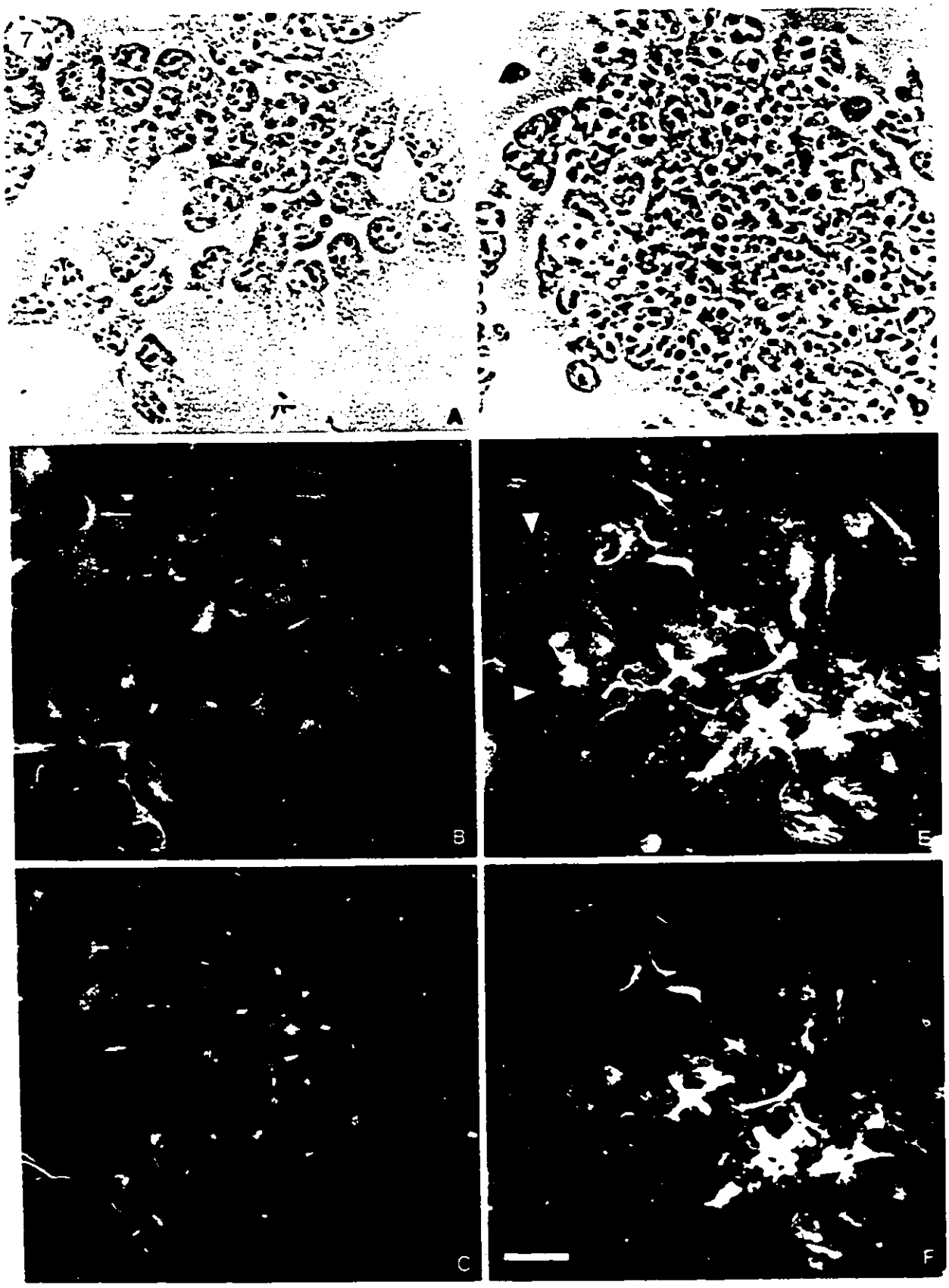
A
B
C
D
E
F

G
H
I

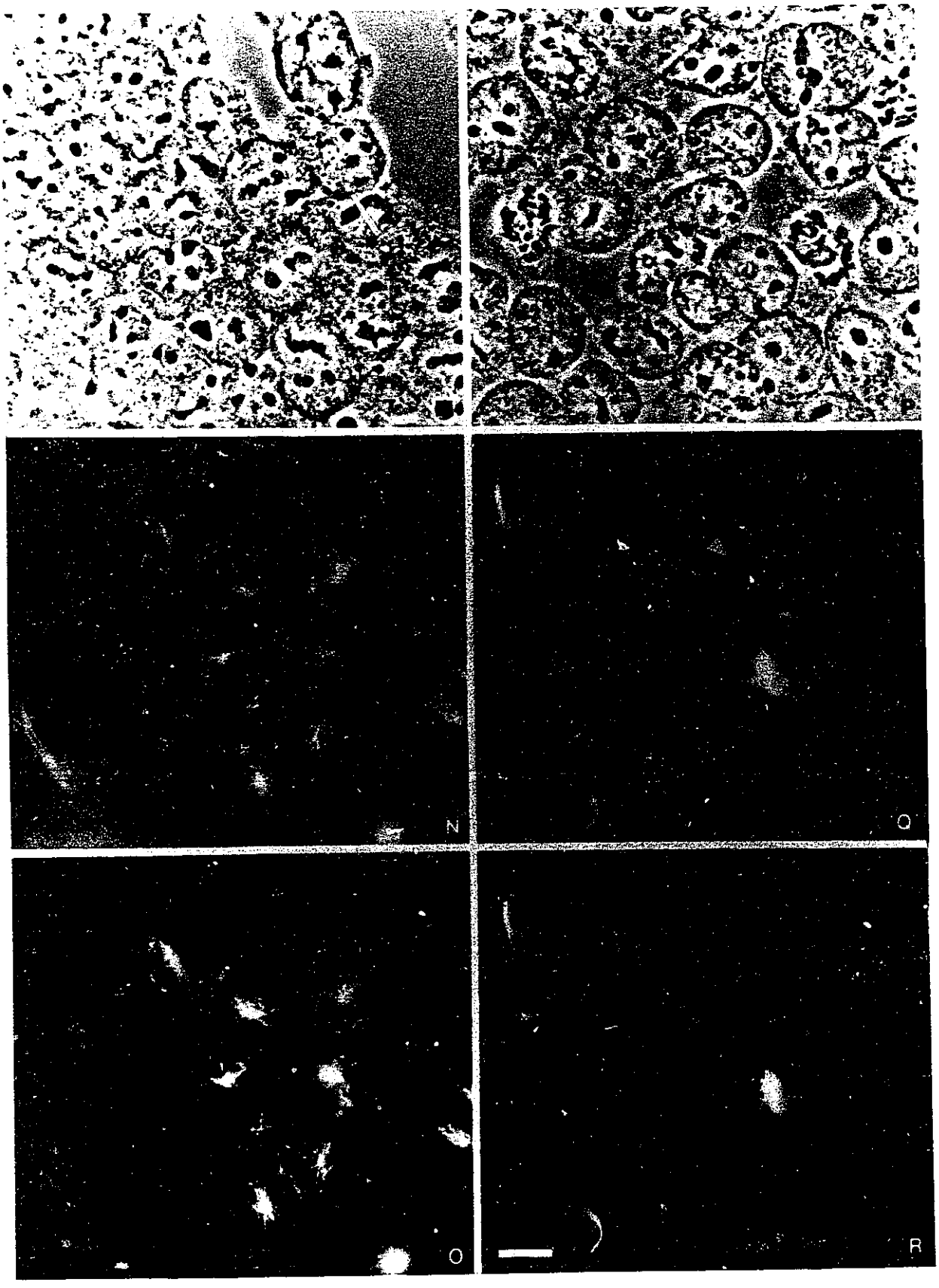
P
N
O
O
R

B) Quantitative Immunoblotting

Total tubulin and acetylated-tubulin levels were analyzed quantitatively by western immunoblotting and detected by ^{125}I-labelled secondary antibodies in whole cell extracts, MT polymer extracts and colchicine-stable MT polymer extracts of undifferentiated and one day neurally-induced EC cells. DNA measurements in all extracts were made using a fluorescence-based assay in an attempt to detect changes in total tubulin and relative acetylated tubulin levels per some constant cell number. Western blotting of PC-Tubulin provided internal standards for densitometric quantification.

Figure 8 shows that although there is no significant difference in the levels of total tubulin in whole cell protein, there is a slight statistically significant increase in the level of tubulin in polymers during early neural differentiation ($p > 0.05$). No significant increase in the amount of tubulin in the colchicine-stable MT extracts was detected after neural induction.

In contrast to the total tubulin levels, the relative levels of ACET tubulin (Fig. 9) however increased approximately two-fold in all of the extracts following neural induction. Unexpectedly, there was no selective incorporation of ACET tubulin into the colchicine stable-MT extracts ($p < 0.05$).

Fig. 8: **Tubulin Levels in Neurally-Induced P19 Cells.** Extracts of whole cell proteins, untreated microtubule polymers, and colchicine-stable microtubule polymers were submitted to electrophoresis and immunoblotted. Quantification of tubulin was accomplished using the DM1B anti-tubulin antibody followed by ^{125}I-labelled secondary antibody and densitometry. (See Materials and Methods for details). Bars represent standard errors.

8

Tubulin Levels in Neurally-induced P19 Embryonal Carcinoma Cells

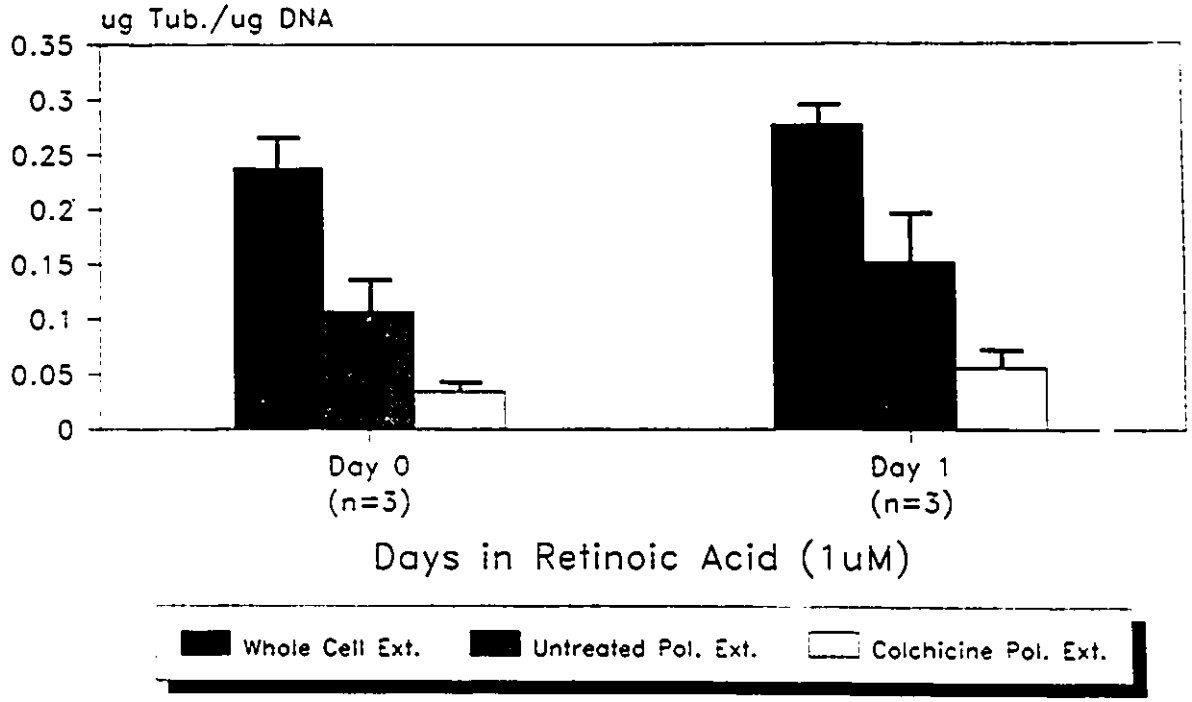

Fig. 9: **Relative Acetylated Tubulin Levels in Neurally-Induced P19 Cells.** Relative levels of acetylated tubulin were determined using the 6-11B-1 antibody followed by ^{125}I-labelled secondary antibody and densitometry. (See Materials and Methods for details). Bars represent standard errors.

9

Relative Acetylated-Tubulin Levels in neurally-induced P19 cells

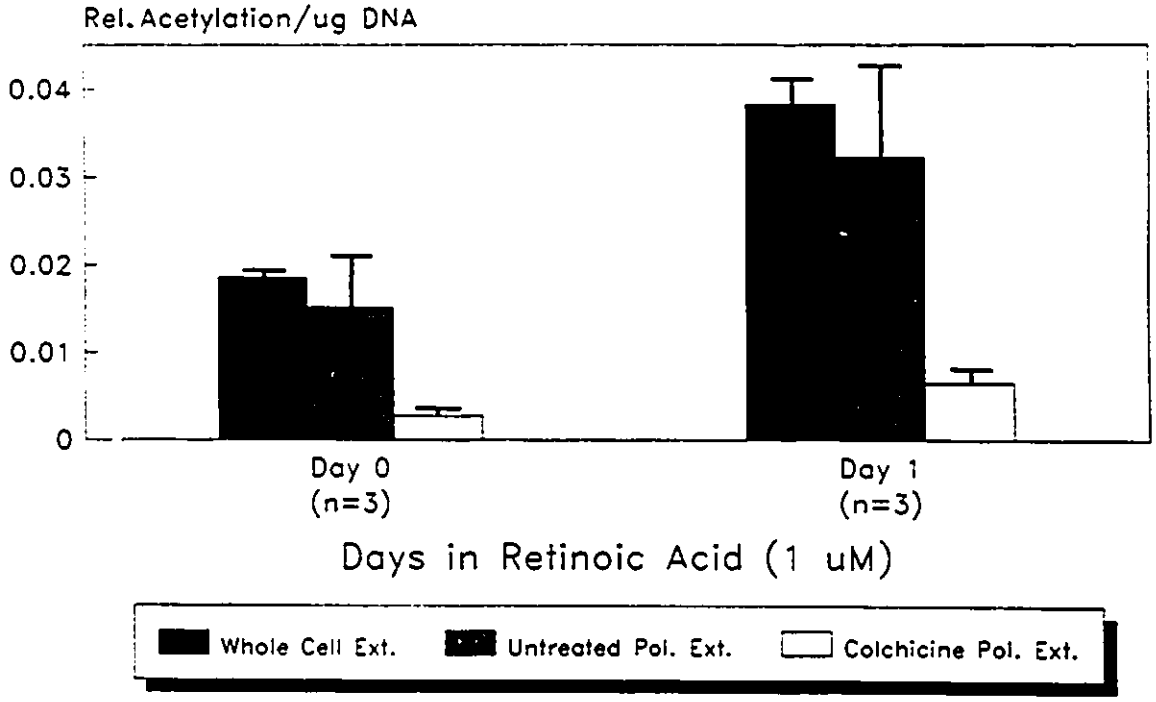

II. Tubulin Purification and Biotinylation

MT protein was purified from beef brain by temperature-dependent cycles of assembly/disassembly. Typically, from a beef brain wet weight of 500 grams, the yield of MT protein in the S3 fraction (see Materials and Methods) after two cycles of assembly/disassembly varied between 1.8 to 2.0 gm. Fig. 10 illustrates the progress of tubulin purification on an SDS-polyacrylamide gel stained with Coomassie Blue. Prior to loading onto the phosphocellulose column, the S3 fraction was cycled once more. As MT protein preparations were cycled, some high molecular weight proteins were detected to co-purify with tubulin. These proteins were eluted by increasing the ionic strength of the column buffer (Fig. 11) and were identified as microtubule-associated proteins (MAPs) by immunoblotting (Fig. 12).

PC-Tubulin was biotinylated to serve as a labelled probe for assaying MT turnover in EC cells. Biotin-tubulin (B-Tb) was first detected by immunoblotting (Fig. 13). From a starting amount of 22.8 mg PC-Tubulin, a total of 2.064 mg of labelled protein was recovered.

Fig. 10: **SDS Gel Electrophoresis of Tubulin Purification from Beef Brain by Cycles of Assembly/Disassembly.** 20μg of protein was loaded in each lane. S1, S2, S3 and S4 are cold supernatants in the progressive purification procedure. The S4 fraction was applied to a phosphocellulose (PC) column to separate tubulin from microtubule-associated proteins (MAPs).

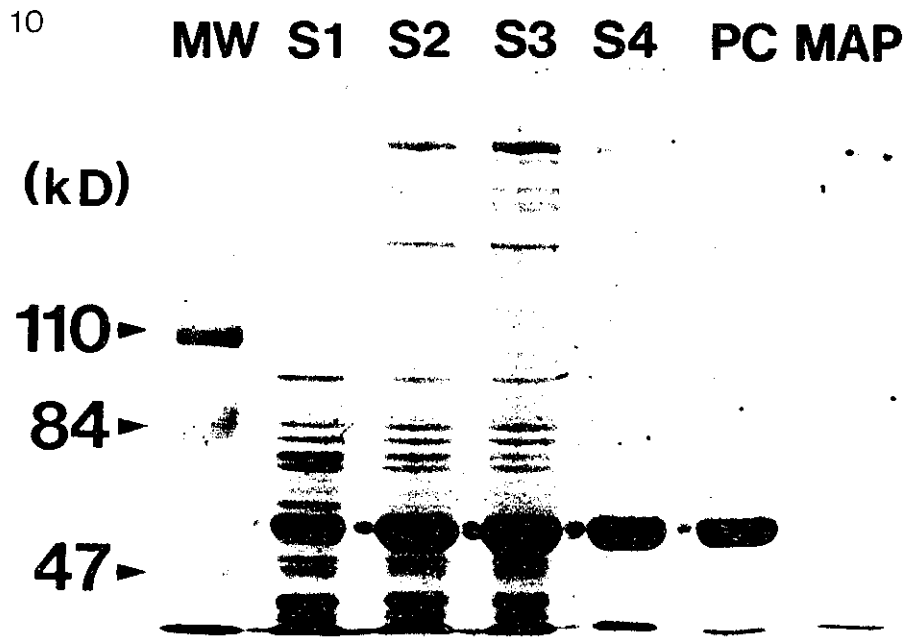
10
MW
S1
S2
S3
S4
PC
MAP
(kD)
110
84
47

Fig. 11: **Elution Profile of Microtubule Proteins purified by Phosphocellulose Chromatography.** Tubulin protein always eluted at Peak #1. MAPs eluted at Peak #3. Peak #2 is assumed to be GTP, that was present in the column buffer.

Phosphocellulose Column Scan of Microtubule Proteins

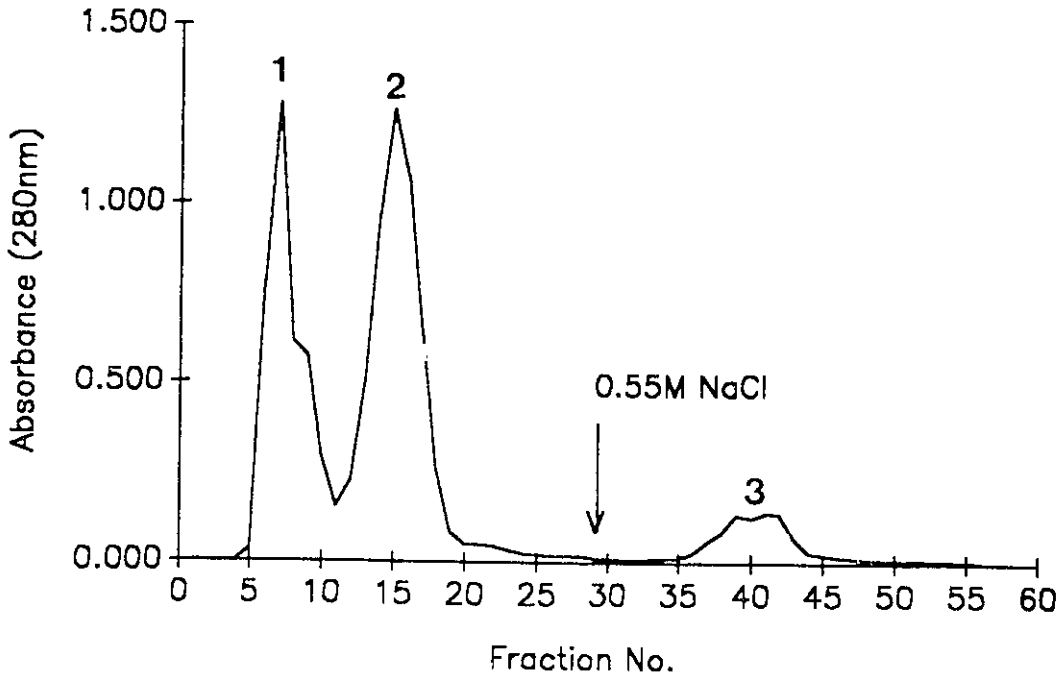

Fig. 12: **Western Blot of MAPs.** The MAP fraction (Peak #3; Fig. 12) was electrophoresed and transferred to a nitrocellulose membrane. MAPs were detected using the anti-MAP antibodies indicated followed by the appropriate biotinylated secondary antibodies. (See Materials and Methods for details). This fraction did not contain any tubulin (tub) as visualized by the absence of immunoreactivity to the 5A6 anti-tubulin antibody.

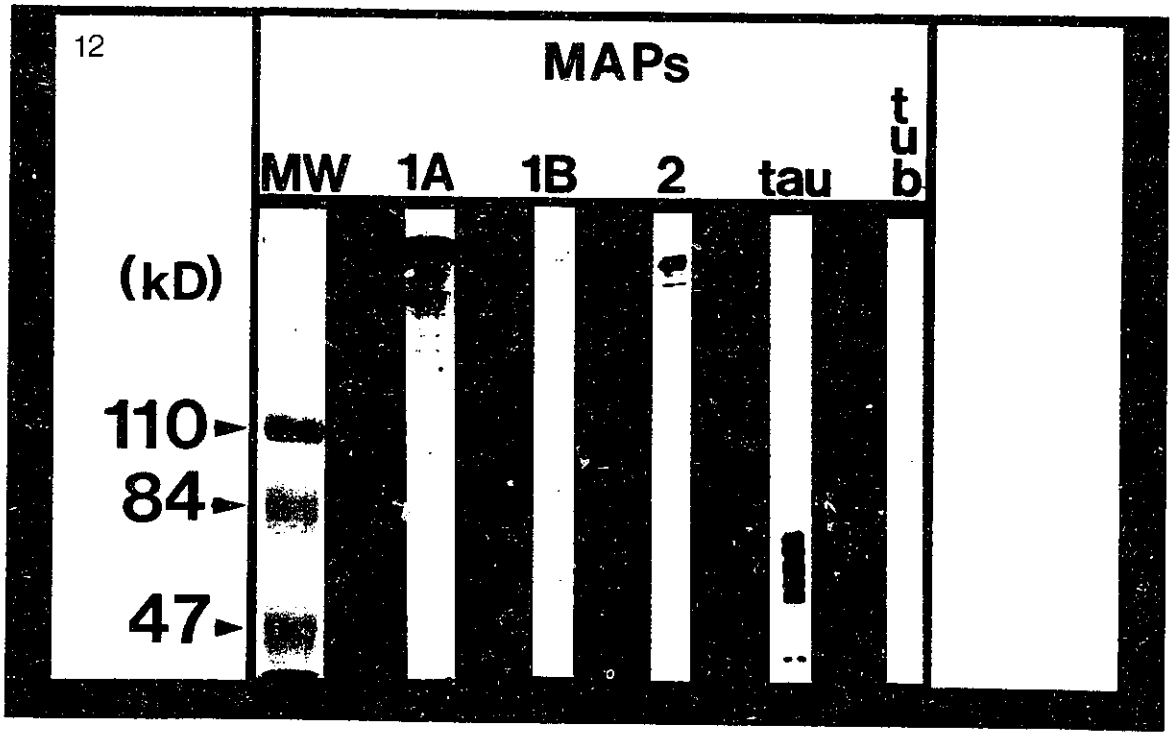
12
MAPs
MW
1A
1B
2
tau
tub
(kD)
110
84
47

Fig. 13: **Western Blot of Biotinylated Tubulin.** Phosphocellulose-purified tubulin (PC), and biotinylated tubulin (B-Tb) in PIPES buffer (P) or microinjection buffer (M) was electrophoresed and transferred to a nitrocellulose membrane. B-Tb was detected colorimetrically using the Streptavidin-Horseradish peroxidase system.

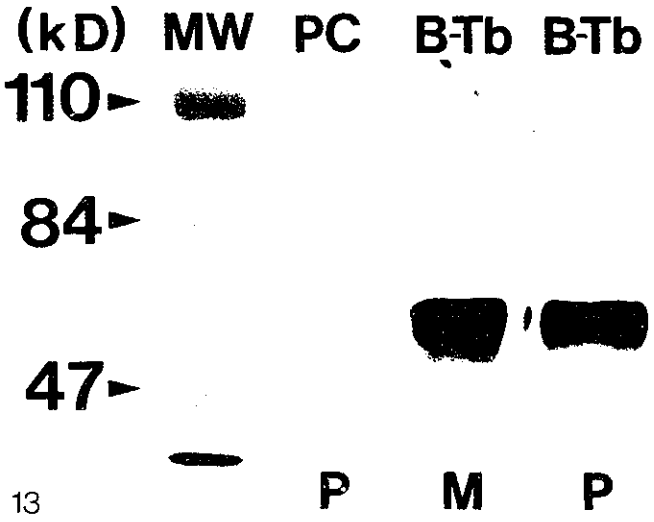

13

III. In Vitro MT Assembly Experiments

The assembly competence of B-Tb was tested by polymerizing it with PC-Tubulin at varying ratios, off ciliary axonemes isolated from Tetrahymena. It was necessary to determine if the B-Tb interferes with assembly of unmodified tubulin. The final tubulin concentration for assembly was 1.3mg/mL. Length measurements of MTs polymerizing from the "plus" end and the "minus" end of axonemes are shown in Table 1. See Fig. 14 for identification of growth polarity of MTs polymerizing off axonemes. Fig. 15 illustrates the detection of B-Tb polymerizing off axonemes by immunogold electron microscopy. Statistical analyses have shown that the mean MT lengths between the various B-Tb:PC-tubulin molar ratios were significantly different from those polymerized with PC-Tubulin alone (TUKEY test, $p < 0.0005$). What is significant is that lower molar ratios of B-Tb:PC-Tubulin produced MT lengths that were greater than those MTs polymerized from higher molar ratios.

Table 1: In Vitro Assembly of Biotin-Tubulin off Axonemes.

		Treatment				
		[1]PC-Tubulin	[2]B-Tb (1:9)	B-Tb (1:4)	B-Tb (1:1)	B-Tb (1:0)
"PLUS" END MICROTUBULE ASSEMBLY	n	116	103	102	59	52
	Mean Length (μm)	4.39	3.51	3.02	1.71	1.15
	Stdn. Err. (μm)	0.13	0.11	0.11	0.11	0.06
"MINUS" END MICROTUBULE ASSEMBLY	n	84	68	49	21	16
	Mean Length (μm)	0.69	0.51	0.36	0.22	0.18
	Stdn. Err. (μm)	0.03	0.02	0.04	0.03	0.03

[1]PC-Tubulin = phosphocellulose-purified tubulin (1.3mg/mL).

[2]B-Tb = biotinylated tubulin (ratios in parentheses indicate mixtures of B-Tb to PC-Tubulin at a final concentration of 1.3mg/mL).

Fig. 14: **Microtubule Growth off Axonemes.** Exogenous tubulin (1.3 mg/ml) was added to ciliary axonemes isolated from Tetrahymena to test the assembly competence of PC-tubulin. The " + " end has more microtubule assembly than the " - " end. Bar = 0.5 μm.

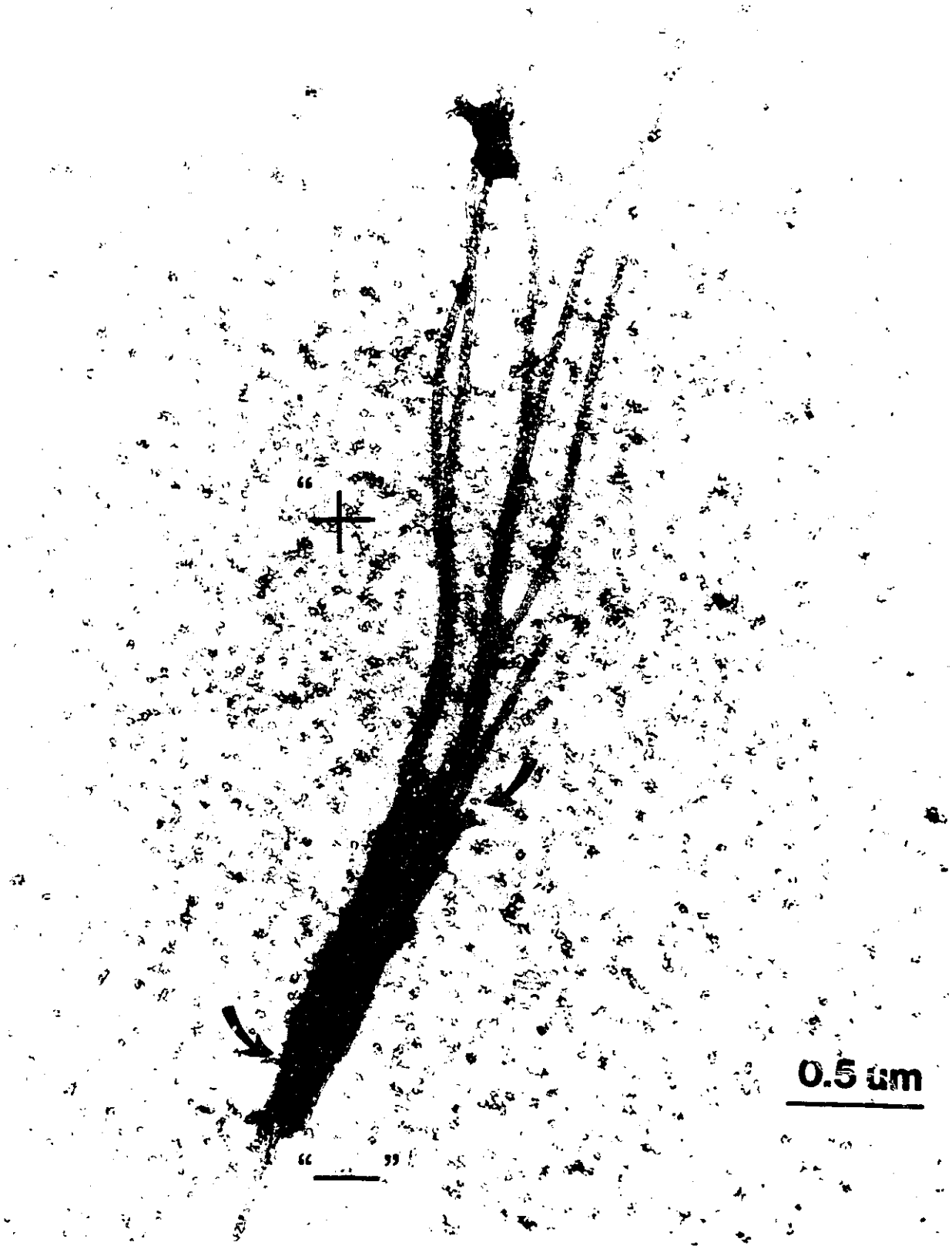
0.5 µm

Fig. 15: **Polymerization of Biotin-Tubulin off Axonemes.** Assembly of molar ratios of Biotin-Tubulin:PC-Tubulin at 0:1 (A,B); 1:9 (C,D,E); 1:4 (F,G); 1:1 (H,I,J,K); and 1:0 (L,M) off Axonemes. Detection of biotin-tubulin (small arrows) polymerizing off axonemes (arrowheads) was by immunogold labelling with rabbit anti-biotin antibodies followed by 10 nm colloidal gold-conjugated goat anti-rabbit antibodies. (See Materials and Methods for details). Bars (A, C-E, I-M) = 1 μm and (B,F,G,H) = 0.5 μm.

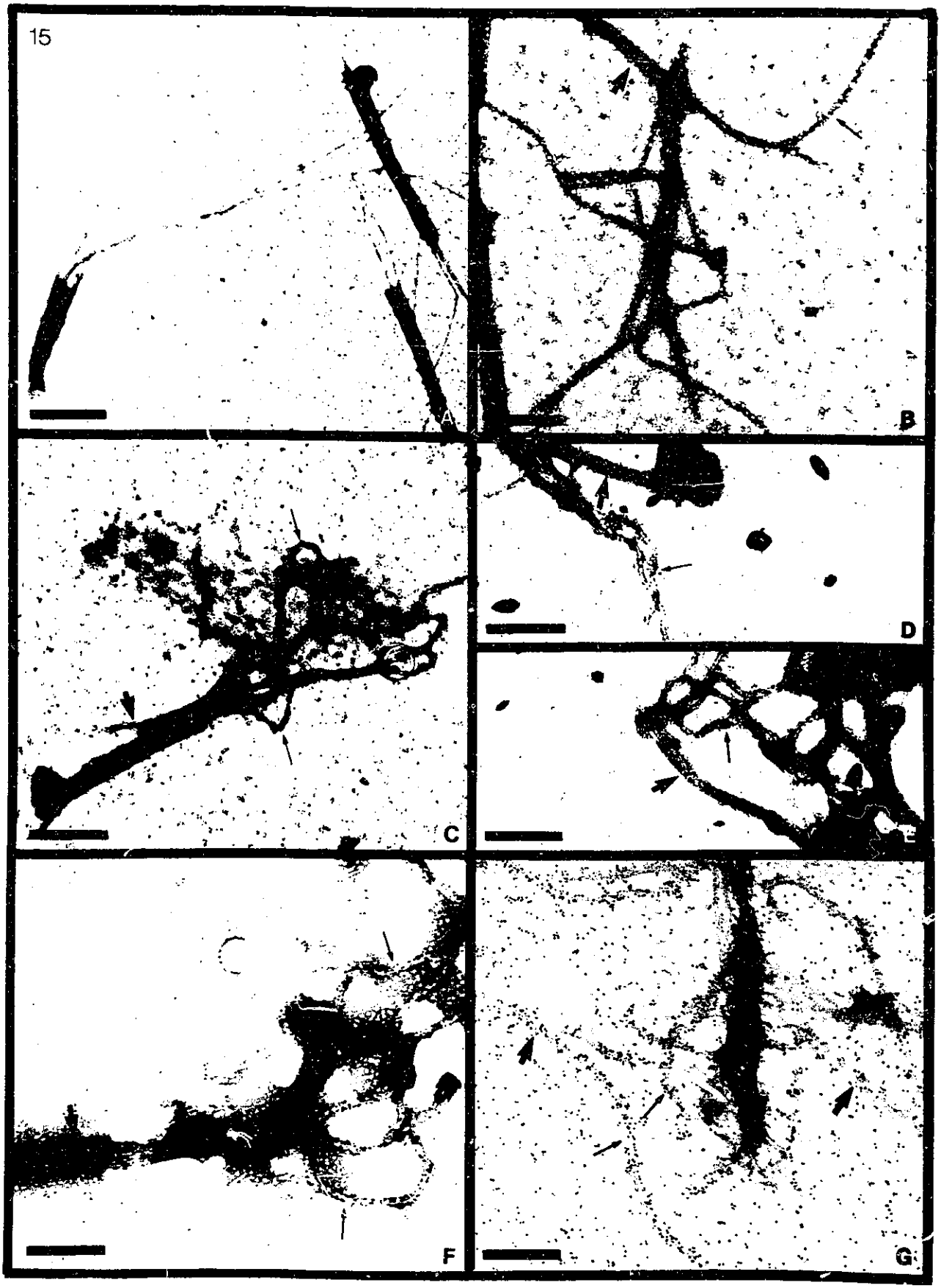
15
A
B
C
D
E
F
G

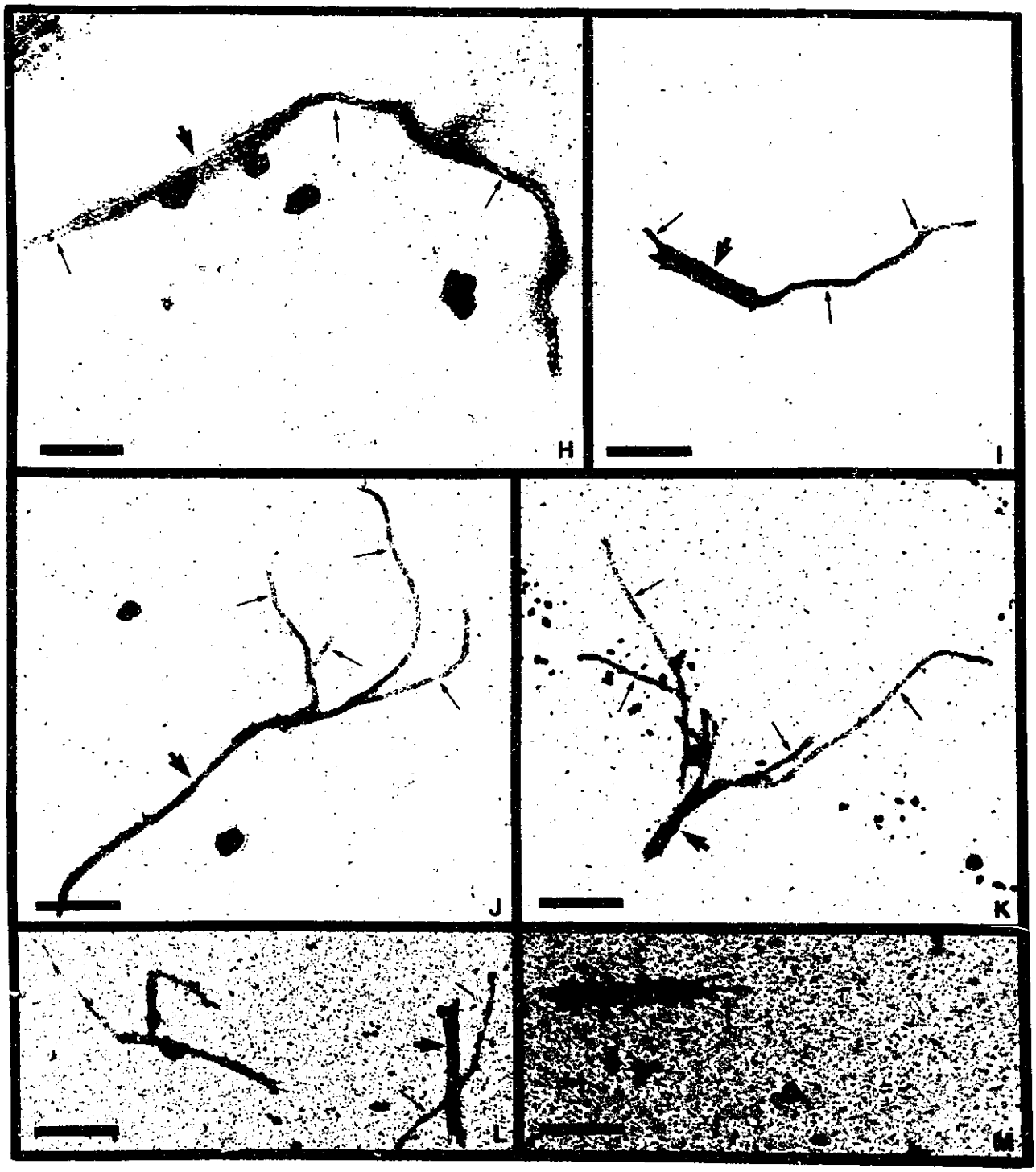
H
I
J
K
L
M

IV. Microinjection Technique

A) Microinjection of Pt K2 Cells

Pt K2 cells were microinjected with the 5A6 anti-tubulin antibody to learn the technique and to see if the MT array could be kept intact after the trauma of injection. The MT network was not altered in microinjected cells compared to control uninjected Pt K2 cells if the pressure used for microinjection was less than 60 hPa (see Fig. 16). Higher pressures that did not cause cell lysis did, however, result in the disruption of the MT array and in some instances fragmented MTs were observed.

B) Microinjection of EC Cells

Microinjection of EC cells proved to be a much more difficult task. Many cells cultured on untreated coverslips either lysed, lifted off upon the entry of the needle, or had fragmented MT arrays when microinjected (Fig. 17B,b,C,c). When access to the cytoplasm for injection was difficult, the nuclei were injected (Fig. 17B,b).

To overcome these obstacles, EC cells were cultured on 0.1% gelatin-coated coverslips to promote spreading and adhesion to the coverslip. EC cells, in contrast to flat cells such as Pt K2 cells, have a round morphology and, therefore, the angle of microinjection had to be increased to approximately 60° for a cleaner entry and withdrawal of the needle from the cell.

Fig. 16: **Microinjection of Pt K2 Cells with the 5A6 Anti-Tubulin Antibody.** (A) 5A6 anti-tubulin staining of control uninjected cells showing intact microtubule arrays. A secondary antibody staining control was performed in uninjected cells (B) to evaluate the extent of background. Microinjection of Pt K2 cells was performed at 100 hPa (C), 80 hPa (D), 60 hPa (E), and 40 hPa (F). At higher injection pressures the extent of fragmentation of the microtubule array is greater than in those cells microinjected with lower injection pressures. Bar = 10 μm.

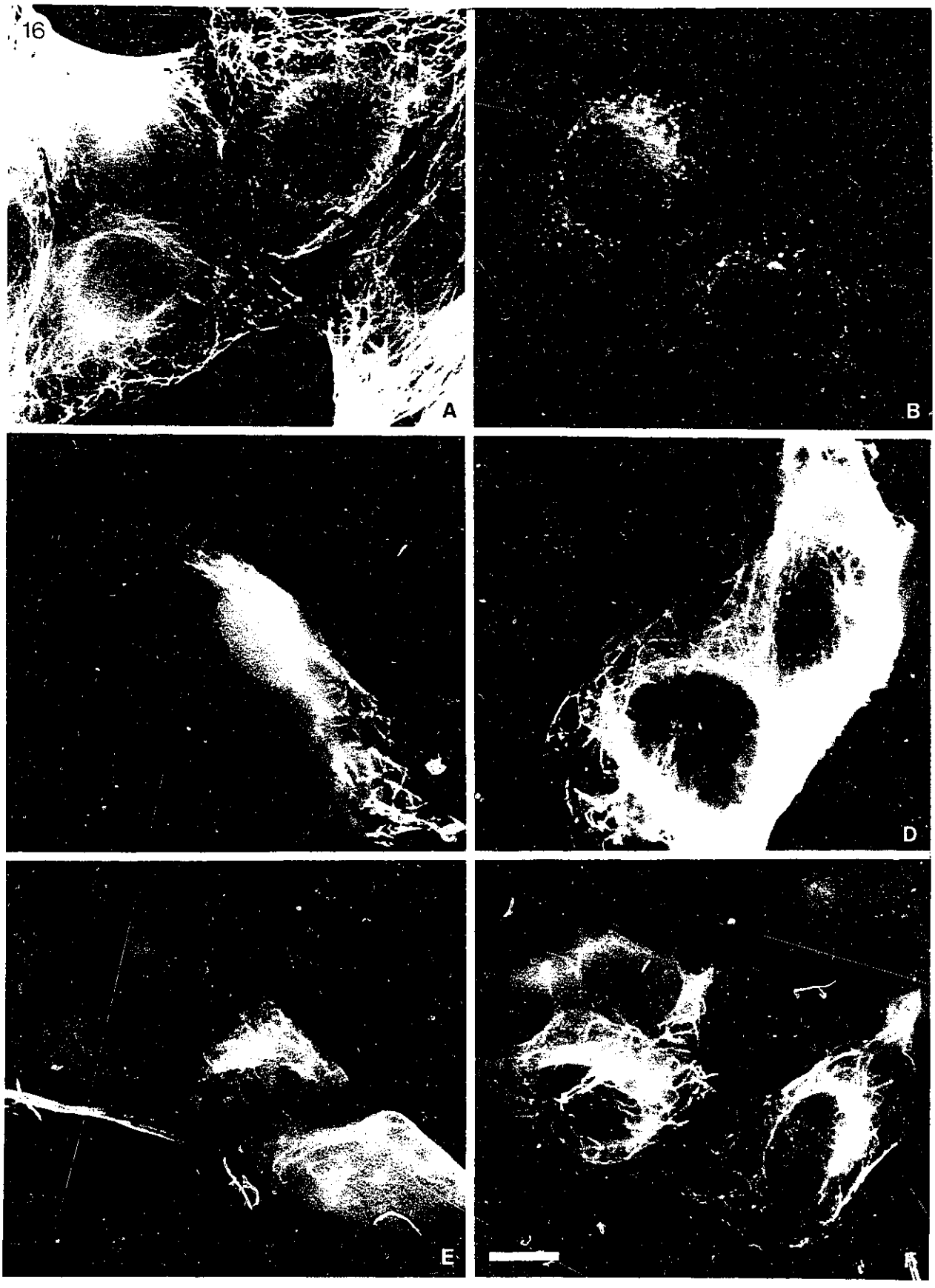
16
A
B
D
E

Fig. 17: **Microinjection of P19 EC Cells with the 5A6 Anti-Tubulin Antibody.** (A-F) 5A6 anti-tubulin staining, (a-f) Phase contrast images. (A,a) 5A6 anti-tubulin staining of control uninjected cells show intact microtubule arrays. Unsuccessful injections occurred frequently (B,b,C,c) when EC cells, cultured on uncoated coverslips, were microinjected at lower angles. Often, the microinjected antibody was detected in the nucleus instead of in the cytoplasm (arrow in B). Disruption of the microtubule array (C) also occurred frequently. Successful microinjections were performed using higher angles for injection and culturing cells on gelatin-coated coverslips (D,d,E,e,F,f). Examples of successful injections into interphase (D,d), anaphase transition (E,e) and telophase (F,f) cells are shown. Bars throughout = 10 μm.

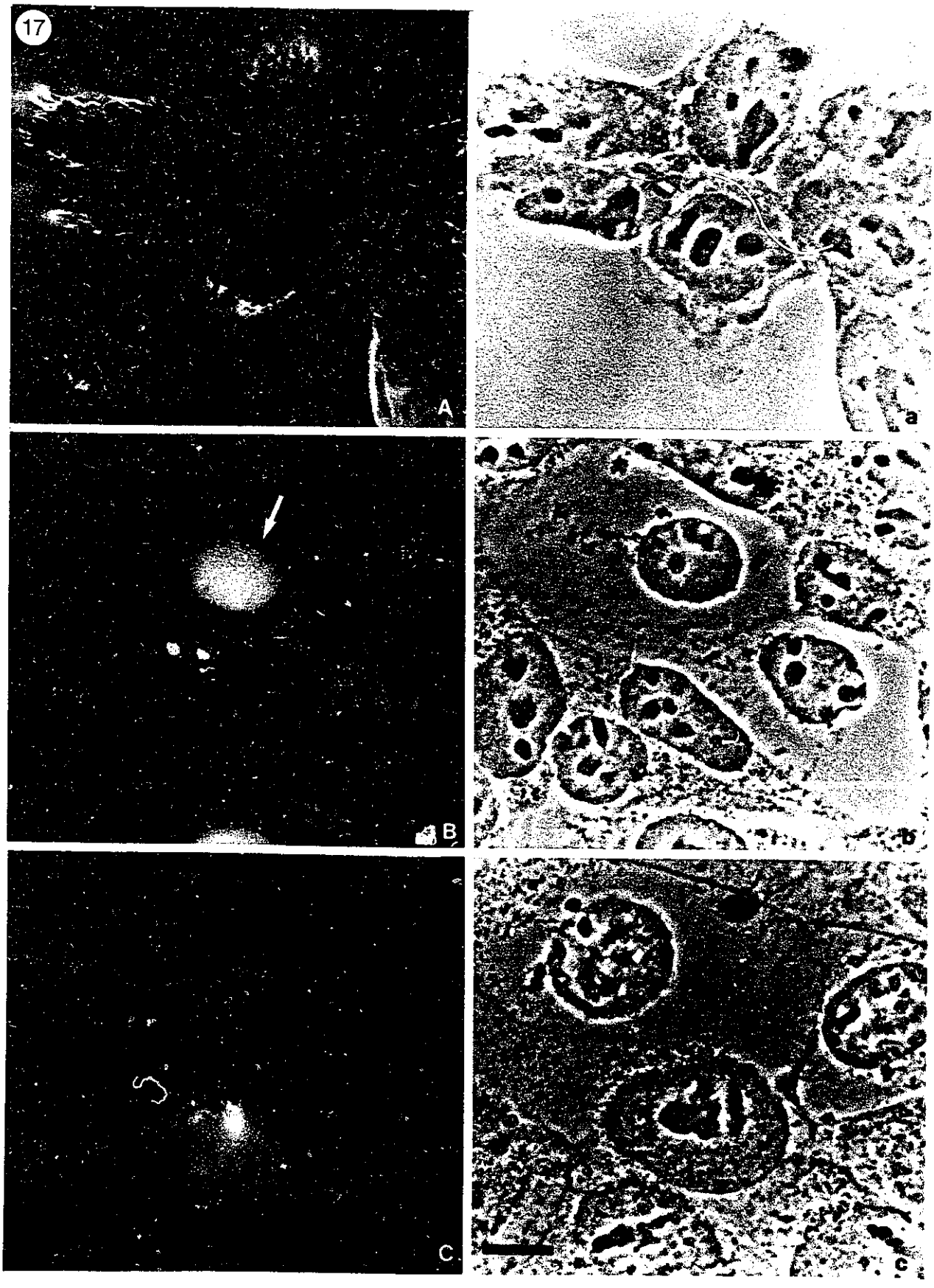
17
A
a
B
b
C
c

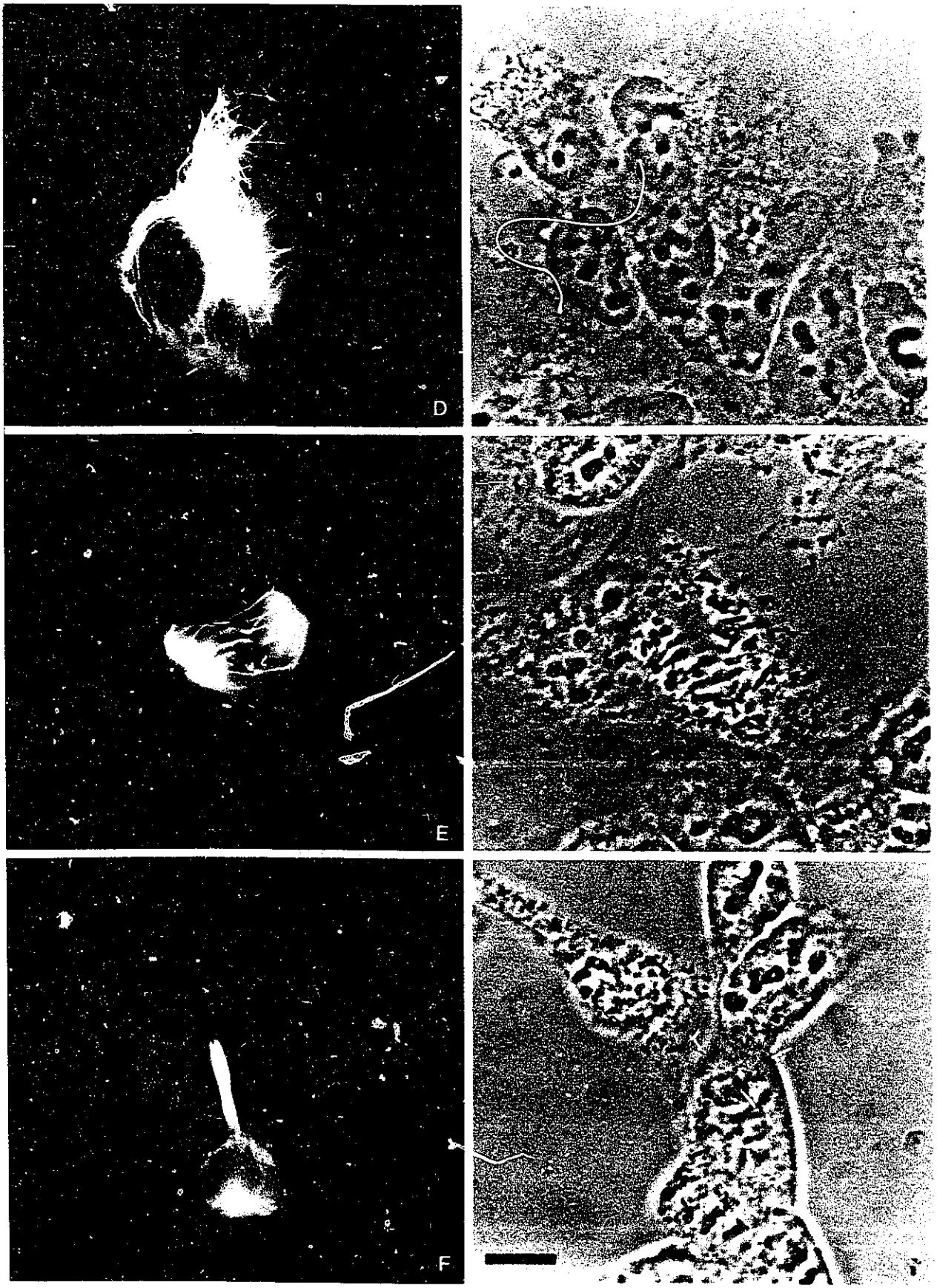
D
E
F

V. Microinjection of B-Tb in L6E9 Cells

Fig. 18 illustrates the incorporation of B-Tb microinjected at a concentration of 2.39 mg/ml into L6E9 cells. At one minute after injection (Fig. 18B,b,C.c), B-Tb is seen to incorporate at the distal ends of growing MTs. Two minutes (Fig. 18D,d) and five minutes (Fig. 18E,e) after injection the length of growing MTs is increasing. By 10 minutes MT turnover is not complete and growing MTs can still be identified (see arrows in Fig. 18F,f). By 15 minutes (Fig. 18G,g) and 20 minutes (Fig. H,h) the incorporation of B-Tb is greater. By 30 minutes (Fig. 18I,i) most of the MT array has turned over. These observations are consistent with those made on other established cell lines Schulze and Kirschner (1986). These results indicated that the B-Tb probe is assembly competent in vivo, and was then used to analyze MT turnover in EC cells.

VI. Video Microscopy

A) Image Averaging

Unaveraged images, initially grabbed by the optical digitizer (the frame grabber boards), appeared noisy when viewed on the video monitor. This is illustrated in phase contrast and fluorescent images in Fig. 19. Compare unaveraged images in Fig. 19A,C and E, with their averaged counterparts in Fig. 19B,D and F, respectively. The background noise was reduced by accumulating and averaging the last successive 32 digitized images, prior to terminating the integration program. After averaging, more detail and information of the original optical image was revealed.

Fig. 18: **Microinjection of Biotin-Tubulin in L6E9 Cells.** Anti-biotin staining (A-I) and 5A6 anti-tubulin staining (a-i) show the incorporation of biotin-tubulin (B-Tb) into the existing microtubule array at 1 minute (B,b,C,c), 2 minutes (D,d), 5 minutes (E,e), 10 minutes (F,f), 15 minutes (G,g), 20 minutes (H,h) and 30 minutes (I,i) after microinjection. Control uninjected cells are shown in (A) and (a). At shorter time intervals after injection, B-Tb is seen to incorporate at the ends of growing microtubules (arrows throughout). At longer times, the incorporation of B-Tb is greater and by 30 minutes after injection, most of the microtubule array has turned over. Bars throughout = 10 μm.

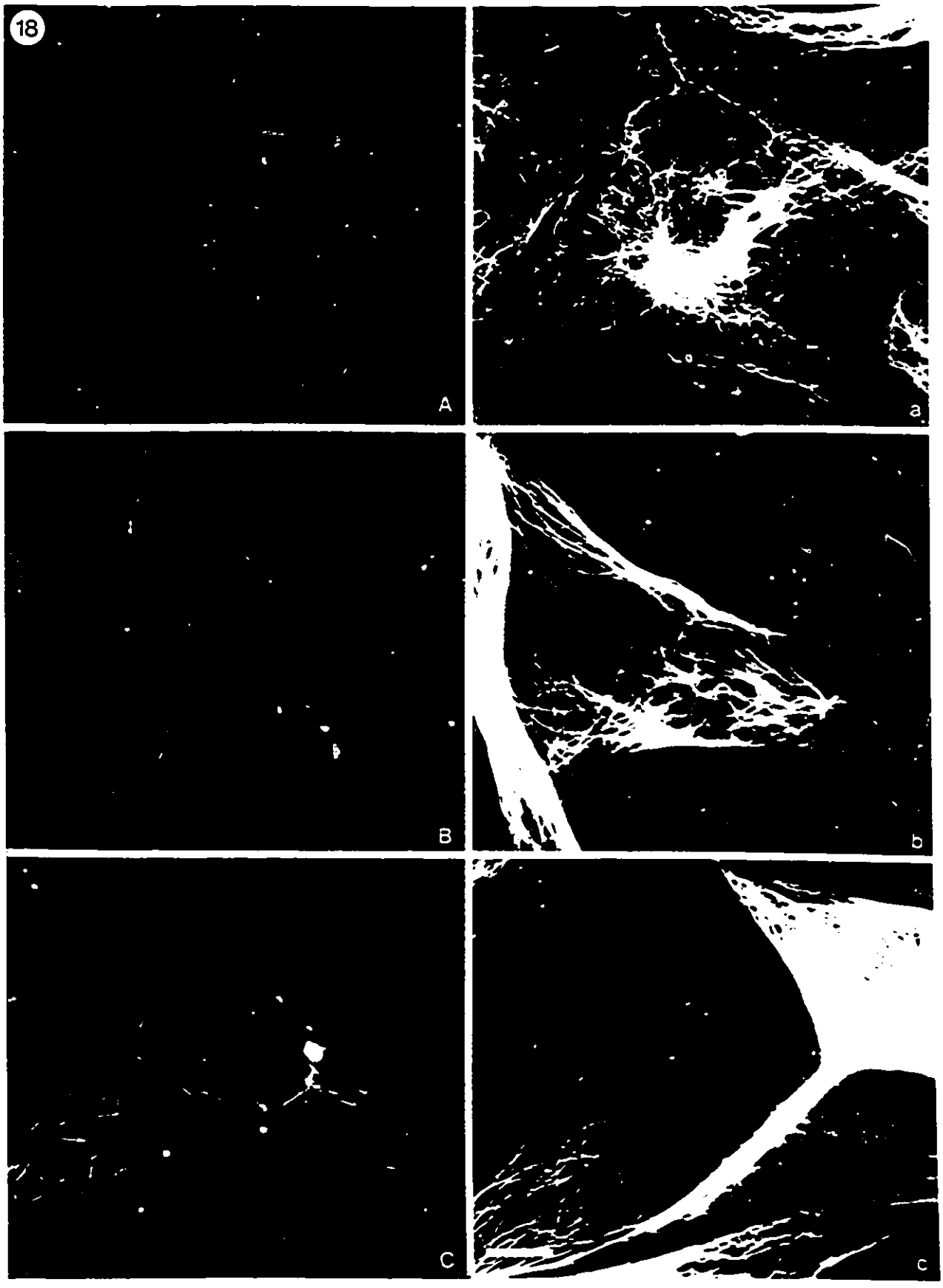
18
A
a
B
b
C
c

D
E
F

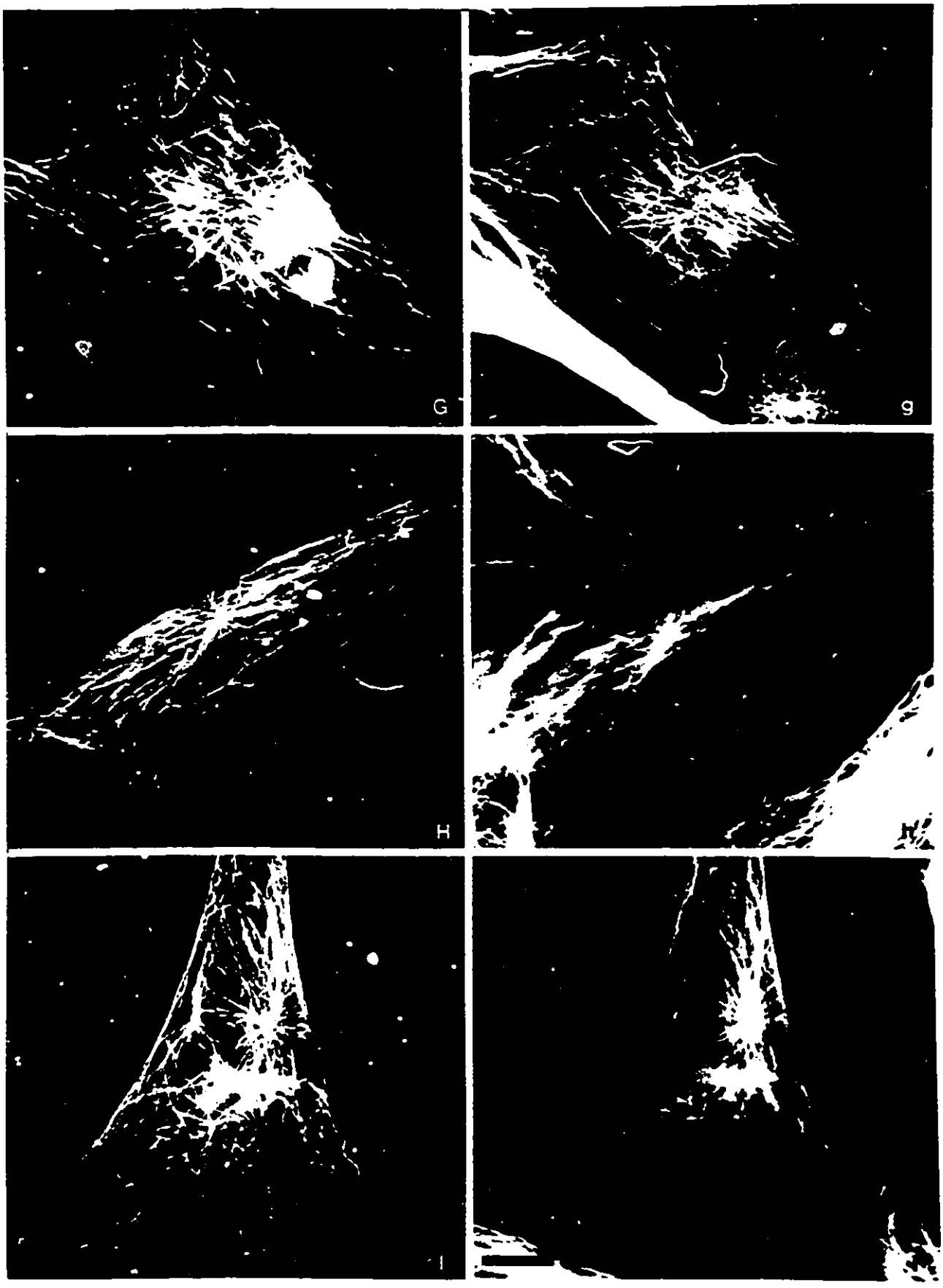
G
g
H
I

Fig. 19: **Image Averaging of Phase Contrast (A-D) and Fluorescent Images (E,F) in EC cells.** Compare unaveraged images (A,C,E) with their averaged counterparts (B,D,F) respectively. Note that after averaging, the signal-to-noise ratio dramatically increases. Bar in (B) = 30μm. Bar in (F) = 10μm.

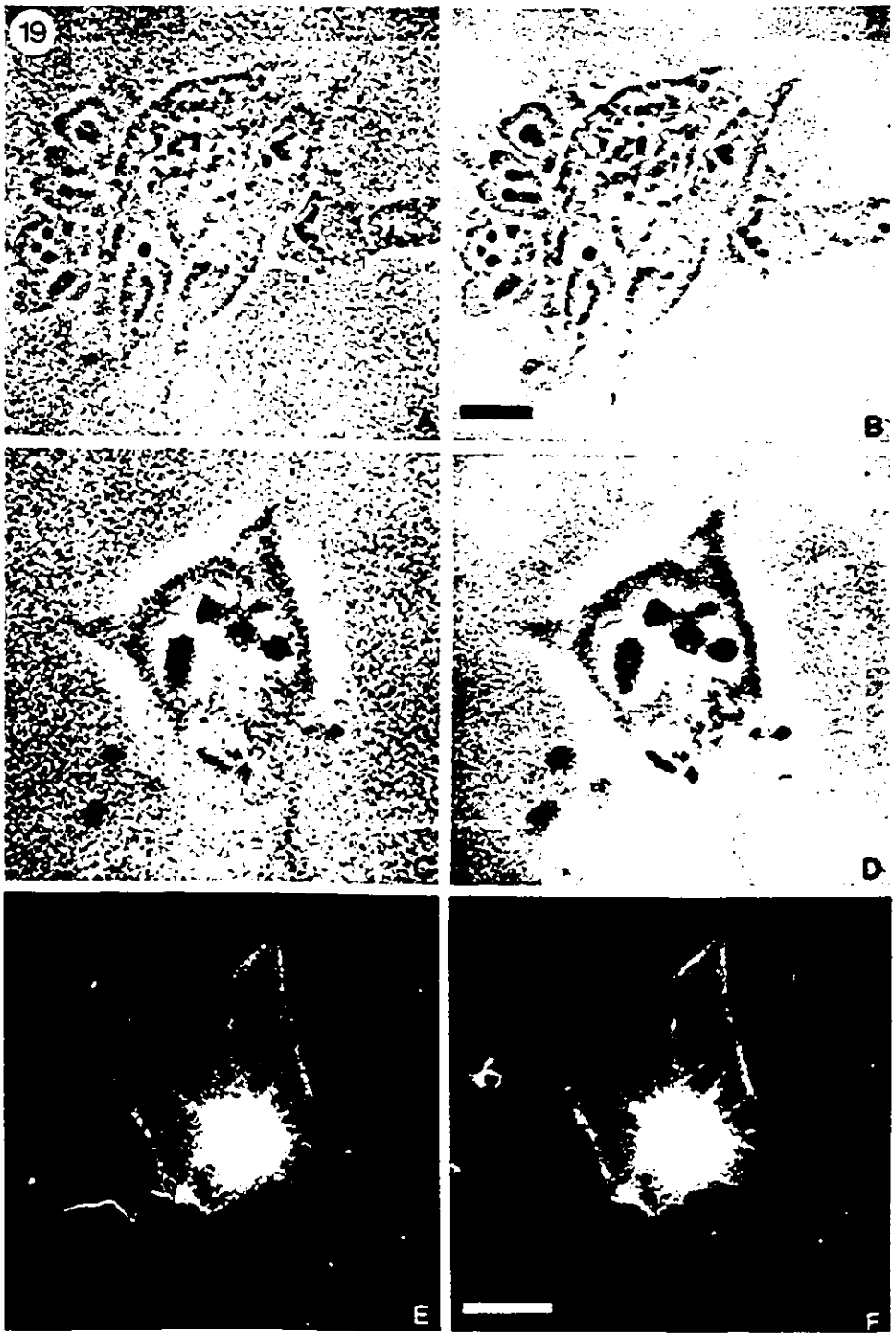
19
A
B
C
D
E
F

B) Image Processing

An averaged digital image was further processed to improve the quality and enhance contrast. Fig. 20 illustrates some methods by which an averaged fluorescent image of MTs in EC cells was processed. The Run Contrast program used on the averaged image illustrated in Fig. 20B improved the quality of the image (Fig. 20C), however, MTs were not clearly resolved in the centre of the cell. When the averaged image was deconvoluted (Fig. 20D), there was a slight increase in noise, but individual MTs were more clearly resolved than in Fig. 20C. To improve the quality of the digital image even further, the Run Contrast and Deconvolution programs were applied in combination to the averaged image. Fig. 20E represents the image that was contrasted first and then deconvoluted, whereas Fig. 20F is the image that was deconvoluted first, and then subjected to the Run Contrast operation. Although both images are significantly better than those manipulated by contrast or deconvolution alone, Fig. 20F has the best resolution. Towards the centre of the cell, there is still an oversaturation of grey levels, but it has been markedly reduced.

Fig. 20: **Digital Image Processing of Fluorescent Images in an EC cell by Grabbing (A), Averaging (B), Contrast (C), Deconvolution (D), Contrast/Deconvolution (E) and Deconvolution/Contrast (F).** Note that deconvolution (D) provides more resolution than contrast alone (C). Manipulations in (E) and (F) significantly improve the quality of the video image but the latter displays better resolution and gives more information. Bar = 10μm.

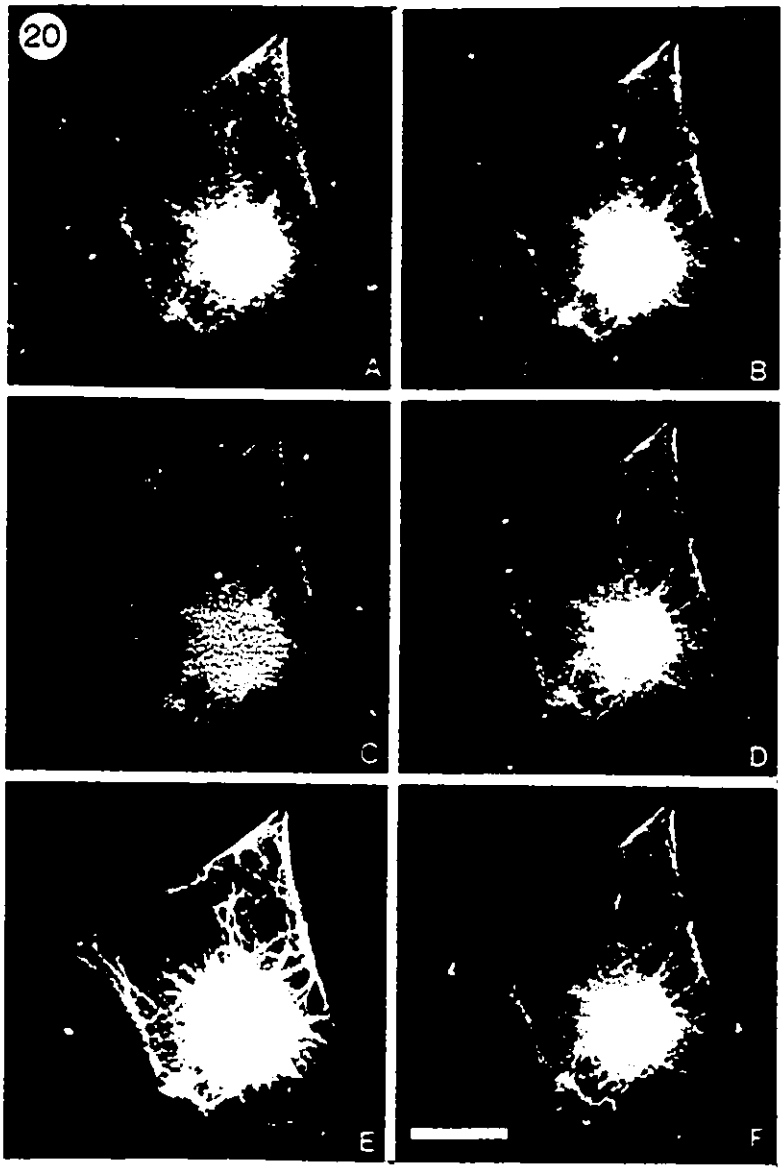
20
A
B
C
D
E
F

C) Tracing of Microtubules

Fig. 21 is a tutorial that illustrates the step-by-step procedure for tracing MTs. See Materials and Methods for details. For illustration purposes only, the background fluorescence was eliminated from the digital image of the first focal plane (Fig. 21A). MTs were traced using the "Dr. HALO" software program and a pointing device (Fig. 21B). After the tracing was completed from the first focal plane (Fig. 21C), it was selectively retrieved (Fig. 21D) by subtracting the highest grey level of the original image (Fig. 21A) and then intensifying the brightness of the cartoon by multiplying every pixel with the appropriate constant. The next step involved the superimposition of the first tracing onto the processed digital image of the second focal plane (see Fig. 21F). The arrows in Fig. 21F show the points where MTs from the first focal plane are continuous with those in the second focal plane.

The complete tracing of the total MT network in an EC cell, illustrated in Fig. 22, was derived by using the same methodology depicted in Fig. 21. The tracing begins at the top of the cell (Fig. 22A) and continues to the bottom (Fig. 22U). A grey level of 255 is the brightest unit of a pixel in any video image. In preparation for tracing, the averaged images were only deconvoluted because the combination of deconvolution and contrast manipulations resulted in certain areas of the cell having a grey level of 255. This was important because the pixels occupying the trace also had a grey level of 255 and the selective retrieval of the cartoon would have been impossible.

In Fig. 22M, towards the centre of the cell, there is an oversaturation of intensity yielding no descriptive information. Since individual MTs that extended into this area

could not be resolved their tracing was estimated (see Fig. 22O). Once the tracing of MTs became more complex (Fig. 22O), their superimposition onto the next focal plane (Fig. 22Q) produced only little more information. (See arrow in Fig. 22O and R). The superimposition of the cartoon in Fig. 22R onto the last focal plane shown in Fig. 22T revealed no further information. Hence, the tracings in Fig. 22R and U are identical.

Fig. 21: **Tutorial for Tracing the MT Network in EC cells.** A processed image of the first focal plane (A) is traced (B,C) and selectively retrieved (D). A processed image of the second focal plane (E) is then superimposed with the tracing from the first focal plane (F). Note that arrows in (F) indicate the positions where MTs from (D) are continuous. Bar = 5μm.

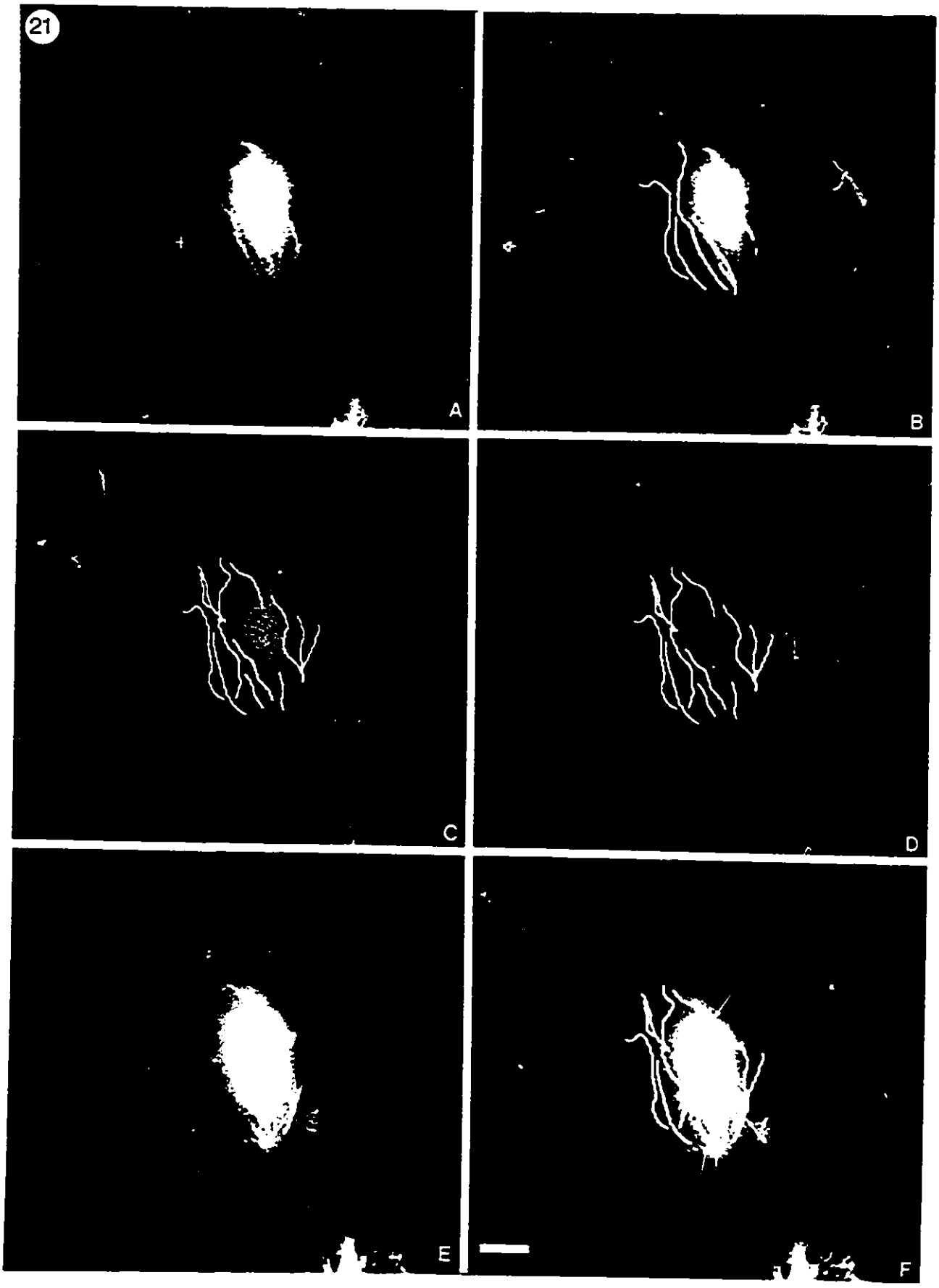
21
A
B
C
D
E
F

Fig. 22: **Reconstruction of the MT Network in an EC Cell on One Focal Plane.** (A-C) = first, (D-F) = second, (G-I) = third, (J-L) = fourth, (M-O) = fifth, (P-R) = sixth and (S-U) = the seventh focal plane. Averaged images (A,D,G,J,M,P and S) are deconvoluted (B,E,H,K,N,Q and T) and traced (C,F,I,L,O,R and U). See Materials and Methods for details. Arrows in (O) and (R) indicate positions where only little more information can be obtained as the trace becomes more complex. Traces illustrated in (R) and (U) are identical since the image from the seventh focal plane was not able to provide additional information. Bars throughout = 5μm.

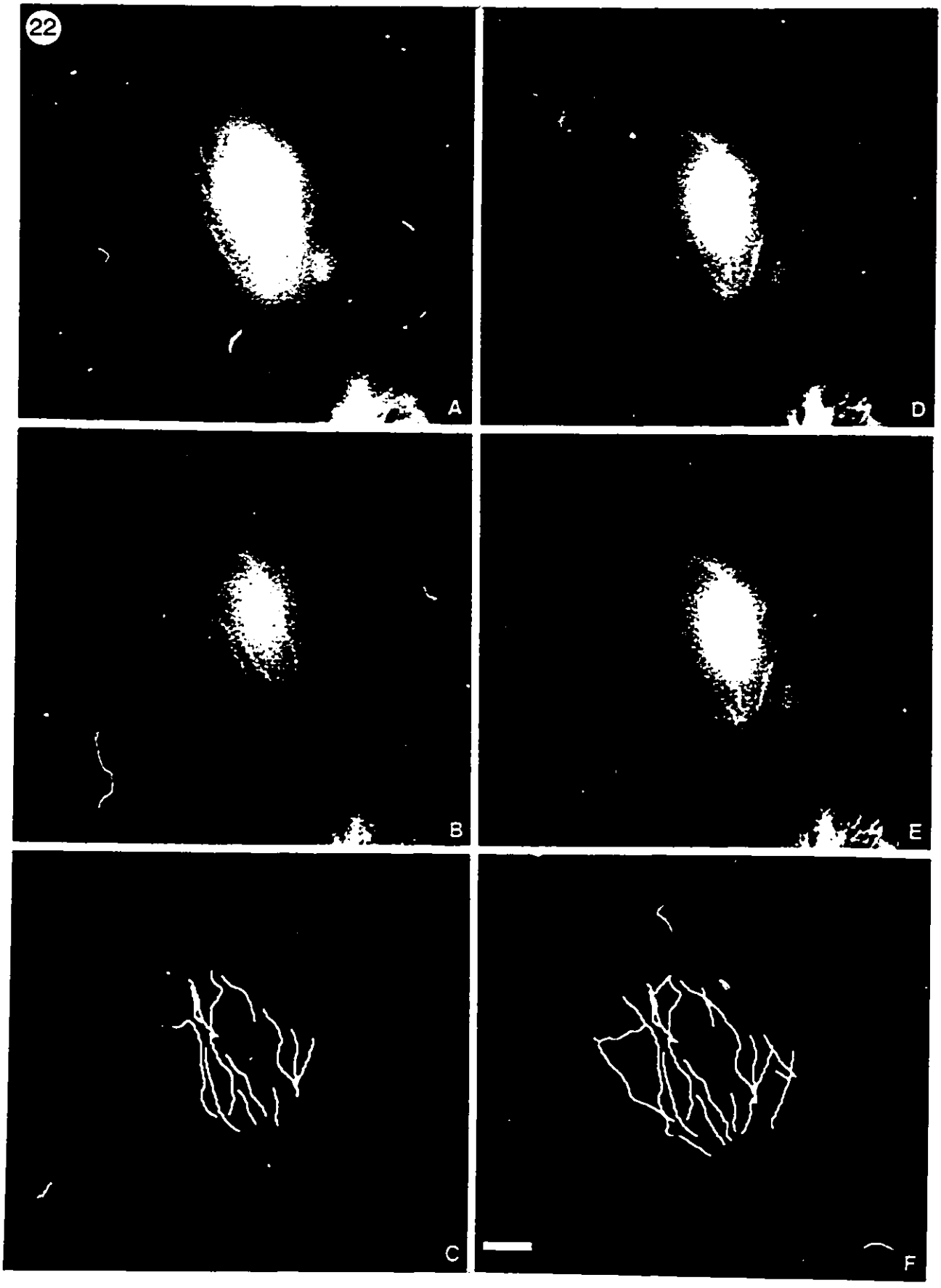
22
A
D
B
E
C
F

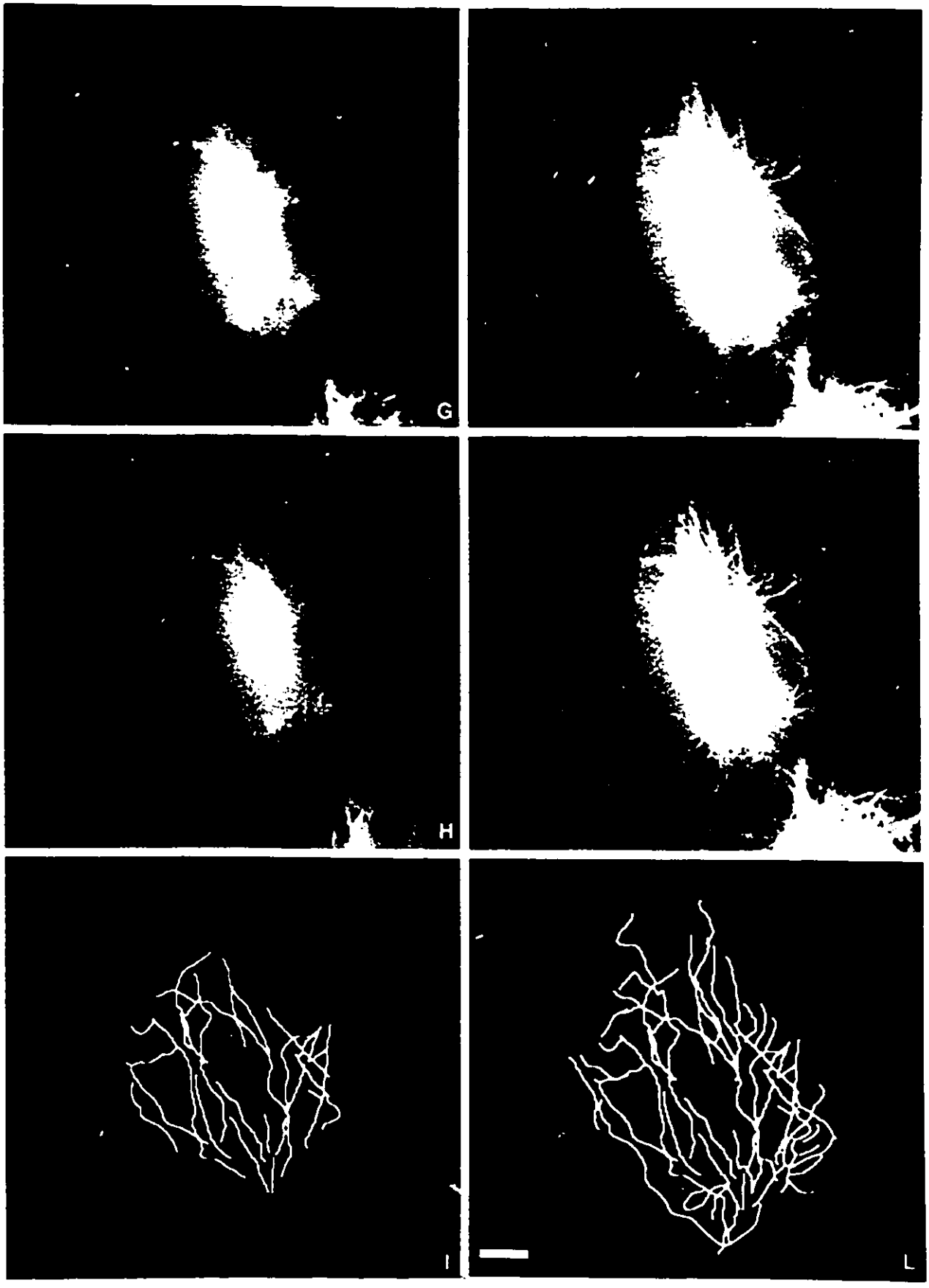
G
H
I
L

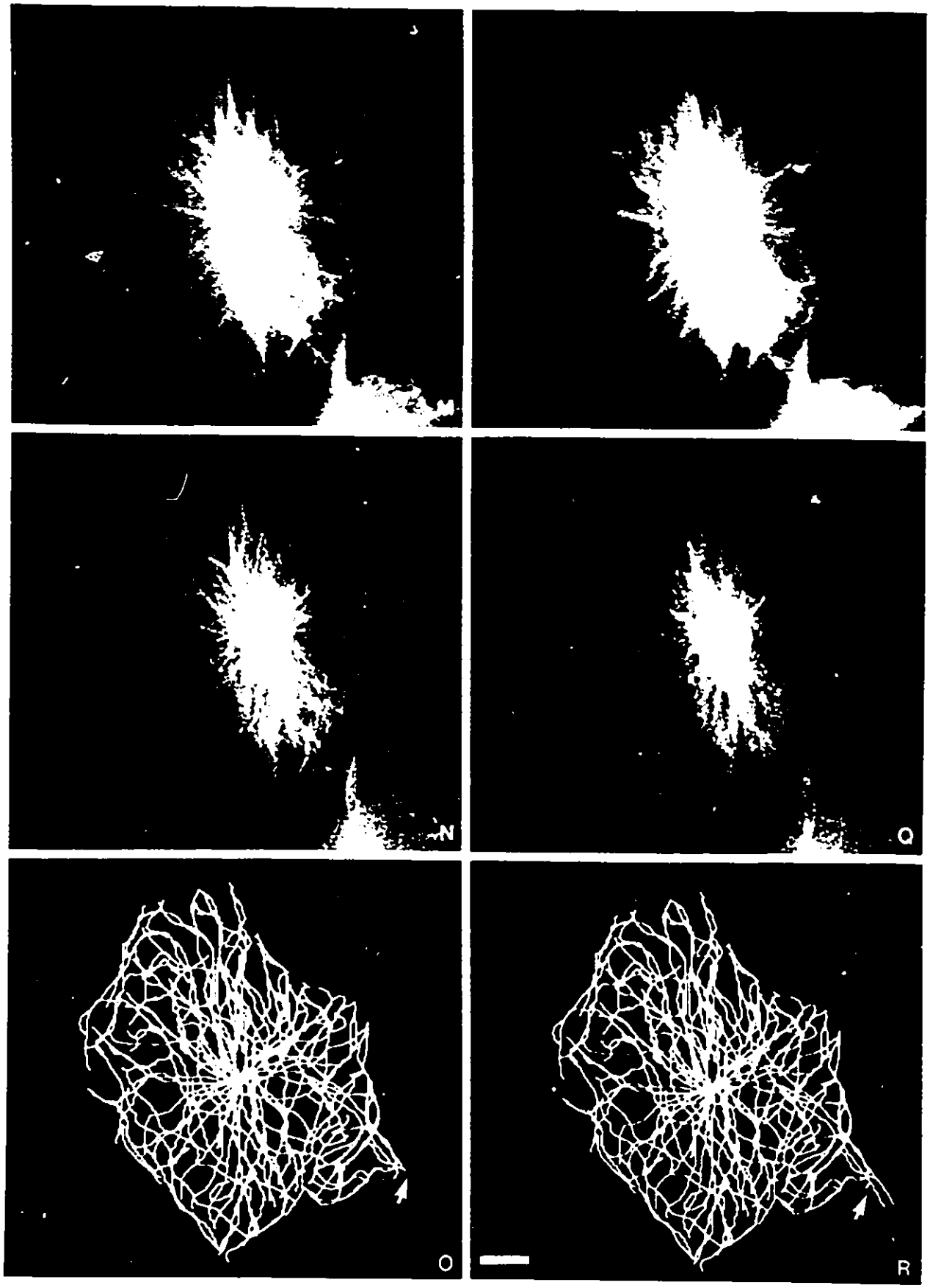
N
Q
O
R

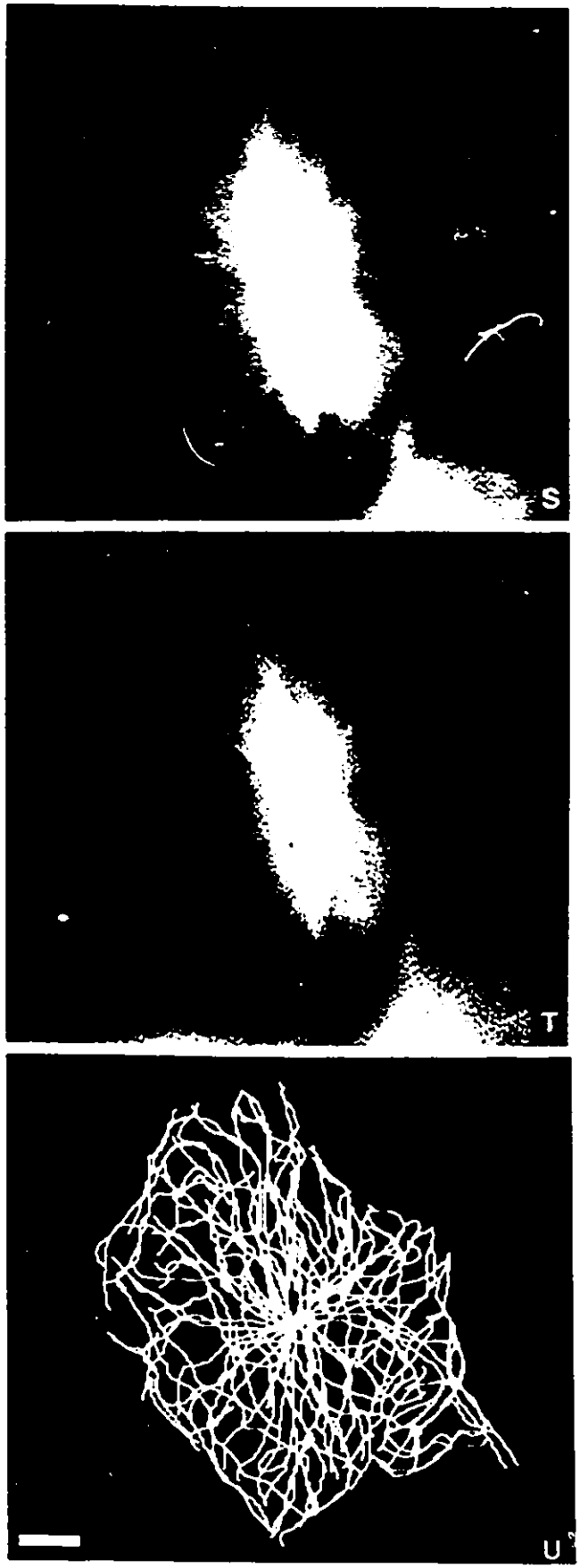
S
T
U

VII. Microtubule Dynamics in EC Cells

To analyze MT dynamics in EC cells, it was necessary to visualize the entire MT array on one focal plane as illustrated in the Model for MT Turnover in Fig. 5. (see Materials and Methods). Therefore, reconstruction of the biotin-labelled MT array and the total MT array in EC cells was done using a computer-aided imaging system. A MT is defined as having turned over if the B-Tb signal is uniform over the entire length (Schulze and Kirschner, 1986).

Figs 23 to 26 show representative examples of undifferentiated and RA-induced EC cells microinjected with B-Tb and Table 2 summarizes the microinjection results. Analysis of MT turnover in undifferentiated EC cells indicates that the results are quite homogeneous. Ten minutes after microinjection of B-Tb, 65.4 $\pm$ 2.2% (S.D.; n = 7) of the total MT array has turned over in undifferentiated cells. This corresponds to a half-time of less than 10 minutes. By 30 minutes, 92.4 $\pm$ 3.02% (S.D.; n = 5) of the MT array has uniformly incorporated B-Tb.

In RA-induced cells however, the results are quite variable. While 54.5 $\pm$ 10.6% (S.D.; n = 3) of the MT array has turned over by 10 minutes, 52.8 $\pm$ 19.37% (S.D.; n = 6) of the population of MTs has uniformly incorporated B-Tb, 30 minutes after microinjection. This wide range in the extent of MT turnover in RA-induced cells indicates that there are varying degrees in MT stability. There is a clear difference between the percent MT turnover in undifferentiated and one-day RA induced EC cells, 30 minutes after microinjection of B-Tb ($p < 0.0025$). These findings show that MTs in most EC cells are dynamic and become less dynamic in some RA-induced EC cells,

prior to morphogenesis.

Fig. 23: **Detection of Biotin-Tubulin Incorporation in Two Undifferentiated EC Cells 10 Minutes After Microinjection.** Video images of anti-biotin staining (A) and anti-tubulin staining (B) at one focal plane. Reconstruction of the biotin-labelled microtubule array (C) and the total microtubule array (D) was accomplished using the procedures outlined in Materials and Methods. The reconstructions were retraced onto acetate (E) to facilitate the enumeration of MT turnover. Bar (A-D) = 10 μm.

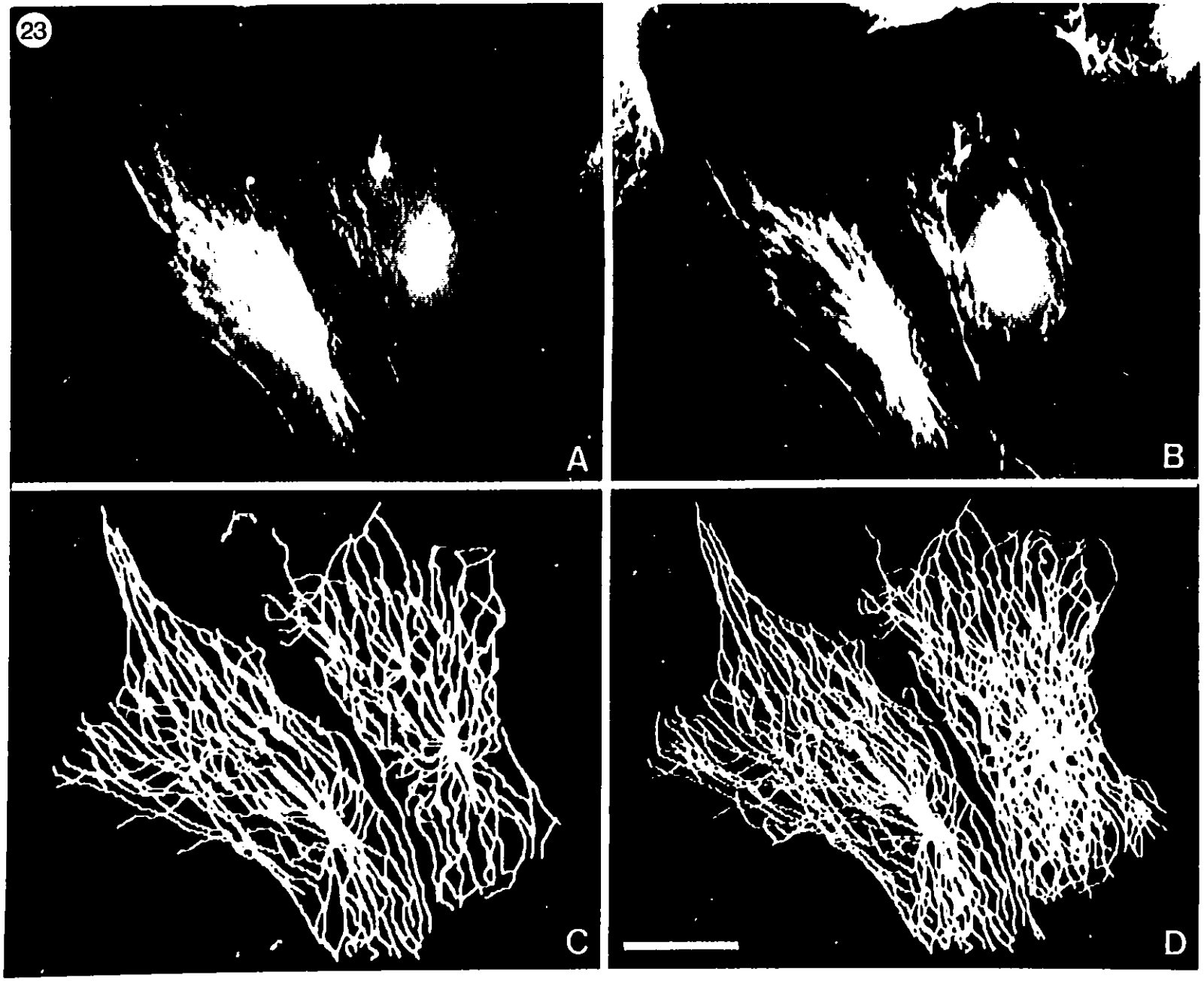
23
A
B
C
D

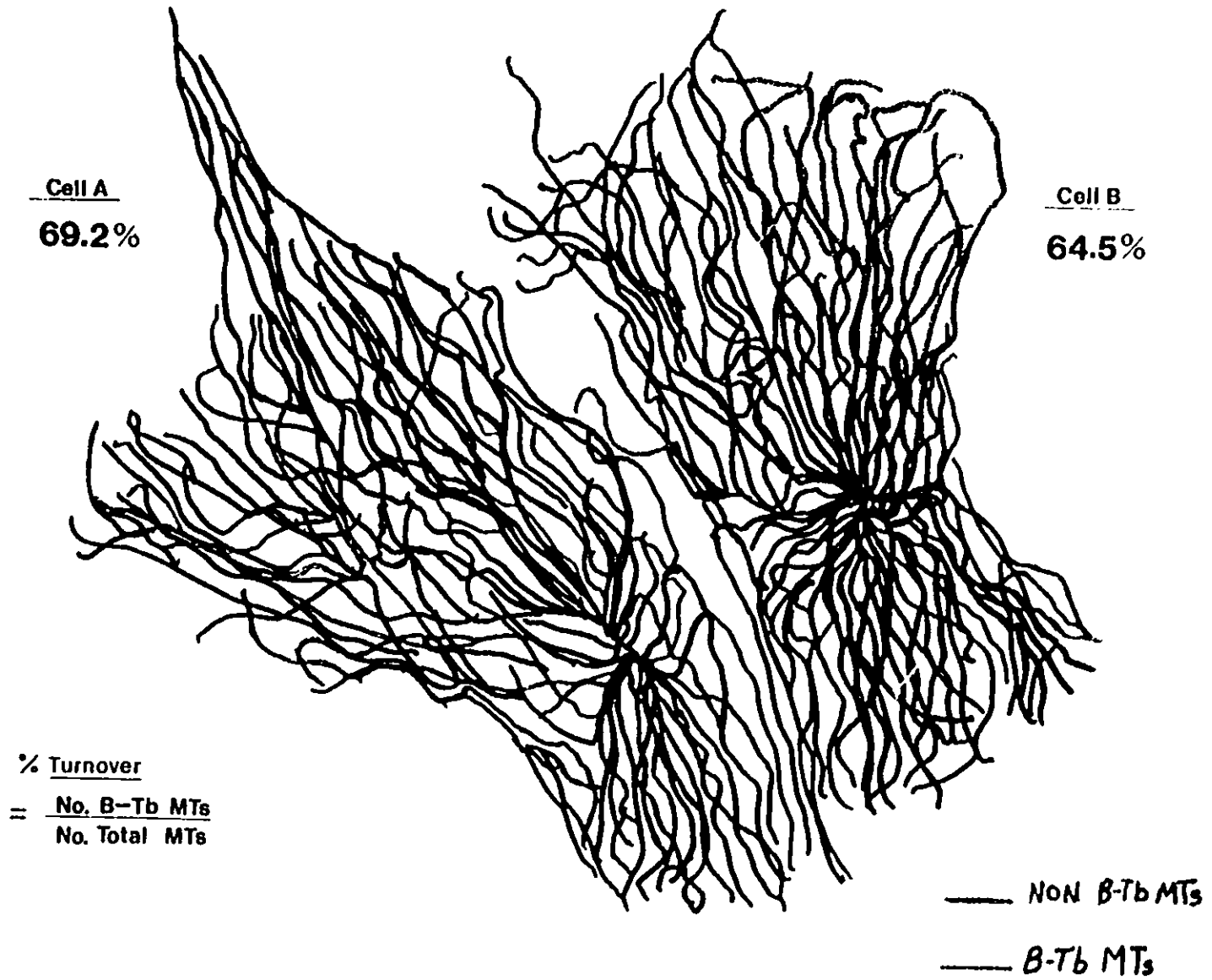

(E)

10 min Post MIJ

Fig. 24: **Detection of Biotin-Tubulin Incorporation in Two Undifferentiated EC Cell 30 Minutes After Microinjection.** Video images of anti-biotin staining (A,A') and anti-tubulin staining (B,B') at one selected focal plane. Reconstructions of the biotin-labelled microtubule arrays (C,C') and the total microtubule arrays (D,D') were accomplished using the procedures outlined in Materials and Methods. The cells in (A-D) and (A'-D') have 92.4% and 96.1% of their total microtubule arrays turned over. Note that the incorporation of B-Tb is more extensive at 30 minutes than at 10 minutes (compare this Figure with Figure 23). Bars = 10 μm.

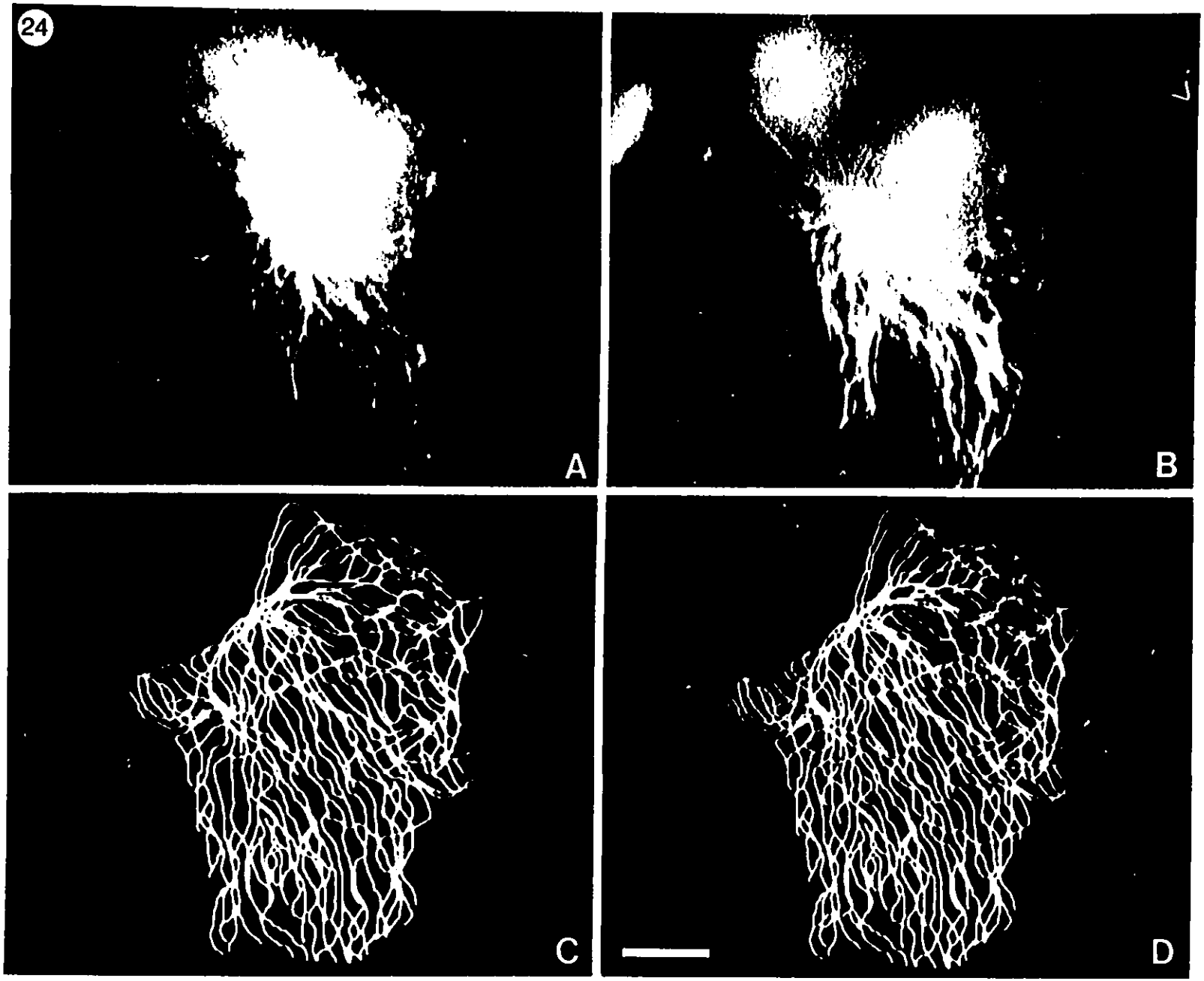
24
A
B
C
D

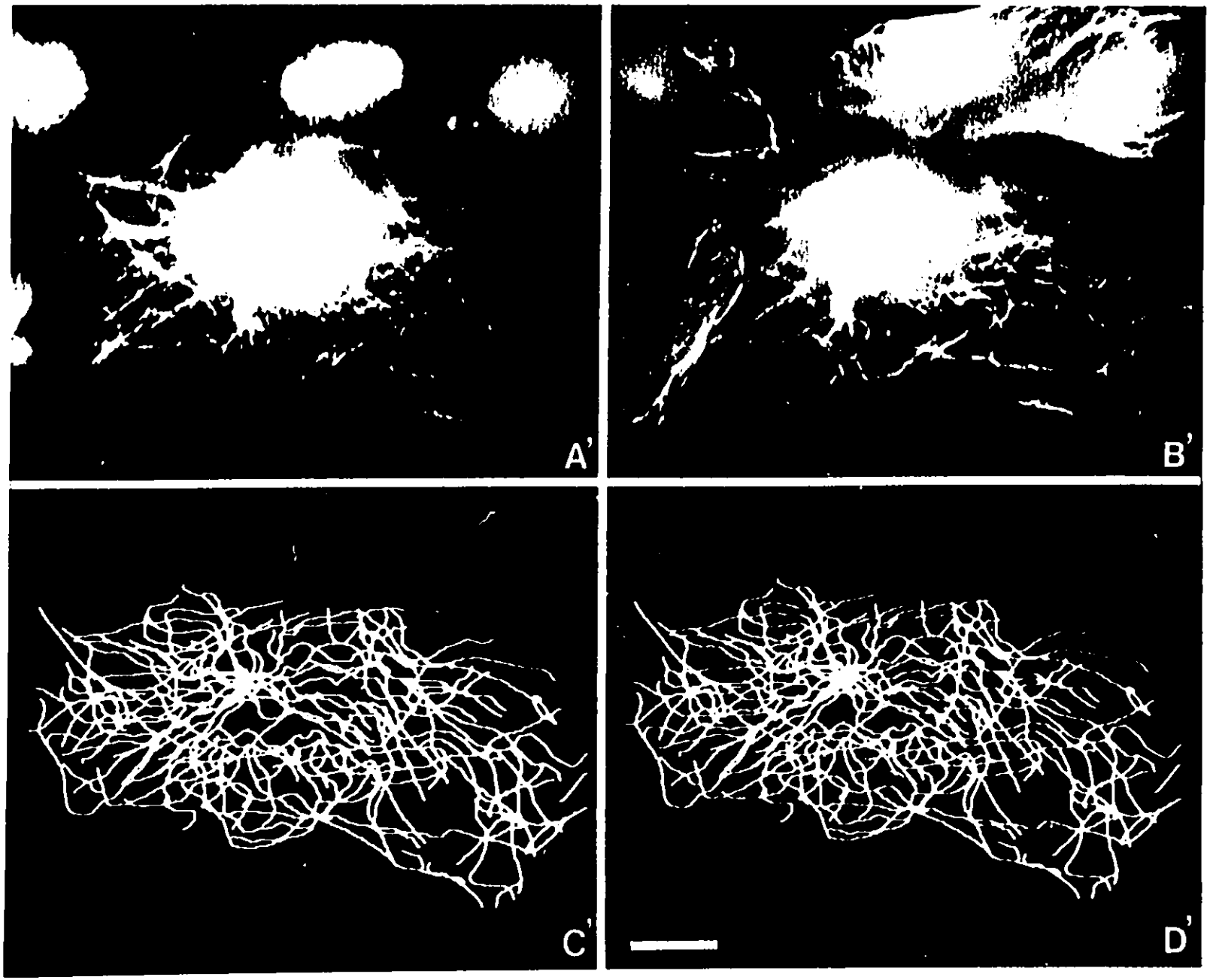
A'
B'
C'
D'

Fig. 25: **Detection of Biotin-Tubulin Incorporation in a One-Day Neurally Induced EC Cell 10 Minutes After Microinjection.** Video images of anti-biotin staining (A) and anti-tubulin staining (B) at one focal plane. Reconstruction of the biotin-labelled microtubule array (C) and the total microtubule array (D) was accomplished using the procedures outlined in Materials and Methods. This cell has 58.6% of its total microtubule array turned over. Bar = 10 μm.

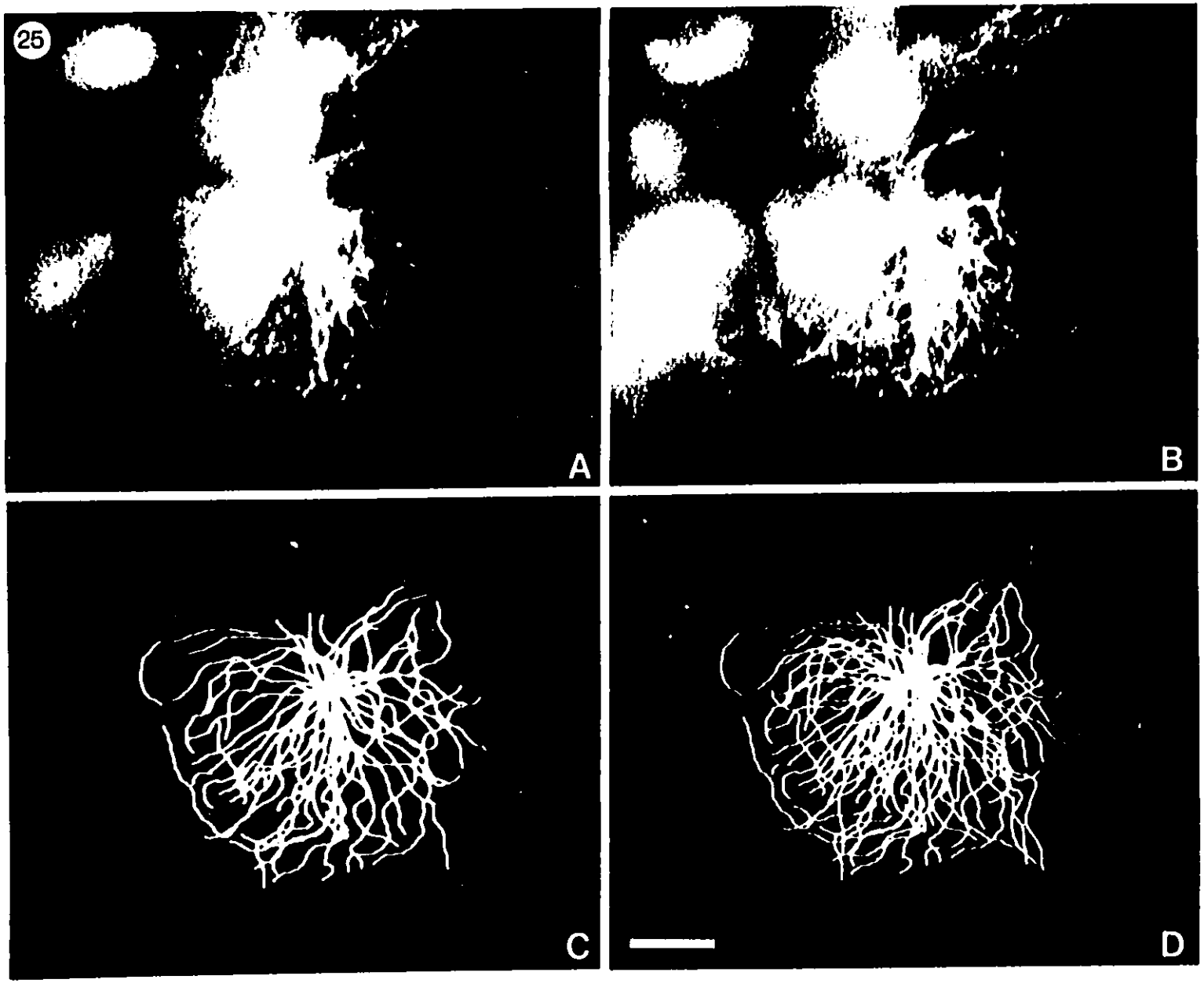
25
A
B
C
D

Fig. 26: **Detection of Biotin-Tubulin Incorporation in Three One-Day Neurally Induced EC Cells 30 Minutes After Microinjection.** Video images of anti-biotin staining (A,A') and anti-tubulin staining (B,B') at one selected focal plane. Reconstruction of the Biotin-labelled microtubule array (C,C') and the total microtubule array (D,D') was accomplished using the procedures outlined in Materials and Methods. The cell in (A-D) has 72.9% of the microtubule array turned over. The top cell and the bottom cell in (A'-D') have 40.4% and 36.5% of the microtubule arrays turned over. Bars = 10 μm.

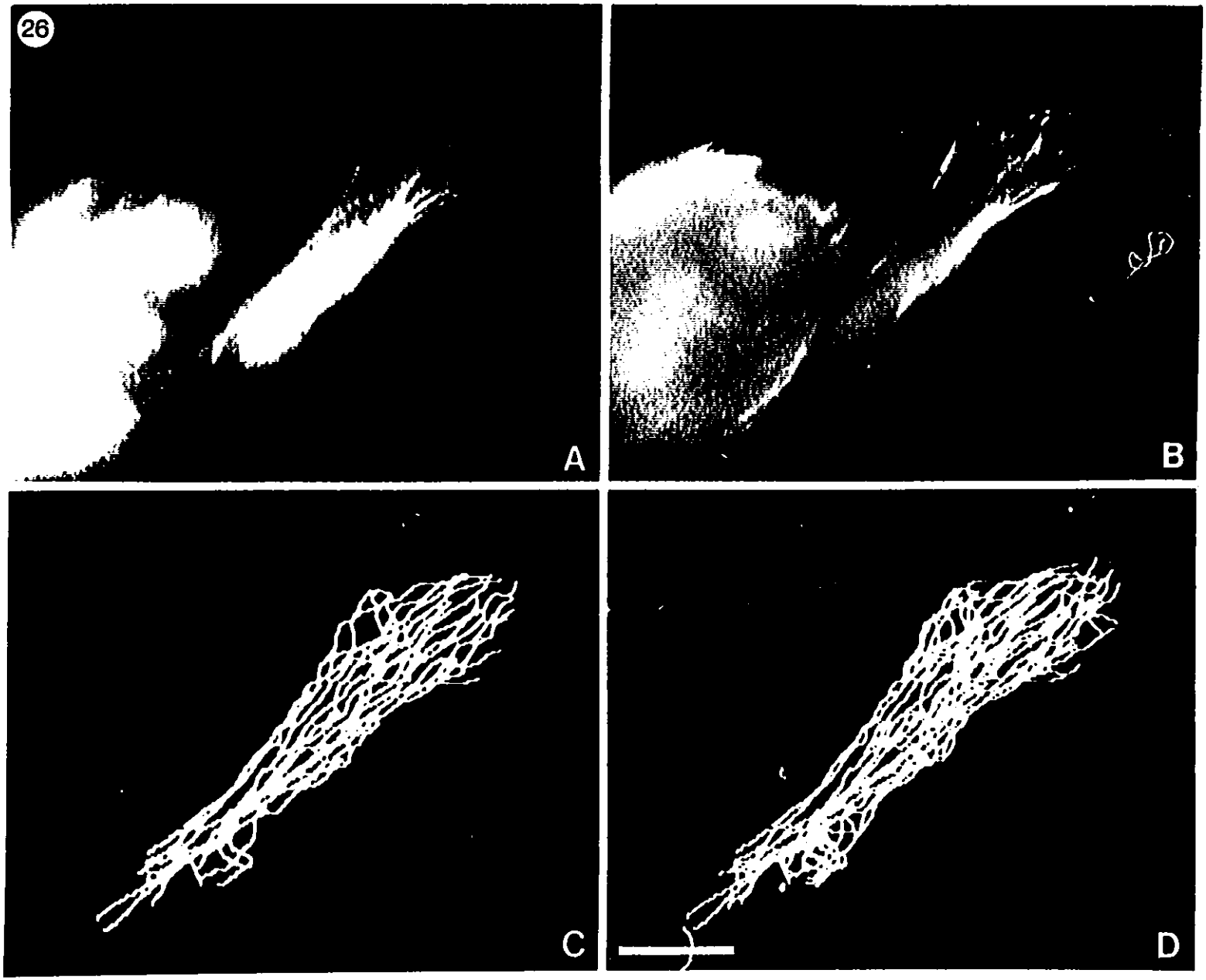
26
A
B
C
D

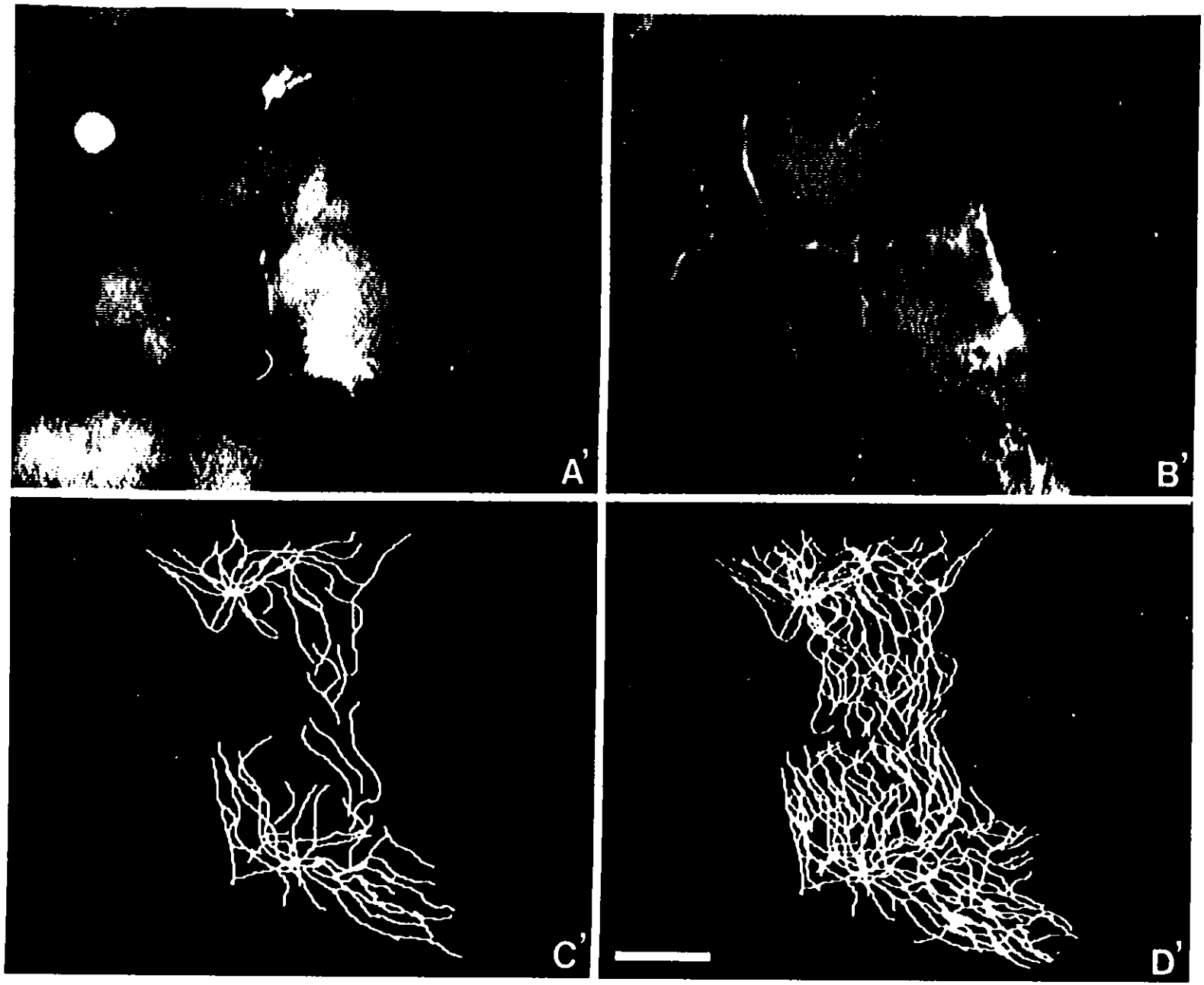
A'
B'
C'
D'

Table 2: Microtubule Dynamics in P19 Cells.

Stage of Differentiation	[1]Percent Microtubule Turnover	
	[2]10 min.	[2]30 min.
Undifferentiated EC Cells	65.4±2.2% (n = 7)	92.4±3.02% (n = 5)
Retinoic Acid-Induced EC Cells	54.5±10.60% (n = 3)	52.8±19.37% (n = 6)

1 Mean ± S.D.

2 Cells were fixed at the indicated time points after microinjection of B-Tb.

DISCUSSION

I. Immunofluorescence Microscopy and Immunoblotting

The objective of this study was to examine MT dynamics, prior to neurogenesis, in RA-induced P19 EC cells and to determine if the extent of acetylation of tubulin correlated with the degree of MT stability in this system. For the experiments conducted in this study, stable MTs were operationally defined as those resistant to depolymerization by a 45 minute treatment with 1 μg/mL colchicine at 37°C. Altered MT stability, assayed by resistance to depolymerization by colchicine, during early RA-induced differentiation was initially examined by immunofluorescence microscopy. The undifferentiated EC cell population was quite homogeneous in terms of its sensitivity to colchicine; the majority of the EC cell population had no polymerized MTs after colchicine treatment.

One day following neural induction with 1 μM RA most EC cells had ACET MTs. Only a subpopulation of these RA-induced cells was detected to have colchicine-resistant MTs that were acetylated. Within this subpopulation, some cells had more colchicine-stable MTs than others, and the organization of the MT array differed (see Fig. 7E,N,and Q). This heterogeneity in colchicine resistance suggested that there were varying degrees of MT stability in cells at this stage of differentiation, prior to morphogenesis.

Quantitative immunoblotting showed that although there was no change in the level of total cellular tubulin following RA induction, there was an increase in the level of tubulin in polymer form. This suggests that undifferentiated EC cells are tightly

regulating the levels of MT assembly. The increase in the level of tubulin in polymers following RA induction suggests that more MT assembly is required prior to morphogenesis. In contrast, Drubin et al., (1985) have shown that prior to neurite outgrowth of PC 12 cells total tubulin levels increased and no appreciable increase in MT assembly was detected. This increase in tubulin was not sufficient to drive MT assembly in the PC 12 system. Tau protein and MAP 1 seemed to be limiting for net MT assembly (Drubin et al., 1985), i.e., MT assembly was driven after the levels of tau and MAP1 increased. The regulation of MT assembly early in differentiation of P19 EC cells might possibly be due to some physiological assembly promoting factors such as GTP or other proteins such as MAP 1B. If MAP 1B levels were increased early in differentiating P19 cells, this protein could drive MT assembly. Currently there is no available data reporting quantitative levels of MAP 1B during neural differentiation of P19 cells.

An unexpected finding was that there was no difference in the levels of tubulin in colchicine-resistant MTs between undifferentiated EC cells and one day RA-induced cells. The immunofluorescence staining results clearly showed that there was an increase in the colchicine-resistant MTs; however, this occurred in only a small percentage of the cells and the immunoblotting method was not sensitive enough to detect the change.

Acetylation of α-tubulin was used as a marker for MT stability in this study. Other markers such as detyrosination of α-tubulin could have been used but only antibodies to ACET tubulin were available. Immunoblotting results showed that although relative levels of ACET tubulin did increase by two fold during early differentiation, there was no selective incorporation of ACET tubulin in colchicine-resistant MTs in RA-

induced cells. Immunofluorescence microscopy observations showed that the persistence and number of ACET MTs after colchicine treatment occurred in only a small population and once again the immunoblotting technique was not sensitive enough to detect this change. If stable MTs were operationally redefined as those resistant to depolymerization by colchicine for shorter treatment times, then a preferential inclusion of ACET tubulin into colchicine-stable MTs might be detected by immunoblotting. Many studies have reported that if MTs are stable to depolymerization for a sufficient period of time, they are likely to be post-translationally modified by detyrosination (Gundersen and Bulinski, 1986; Gundersen et al., 1989) and/or acetylation (Piperno et al., 1987; Black et al., Webster and Borisy, 1989). Therefore, the increase in the levels of acetylation of MTs following RA induction strongly suggests that such MTs are more stable than those in undifferentiated cells.

II. Microtubule Dynamics

There are two possible mechanisms that could account for the increase in the levels of ACET tubulin following RA induction of P19 cells: (a) an increase in the activity of the tubulin acetyltransferase enzyme; or (b) an alteration in MT dynamics. I have tested the second possibility directly. The immunofluorescence observations have suggested that the MT array in undifferentiated EC cells is initially dynamic and becomes less dynamic in a subpopulation of RA-induced cells, prior to morphogenesis. To test this, MT dynamics were directly measured by microinjecting biotin-tubulin (B-Tb) in undifferentiated and in RA-induced EC cells. The incorporation of B-Tb into the

endogenous MT arrays of such cells was detected by hapten-mediated immunocytochemistry.

Prior to microinjection of cells, B-Tb was initially tested for assembly competence in vitro by polymerizing it off isolated axonemes from Tetrahymena. Various molar ratios of B-Tb to PC-Tubulin were used to initiate MT assembly. This was done because when B-Tb is microinjected into cells, it gets mixed with the endogenous tubulin pool. There is no exclusive incorporation of B-Tb into cellular MTs; polymerized MTs in vivo would consist of B-Tb and unmodified endogenous cellular tubulin (Schulze and Kirschner, 1986). Therefore, it was necessary to determine which molar ratios of B-Tb to PC-Tubulin would yield MT lengths that were similar to those MTs polymerized with PC-Tubulin alone.

In vitro MT assembly experiments in this study have shown that all molar ratios of B-Tb to PC-Tubulin tested, produced mean MT lengths that were statistically lower than those MTs polymerized with PC-Tubulin alone. However, lower molar ratios (e.g. 1:4 and 1:9) produced mean MT lengths that were higher than those MTs polymerized with higher molar ratios of B-Tb to PC-Tubulin (e.g. 1:0 and 1:1). These observed trends in MT lengths are consistent with those reported by Kristoffersen et al., (1986) and Schulze and Kirschner, (1986). It should be noted that a B-Tb to PC-Tubulin molar ratio of 1:19 yielded a mean MT length statistically identical to control (Schulze and Kirschner, 1986).

MT assembly in vitro using a molar ratio of 1:19 of B-Tb to PC-Tubulin was not used but a molar ratio of 1:9 was used. The reason for this is that previous

microinjection studies have estimated the ratio of injected tubulin to endogenous tubulin to be 1:9. This increase in tubulin by an estimated factor of 10, did not significantly perturb MT dynamics and that cells underwent normal mitosis (Schulze and Kirschner, 1986; Sammak and Borisy, 1988). This estimation was based on assessing the degree of swelling observed when cells were microinjected with B-Tb at a concentration similar to the intracellular tubulin concentration of 2 to 2.2 mg/mL (Hiller and Weber, 1978). Since microinjecting EC cells proved to be a difficult task, it was impossible to estimate the degree of swelling and to estimate how much tubulin was being introduced intracellularly. However, only successful injections were used to quantify the extent of MT turnover.

The assembly competence of B-Tb in vivo was first tested by microinjecting it at a concentration of 2.39 mg/mL into undifferentiated L6E9 rat myoblast cells. These cells were chosen due to the relative ease by which they can be successfully microinjected. The results show that the pattern and extent of incorporation of B-Tb into the endogeneous MT array were similar to those reported in previous studies and thus demonstrating its assembly competence in vivo (Schulze and Kirschner, 1986, 1987; Sammak et al., 1987). B-Tb was then used to probe MT dynamics during early RA-induced neural differentiation of P19 EC cells.

For EC cells it became necessary to visualize the entire MT array on one focal plane to quantify MT turnover. Therefore computer-aided video imaging with a silicon-intensified target (SIT) camera was used to reconstruct the MT array in EC cells on one focal plane. This technique is illustrated in Fig. 21 and an example of the full

reconstruction is presented in Fig. 22. Utilizing this technique, the B-Tb labelled MT array and the total MT array were reconstructed in microinjected undifferentiated and RA-induced EC cells. The extent of MT turnover was then quantified. It should be noted that quantification of MT turnover in RA-induced cells was restricted to cells having MT arrays similar in distribution in undifferentiated cells. It was not possible to analyze MT dynamics in the minor population of RA-induced cells having the bundle of MTs. At the level of immunofluorescence microscopy, individual MTs within the bundle cannot be resolved. For such an analysis, MT turnover would have to be quantified by introducing fluorescently-labelled tubulin and using photobleaching procedures described by Sammak and Borisy (1988).

In undifferentiated EC cells, it was shown that by 10 minutes after the microinjection of B-Tb approximately 65% of the MT population had turned over. It was necessary to show that longer times after microinjection, a greater percentage of the total MT array would uniformly incorporate B-Tb. 30 minutes after microinjecting B-Tb, greater than 90% of the MT array had turned over. These results indicate that the MT array in undifferentiated EC cells is very dynamic because similar MT dynamics have been reported in other established cell lines (Schulze and Kirschner, 1986; Sammak et al., 1987; Webster et al., 1987a; Geuens, et al., 1989).

In RA-induced cells, the extent of MT turnover was different from undifferentiated EC cells. 10 minutes after microinjection approximately 50% of the MT array had turned over. By 30 minutes, the range of MT turnover was from 29.5% to 72.9% indicating that there are varying degrees of MT stability. These results are

consistent with the immunofluorescence observations of colchicine-resistant MTs in RA-induced EC cells. Clearly there is a difference in the extent of MT turnover by 30 minutes between undifferentiated and RA-induced EC cells. These results support the hypothesis that MTs become less dynamic following RA induction of EC cells prior to morphogenesis. This alteration in MT dynamics prior to neurogenesis has not previously been reported and it may be a critical event in determining the developmental fate of these cells. The only alteration in MT stablity that has been documented was after neurites had been elaborated (Okabe and Hirokawa, 1988, 1990; Lim et al., 1989, 1990; Keith, 1990; Shea and Beermann, 1990).

The role of ß-tubulin isotypes for generating stable MTs during neural differentiation of P19 EC cells has been described by Falconer et al., (submitted). The experiments conducted in this study does not permit us to distinguish the incorporation of specific α-tubulin or ß-tubulin isotypes into growing MTs prior to and following RA induction of EC cells. This may be achieved by purifying these isotypes from brain by affinity chromatography, labelling them with biotin and then microinjecting them into EC cells to analyze their effect on MT dynamics.

It has been shown in vitro that MTs polymerized from adult brain tubulin, containing a high proportion of acidic isoelectric variants, are more resistant to depolymerization than those MTs polymerized from neonate tubulin having reduced levels of acidic isoelectric variants (Lee et al., 1990c). Therefore, the microinjection of adult brain tubulin into undifferentiated EC cells might alter the dynamic properties of MTs. To rule out this possibility, tubulin prepared from various developmental stages would

have to be microinjected into tissue culture cells and assess its effect on MT dynamics.

There is an increasing interest in understanding the role of stable MTs during cell differentiation and cell motility in a wide variety of systems. For example, stable MT bundles are known to play a role in generating cellular asymmetry, leading to the formation of the marginal band in differentiating erythrocytes (Winckler and Solomon, 1991).

Stable MTs also have been implicated in cell motility. Gundersen and Bulinski (1988) have used experimentally wounded monolayers of fibroblasts in culture to examine MT stability during cell migration. MTs in such cells have specialized MT arrays that a) are oriented towards the direction of migration, b) are post-translationally modified by detyrosination (GLU MTs) and c) are stable to depolymerization by anti-MT drugs. These events occurred prior to active cell migration. Although the role of stable MTs in these cells is unclear, their orientation toward the direction of migration is suggestive. Gundersen and Bulinski (1988) have speculated that these stable MTs could serve as tracks for the transport of membrane components toward the leading edge of migrating cells.

During reduced serum-induced muscle cell differention of L6 rat myoblasts, an accumulation of detyrosinated tubulin (GLU tubulin) and acetylated tubulin (ACET tubulin) was detected in stable MT arrays (Gundersen et al., 1989). This enrichment of GLU and ACET tubulin occurred early in differentiation and such enriched MTs were oriented in a direction parallel to the elongation of the differentiating muscle cells. They proposed that stable MTs served as tracks for the generation of bipolar morphologies

during muscle cell differentiation (Gundersen et al., 1989; Bulinski and Gundersen, 1991).

The role of stable MTs, enriched in post-translationally modified tubulin, during neurogenesis has been most extensively investigated. It is well documented that stable MTs accumulate during neuronal differentiation in a wide variety of nerve cell culture systems (Black and Greene, 1982; Black and Keyser, 1987; Falconer et al., 1989a, 1989b; Ferreira and Caceres, 1989; Lim et al., 1989; Baas and Black, 1990; Shea and Beermann, 1990; Shea et al., 1990). In some systems, such as PC 12 cells (Black and Greene, 1982; Black et al., 1986, 1989) and NB2a/d1 neuroblastoma cells (Shea and Beermann, 1990; Shea et al., 1990), the accumulation of colchicine-resistant MTs was detected after neurites had been elaborated. In the P19 EC cell system, Falconer et al., (1989a, 1989b) have documented the presence of colchicine-resistant MTs, enriched in GLU and ACET tubulin, prior to the onset of neurogenesis and have proposed that such MTs might serve as nucleating structures for neurite elongation.

This thesis has examined changes in MT dynamics that accompany changes in colchicine susceptibility and acetylation of tubulin. Two aspects of this alteration in MT stability that must be examined next are a) factors that contribute to the generation of stable MTs and b) the developmental fate of RA-induced EC cells having these stable MT arrays.

III. Model for Generating Stable Microtubules

A model for the generation of stable MTs, present in one day RA-induced P19 EC cells, is illustrated in Fig. 27. This model is based as an extension of the dynamic instability model for cellular morphogenesis, originally presented by Kirschner and Mitchison (1986). It also takes into account the current available evidence on the dynamics of post-translational modifications of tubulin and the expression of various cytoskeletal proteins in neurally differentiating P19 EC cells documented by Falconer and Brown, (1989) and Falconer et al.,(1989a, 1989b).

In undifferentiated EC cells, MTs are very dynamic and turn over with $t_{1/2}$ of less than 10 minutes. Following neural induction with RA, there is a selective stabilization of a subset of MTs. Since dynamic instability is the widely accepted model for MT dynamics in vivo, it can be suggested that after induction with RA, dynamic MTs would largely depolymerize and be replaced by those that have been selectively stabilized. How this occurs is still not known.

The model illustrated in Fig. 27 suggests that for selective stabilization to occur, there would first be an incorporation of the major brain-specific ß-tubulin isotype (ß-II) into the initial MT arrays following neural induction. Falconer et al., (submitted) previously have shown by immunofluorescence microscopy that there is increased expression of ß-II tubulin in early neurally differentiating EC cells. Since this thesis has reported no change in the level of total tubulin following neural induction, more of the ß-II tubulin would be incorporated into MTs than other ß-tubulin isotypes. Those MTs

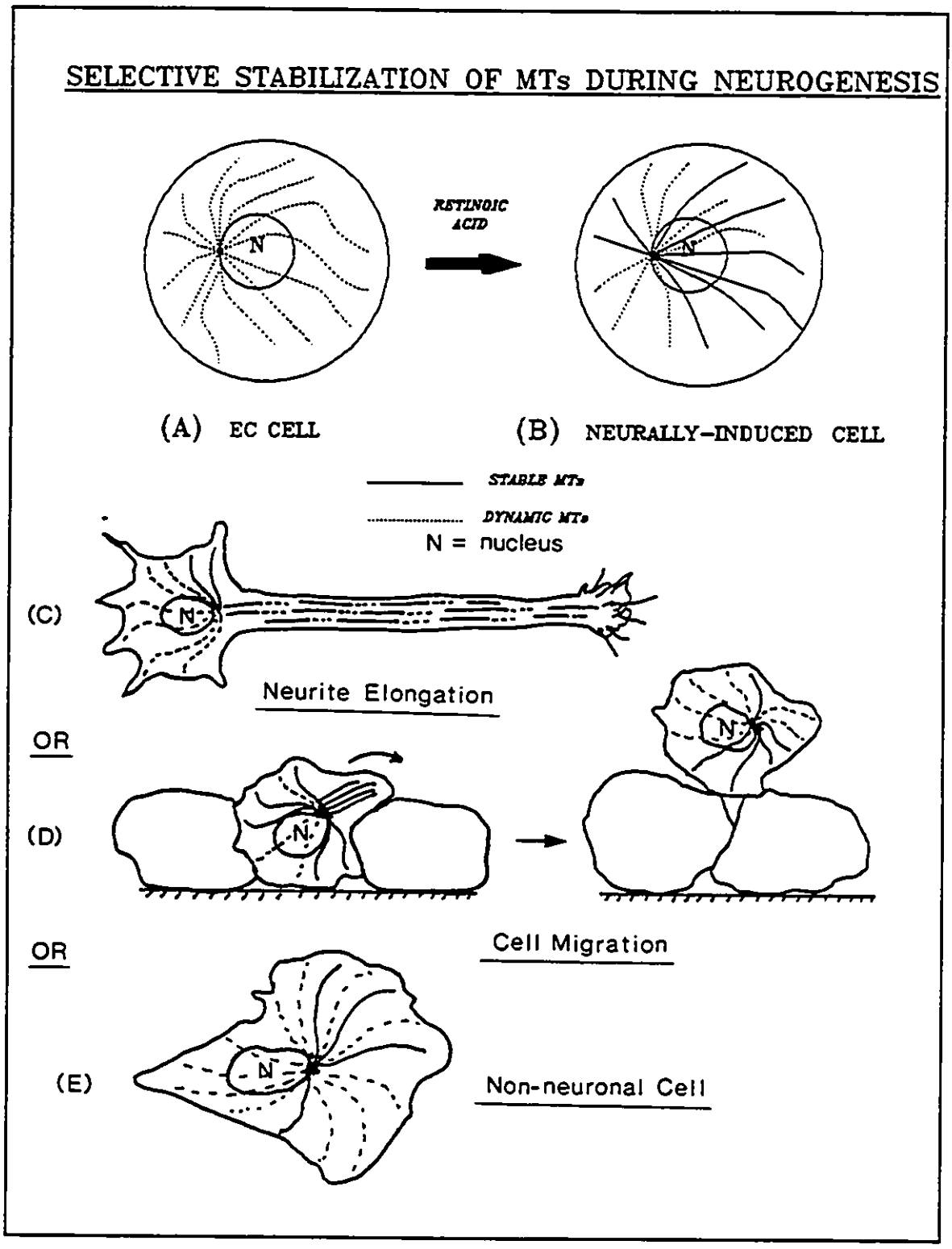

Fig. 27: Selective Stabilization of MTs During Neural Differentiation of P19 EC Cells. (Modified from Kirschner and Mitchison, 1986).

enriched in the ß-II tubulin isotype would be more stable to depolymerization than those not as enriched. Banerjee et al., (1989) have shown that MTs polymerized from purified heterodimers of tubulin consisting of ß-II tubulin were more stable than those MTs polymerized from unfractionated tubulin.

After MTs enriched in the ß-II tubulin isotype are polymerized, they would be stable long enough to be post-translationally modified by the enzymes tubulin acetyl transferase and/or tubulin carboxypeptidase that acetylate and detyrosinate MTs respectively. These enzymes are known to function preferentially on polymerized MTs (Maruta et al., 1986; Gundersen et al., 1987; Black et al., 1989). Thus, a MT not as enriched with the ß-II tubulin isotype would not be extensively detyrosinated and/or acetylated. Using pulse-chase protocols it has previously been shown in cultured neurons that the turnover of ACET MTs is biphasic. As measured by acetate turnover, 30 to 50% of acetate turns over with $t_{1/2}$ of 2 hours and the remainer turns over with $t_{1/2}$ greater than 5 hours (Black et al., 1989). This indicates that even ACET MTs can differ in their stability. The mechanism by which MTs acquire increased stability beyond this point at this early stage of neural differentiation is not known.

One factor that might play a role for stabilizing MTs is the presence of MAP 1B. This protein was detected in both undifferentiated and one day RA-induced EC cells (Falconer et al., submitted). The tubulin binding region of MAP 1B was found to be very basic (Noble et al., 1989). The characterization of MAP 1B binding to tubulin by ionic interactions has been investigated by Avila (1991). Thus it is possible that MAP 1B would bind to MTs that have an enhanced negative charge and thus would increase

MT stability.

Another factor than might influence the stability of MTs in RA-induced P19 cells is intermediate filaments (IFs). Extensive crosslinking between the neurofilament and MT network has been demonstrated in vivo (Hirokawa, 1982) and in vitro (Hisanaga and Hirokawa, 1990). Blose et al., (1984) also have shown that the IF network collapsed after certain monoclonal and polyclonal antibodies to tubulin were microinjected in living fibroblasts. This suggested that there was an intimate association between the IF network and the MT array.

Falconer et al., (1989b) previously have attempted to determine the role of vimentin IFs for stabilizing MTs by treating RA-induced P19 cells with acrylamide. Acrylamide has been shown to disrupt the IF network (Eckert, 1985). After acrylamide treatment, colchicine was added to induce depolymerization of MTs. Those studies concluded that vimentin IFs did not play a role in stabilizing MTs early in differentiation. However, the simultaneous extraction-fixation protocol for immunofluorescence microscopy used in that study was not appropriate for preserving the vimentin IF network and the MT system. Vimentin staining was very diffuse in most undifferentiated and RA-induced cells and a filamentous network was detected in a very restricted population (Falconer et al., 1989b). Klymkowsky (1988) has shown that the vimentin IF network and the MT array can be successfully preserved in human fibroblasts if cells are first extracted in a MT stabilizing buffer and then fixed in cold methanol. Another problem is that the mechanism of action of acrylamide on the IF system is not fully understood. Therefore, the results of Falconer et al., (1989b) regarding the role of vimentin IFs for

stabilizing MTs in RA-induced P19 cells are inconclusive.

The α-tubulins incorporating into stable MTs in RA-induced P19 cells might be rendered more acidic by polyglutamylation (Edde et al., 1990, 1991). Although the function(s) of polyglutamylation is/are unknown, it is proposed that the successive addition of glutamyl residues might serve as to enhance MAP binding during nerve cell maturation (Lee et al., 1990a, 1990b). It is not known if polyglutamylation occurs on preferentially polymerized MTs or on monomeric tubulin. If antibodies to polyglutamylated α-tubulins were generated, they could be used to determine if such modified tubulins are present during early neural differentiation and if they are preferentially incorporated into stable MTs in vivo.

IV. Experimentally Testing Factors Influencing MT Stability

The role of ß-II tubulin, MAP 1B and intermediate filaments for potentially enhancing MT stability can be tested experimentally by a) quantitative biochemical procedures and b) quantitative microscopy. Both techniques rely on introducing antibodies, specific to each of these three components of the cytoskeleton, into RA-induced cells by phospholipid-mediated delivery (Shea et al., 1991c). The advantages of this technique over microinjection are that it can be done in a tissue culture laminar flow hood under sterile conditions, it is simple to perform, many cells can be successfully loaded at a single time and finally the need for purchasing expensive equipment for microinjection is eliminated (T.B. Shea, personal communication).

A) Quantitative Biochemistry

In independent experiments, antibodies to ß-II tubulin can be introduced into RA-induced P19 cells. Controls would include the introduction of pre-immune serum and no antibody. The objective is to prevent the incorporation of the ß-II tubulin isotype into the MT array. After a sufficient period for recovery, the stability of MTs in these cells can be tested by treating the cultures with colchicine. The amount of tubulin in polymer can be measured quantitatively by immunoblotting procedures. Also, the appearance of post-translationally modified form of MTs and their colchicine-stability can be examined by both immunofluorescence microscopy and quantitative immunoblotting. These experiments would attempt to show the role of tubulin isotype sorting and post-translational modifications of tubulin in generating stable MTs.

The role of MAP 1B for potentially stabilizing the MT array in RA-induced cells can be tested by introducing anti-MAP 1B antibodies. The objective is to assay the stability of MTs by preventing their association to MAP 1B. Shea et al., (1991a,b) have analyzed the effect of introducing anti-MAP 1 and anti-tau antibodies by phospholipid-mediated delivery into NB2a/d1 neuroblastoma cells. Their results showed that MAP 1 had no effect on neurite outgrowth early in differentiation but retracted neurites at later stages. In contrast, tau protein prevented initial neurite outgrowth. Their studies however, did not examine the effects of these antibodies directly on MT stability.

The role of intermediate filaments (IFs) for stablizing MTs can be examined by introducing specific anti-IF antibodies to disrupt the IF network. Three independent groups have shown that microinjection of anti-IF antibodies into cultured cells resulted

in the aggregation and collapse of the IF network without affecting cell shape, mitosis and locomotion (Gawlitta et al., 1981; Klymkowsky, 1981; Lin and Feramisco, 1981). A fourth study by Shea et al., (1991a) have shown that anti-vimentin antibodies, introduced by phospholipid-mediated delivery, inhibited initial neurite extension of NB2a/d1 neuroblastoma cells. The antibodies can be introduced into P19 cells by phospholipid-mediated delivery, as described above. After this treatment the amount of tubulin in polymer and in colchicine-treated cell extracts can be quantified using the immunoblotting procedures mentioned above. Using these types of manipulations, it should be possible to determine the effect of a disrupted IF array on MT stability detected in early neurally differentiating EC cells.

B) Quantitative Microscopy

The role of ß-II tubulin, MAP 1B and IFs on MT dynamics also can be examined directly by real-time observations in RA-induced P19 cells. The procedure is to introduce rhodamine-labelled tubulin into undifferentiated P19 cells by the bead loading technique (McNeil and Warder, 1987; McNeil, 1989) or by phospholipid-mediated delivery (Shea and Beermann, 1990; Shea et al., 1991c). After rhodamine-tubulin is uniformly incorporated into the MT array, the cells would be neurally-induced with 1μM RA. Twenty-fours after induction the cells would be introduced with antibodies to either ß-II tubulin, MAP 1B or IFs and can then be observed in real-time using low light level fluorescence video microscopy. Any alterations in MT dynamics would be detected by using the FRAP technique. A laser mounted onto a fluorescence microscope can be used

to photobleach a line across fluorescently-labelled MTs. The recovery of fluorescence can then be used as a measure of MT dynamics.

V. Function(s) of Stable MTs in RA-Induced P19 Cells

The next biological question of interest is to determine the developmental fate of RA-induced P19 cells having stable MTs. The model illustrated in Fig. 27 shows three possible roles for stable MTs in P19 cells. First, it has been suggested that stable MTs would function as nucleating structures for further MT assembly leading to the formation of neurites (Falconer et al., 1989a, 1989b). A second possibility was that stable MTs would serve for cell migration (Falconer et al., submitted). Immunofluorescence observations of P19 cells, two days after neural induction, have shown that cells expressing the neuron-specific ß-III tubulin isotype are localized on top of a monolayer of cells that is largely ß-III negative. Thus it was suggested that stable MTs in one day neurally-induced cells would polarize the cell for migration to the top of the monolayer of cells where it will then differentiate into a neuron. A third possiblity is that stable MTs are in non-neuronal cells.

These three possibilities can be tested directly by introducing rhodamine-labelled tubulin into differentiating P19 cells by the bead loading technique (McNeil and Warder, 1987; McNeil, 1989) or by phospholipid mediated delivery (Shea and Beermann, 1990; Shea et al., 1991c). The determination of the developmental fate of such cells only having stable MT arrays can be achieved using the FRAP technique as described earlier. Those cells having longer fluorescence recovery times can then be followed by real-time

observations. Forty-eight hours after RA induction, the cells can then be fixed and processed for immunofluorescence microscopy. Positive staining with the anti-ß-III tubulin antibody will confirm the developmental fate of cells having less dynamic MT arrays to the neuronal pathway.

This thesis has examined MT dynamics during early RA-induced neural differentiation of P19 EC cells. This is the first study reporting alterations in MT stability that are correlated with changes in MT dynamics occurring prior to morphogenesis. The acetylation of α-tubulin accompanies this change. The mechanisms by which stable MT arrays in RA-induced EC cells are generated still must be examined. A methodology for determining the developmental fate of RA-induced EC cells having stable MTs also has been proposed.

APPENDIX-Detailed Protocols

Paraffin Sectioning

Fixation and Processing

Adult female BALB/C mice were sacrificed and decapitated. Brain tissue was excised and dissected sagitally into the right and left hemispheres. One hemisphere of the brain was fixed in 4% formalin in phosphate-buffered saline (PBS) as described previously by Cambray-Deakin and Burgoyne (1987), and the other hemisphere was fixed in methacarn (60% methanol, 30% chloroform and 10% glacial acetic acid) as per Dardick et al., (1988). All fixations were for 24 hours at 4°C, prior to paraffin embedding.

On the following day, samples were dehydrated in a series of ethanol baths as follows: 3 hours in 70%, 5 hours in 80% and overnight in 95%. In the morning, samples were then immersed in absolute ethanol for three times (1 hour each) and then transferred to xylene for two times (1½ hours each). Following washes in xylene, fixed tissues were immersed in melted paraffin for 3 hours at 60°C and then embedded in fresh paraffin at room temperature.

Thin Sectioning

Prior to sectioning, gelatin-coated glass slides were prepared by pipetting a solution of 0.5% gelatin in distilled water (dH_2O) onto one side of a glass slide. After 10 minutes, the excess gelatin solution was removed and the slides were allowed to air

dry before use. Paraffin blocks were trimmed and 8 micron sections were obtained using a microtome (American Optical Company). Sections were transferred to a warm water bath (37°C) supplemented with 0.5 % gelatin. Great care was taken not to introduce folds in the sections when they were overlayed on the surface of the water. Then, sections were placed onto gelatin-coated glass slides by approaching them from beneath the water. Excess water was wiped off and slides were placed (sample-side-up) onto a slide tray warmer heated to 45°C, for overnight. This allowed the paraffin-embedded sections to attach and stick to the gelatin-coated slides. On the following day, slides were removed and stored at room temperature until use.

Immunocytochemistry

Paraffin sections were stained with mouse monoclonal antibodies specific to MAP 2 (clone AP-18; Tucker et al., 1988), acetylated tubulin (clone 6-11B-1; Piperno and Fuller, 1985), ß-III tubulin (clone TUJ 1; Lee et al., 1990a) and the 160kD neurofilament protein (Amersham; Oakville, Ont.). These antigens were detected by immunofluorescence microscopy. Biotinylated goat anti-mouse antibodies were purchased from Cappel Laboratories. Streptavidin-biotin-FITC and Streptavidin-biotin-HRP conjugates were supplied by Jackson Immunoresearch and Amersham, respectively.

Sections were deparaffinized and rehydrated to PBS, as described above. For some experiments, paraffin sections were blocked with either non-immune goat serum (Sigma), 1% Bovine Serum Albumin (BSA) in PBS, or with 5% Carnation Skim Milk Powder in PBS for 1 hour in a humidity chamber.

After rinsing extensively in PBS for 15 minutes, separate sections were then incubated with mouse monoclonal antibodies to MAP 2 (1:250 dilution), acetylated tubulin (1:10 dilution), NF-160 (1:50 dilution) and ß-III tubulin (1:300 dilution) overnight at 4°C. The slides were then rinsed for 15 minutes in PBS and incubated with a biotinylated goat anti-mouse secondary antibody (1:100 dilution) for 1 hour for signal amplification. The slides were rinsed in PBS as before, and then incubated with streptavidin-FITC (1:100 dilution) for 1 hour. After incubation, paraffin sections were rinsed again in PBS and mounted in p-phenylene-diamine.

All sections were examined with a Zeiss Axiophot microscope equipped with epifluorescence optics and photographed on Ilford XP 1-400 ASA film.

REFERENCES

Aitchison, W.A. and Brown, D.L., 1986, Duplication of the flagellar apparatus and cytoskeletal microtubule system in the alga Polytomella. Cell Mot. Cytoskel. 6: 122-127.

Allen, C. and Borisy, G.G., 1974, Structural polarity and directional growth of microtubules of Chlamydomonas flagella. J. Mol. Biol. 90: 381-402.

Alexander, J.E., Bodnar, W.B., Hunt, D.F., Martino, P.A., Shabanowitz, J., Lee, M.K. and Frankfurter, A., 1990, Polyglutamylation and phosphorylation of neuronal ß-tubulins: Structural analysis by tandem mass spectrometry. J. Cell Biol. 111:173a.

Alexander, J.E., Hunt, D.F., Lee, M.K., Shabnowitz, J., Michel H., Berlin, S.C., Macdonald, T.L., Sundberg, R.J., Rebhun, L.I. and Frankfurter, A., 1991, Characterization of posttranslational modifications in neuron-specific class III ß-tubulin by mass spectrometry. Proc. Natl. Acad. Sci. USA. 88: 4685-4689.

Arce, C.A. and Barra, H.S., 1985, Release of C-terminal tyrosine from tubulin and microtubules at steady state. Biochem. J. 226: 311-317.

Arce, C.A., Hallak, M.E., Rodriguez, J.A., Barra, H.S. and Caputto, R., 1978, Capability of tubulin and microtubules to incorporate and to release tyrosine and phenylalanine and the effect of the incorporation of these amino acids on tubulin assembly. J. Neurochem. 31: 205-210.

Asai, D.J. and Remlona, N.M., 1989, Tubulin isotype usage in vivo: a unique spatial distribution of the minor neuronal-specific ß-tubulin isotype in pheochromocytoma cells. Dev. Biol. 132: 398-409.

Avila, J., 1989, Microtubule Proteins. Prentice Hall.

Avila, J., 1991, Does MAP1B bind to tubulin through the interaction of α-helices? Biochem. J. Lett. 274: 621-622.

Baas, P.W. and Black, M.M., 1990, Individual microtubules in the axon consist of domains that differ in both composition and stability. J. Cell Biol. 111: 495-509.

Baas, P.W. and Heidemann, S.R., 1986, Microtubule reassembly from nucleating fragments during the regrowth of amputated neurites. J. Cell Biol. 103: 917-927.

Baas, P.W., Deitch, J.S., Black, M.M. and Banker, G.A., 1988, Polarity orientation of microtubules in hippocampal neurons: Uniformity in the axon and nonuniformity in the dendrite. Proc. Natl. Acad. Sci. USA. 85: 8335-8339.

Banerjee, A., Roach, M.C., Trcka, P. and Luduena, R.F., 1989, Purification and assembly properties of ß-tubulin isotypes from bovine brain tubulin. J. Cell Biol. 109: 338a.

Barra, H.S., Rodriguez, J.A., Arce, C.A. and Caputto, R., 1973, A soluble preparation from rat brain that incorporates into its own proteins [^{14}C]-arginine by a ribonuclease-sensitive system and [^{14}C]-tyrosine by a ribonuclease-insensitive system. J. Neurochem. 20: 97-108.

Bayley, P.M., 1990, What makes microtubules dynamic? J. Cell Sci. 95: 329-334.

Bayley, P.M., Schilstra, M.J. and Martin, S.R., 1989, A lateral cap model of microtubule dynamic instability. FEBS Lett. 259: 181-184.

Bayley, P.M., Schilstra, M.J. and Martin, S.R., 1990, Microtubule dynamic instability: numerical simulation of microtubule transition properties using a lateral cap model. J. Cell Sci. 95: 33-48.

Beltramo, D.M., Arce, C.A. and Barra, H.S., 1989, Tyrosination-detyrosination of tubulin and microtubules during the development of chick erythrocytes. Mol. Cell. Biochem. 89: 47-56.

Binder, L.I., Frankfurter, A., Rebhun, L.I., 1985, The distribution of tau polypeptides in the mammalian central nervous system. J. Cell Biol. 101: 1371-1378.

Black, M.M. and Baas, P.W., 1989, The basis of polarity in neurons. Trends in Neurosci. 12: 211-214.

Black, M.M. and Greene, L.A., 1982, Changes in the colchicine susceptibility of microtubules associated with neurite outgrowth: studies with nerve growth factor-responsive PC12 pheochromocytoma cells. J. Cell Biol. 95: 379-386.

Black, M.M. and Keyser, P., 1987, Acetylation of α-tubulin in cultured neurons and the induction of α-tubulin acetylation in PC12 cells by treatment with NGF. J. Neurosci. 7: 1833-1842.

Black, M.M., Aletta, J.M. and Greene, L.A., 1986, Regulation of microtubule composition and stability during nerve growth factor promoted neurite outgrowth. J. Cell Biol. 103: 545-557.

Black, M.M., Baas, P.W. and Humphries, S., 1989, Dynamics of α-tubulin deacetylation in intact neurons. J. Neurosci. 9: 358-368.

Blose, S.H., Meltzer, D.I. and Feramisco, J.R., 1984, 10-nm filaments are induced to collapse in living cells microinjected with monoclonal and polyclonal antibodies against tubulin. J. Cell Biol. 98: 847-858.

Brunk, C.F., Jones, K.C. and James, T.W., 1979, Assay for nanogram quantities of DNA in cellular homogenates. Anal. Biochem. 92: 497-500.

Bulinski, J.C. and Gundersen, G.G., 1991, Stabilization and posttranslational modification of microtubules during cellular morphogenesis. Bioessays. 13: 285-293.

Bulinski, J.C., Richards, J.E. and Piperno, G., 1988, Posttranslational modifications of α-tubulin: Detyrosination and acetylation differentiate populations of interphase microtubules in cultured cells. J. Cell Biol. 106: 1213-1220.

Calvert, R. and Anderton, B.H., 1985, A microtubule-associated protein MAP1 which is expressed at elevated levels during development of rat cerebellum. EMBO J. 4: 1171-1176.

Cambray-Deakin, M.A. and Burgoyne, R.D., 1987, Posttranslational modifications of α-tubulin: acetylated and detyrosinated forms in axons of rat cerebellum. J. Cell Biol. 104: 1569-1574.

Cambray-Deakin, M.A. and Burgoyne, R.D., 1990, The non-tyrosinated Mα4 α-tubulin gene product is post-translationally tyrosinated in adult rat cerebellum. Mol. Brain Res. 8: 77-81.

Carlier, M.F. and Pantaloni, D., 1981, Kinetic analysis of guanosine 5'-triphosphate hydrolysis associated with tubulin polymerization. Biochem. 20: 1918-1924.

Chu, D.T.W. and Klymkowsky, M.W., 1989, The appearance of acetylated α-tubulin during early development and cellular differentiation in Xenopus. Dev. Biol. 136: 104-117.

Dardick, I., Parks, W.R., Little, J. and Brown, D.L., 1988, Characterization of cytoskeletal proteins in basal cells of human parotid salivary gland ducts. Virchows. Archiv. A. Pathol. Anat. Histopathol. 412: 525-532.

de la Vina, S., Andreu, D., Medrano, F.J., Nieto, J.M. and Andreu, J.M., 1988, Tubulin structure probed with antibodies to synthetic peptides: mapping of three major types of limited proteolysis fragments. Biochem. 27: 5352-5365.

Drubin, D.G. and Kirschner, M.W., 1986, Tau protein function in living cells. J. Cell Biol. 103: 2739-2746.

Drubin, D.G., Feinstein, S.C., Shooter, E.M. and Kirschner, M.W., 1985, Nerve growth factor-induced neurite outgrowth in PC12 cells involves the coordinate induction of microtubule assembly and assembly-promoting factors. J. Cell Biol. 101: 1799-1807.

Dustin, P., 1986, Microtubules. Springer-Verlag. Berlin.

Echeverri, C.J., Falconer, M.M. and Brown, D.L., 1990, Expression of neural beta tubulins in differentiating EC cells. J. Cell Biol. 111: 413a.

Eckert, B.S., 1985, Alteration of intermediate filament distribution in Pt K1 cells by acrylamide. Eur. J. Cell Biol. 37: 169-174.

Eddé, B., Rossier, J., Le Caer, J.P., Desbruyères, E., Gros, F. and Denoulet, P., 1990, Posttranslational glutamylation of α-tubulin. Science. 247: 246-248.

Eddé, B., Rossier, J., Le Caer, J.P., Berwald-Netter, Y., Koulakoff, A., Gros, F. and Denoulet, P., 1991, A combination of posttranslational modifications is responsible for the production of neuronal α-tubulin heterogeneity. J. Cell. Biochem. 46: 134-142.

Edwards, M.K.S. and McBurney, M.W., 1983, The concentration of retinoic acid determines the differentiated cell types formed by a teratocarcinoma cell line. Dev. Biol. 98: 187-191.

Falconer, M.M. and Brown, D.L., 1989, Beta tubulin isotypes in stable microtubule arrays. J. Cell Biol. 109: 338a.

Falconer, M.M. and Brown, D.L., 1990, Sub-cellular sorting of beta tubulins. J. Cell Biol. 111: 413a.

Falconer, M.M., Vielkind, U. and Brown, D.L., 1989a, Establishment of a stable, acetylated microtubule bundle during neuronal commitment. Cell Mot. Cytoskel. 12: 169-180.

Falconer, M.M., Vielkind, U. and Brown, D.L., 1989b, Association of acetylated microtubules, vimentin intermediate filaments, and MAP2 during early neural differentiation in EC cell culture. Biochem. Cell Biol. 67: 537-544.

Falconer, M.M., Echeverri, C.J. and Brown, D.L., 1991, Differential sorting of beta-tubulin isotypes into colchicine-stable microtubules during neuronal and muscle differentiation of EC cells. (SUBMITTED FOR PUBLICATION).

Ferreira, A. and Caceres, A., 1989, The expression of acetylated microtubules during axonal and dendritic growth in cerebellar macroneurons which develop in vitro. Dev. Brain Res. 49: 205-213.

Gard, D.L. and Kirschner, M.W., 1985, A polymer-dependent increase in phosphorylation of beta-tubulin accompanies differentiation of mouse neuroblastoma cell line. J. Cell Biol. 100: 764-774.

Gawlitta, W., Osborn, M. and Weber, K., 1981, Coiling of intermediate filaments induced by microinjection of a vimentin-specific antibody does not interfere with locomotion and mitosis. Eur. J. Cell Biol. 26: 83-90.

Geuens, G., Hill, A.M., Levilliers, N., Adoutte, A. and DeBrabander, M., 1989, Microtubule dynamics investigated by microinjection of Paramecium axonemal tubulin: lack of nucleation but proximal assembly of microtubules at the kinetochore during prometaphase. J. Cell Biol. 108: 939-953.

Ginzburg, I., 1991, Neuronal polarity: targeting of microtubule components into axons and dendrites. Trends in Biochem. 16: 257-251.

Gu, W., Lewis, S.A. and Cowan, N.J., 1988, Generation of antisera that discriminate among mammalian α-tubulins: introduction of specialised isotypes into cultured cells results in their coassembly without disruption of normal microtubule function. J. Cell Biol. 106: 2011-2022.

Gundersen, G.G. and Bulinski, J.C., 1986, Microtubule arrays in differentiated cells contain elevated levels of a post-translationally modified form of tubulin. Eur. J. Cell Biol. 42: 288-294.

Gundersen, G.G. and Bulinski, J.C., 1988, Selective stabilization of microtubules oriented toward the direction of cell migration. Proc. Natl. Acad. Sci. USA. 85: 5946-5950.

Gundersen, G.G., Kalnoski, M.H. and Bulinski, J.C., 1984, Distinct populations of microtubules: tyrosinated and nontyrosinated alpha tubulin are distributed differently in vivo. Cell 38: 779-789.

Gundersen, G.G., Khawaja, S. and Bulinski, J.C., 1987, Postpolymerization detyrosination of α-tubulin: A mechanism for subcellular differentiation of microtubules. J. Cell. Biol. 105: 251-264.

Gundersen, G.G., Khawaja, S. and Bulinski, J.C., 1989, Generation of a stable, posttranslationally modified microtubule array is an early event in myogenic differentiation. J. Cell Biol. 109: 2275-2288.

Heidemann, S.R. and Euteneuer, U., 1982, Microtubule polarity determination based on conditions for tubulin assembly in vitro. Meth. Cell Biol. 24: 207-216.

Heidemann, S.R., Hamborg, M.A., Thomas, S.J., Song, B., Lindley, S. and Chu, D., 1984, Spatial organization of axonal microtubules. J. Cell Biol. 99: 1289-1295.

Hill, T.L. and Chen, Y.D., 1984, Phase changes at the end of a microtubule with a GTP cap. Proc. Natl. Acad. Sci. USA. 81: 5772-5776.

Hiller, G. and Weber, K., 1978, Radioimmunoassay for tubulin: a quantitative comparison of the tubulin content of different established tissue culture cells and tissues. Cell. 14: 795-804.

Hirokawa, N., 1982, Cross-linker system between neurofilaments, microtubules, and membrane organelles in frog axons revealed by the quick-freeze, deep-etching method. J. Cell Biol. 94: 129-142.

Hisanaga, S. and Hirokawa, N., 1990, Dephosphorylation-induced interactions of neurofilaments with microtubules. J. Biol. Chem. 265: 21852-21858.

Hotani, H. and Horio, T., 1988, Dynamics of microtubules visualized by darkfield microscopy: treadmilling and dynamic instability. Cell Mot. Cytoskel. 10: 229-236.

Inoue, S. and Ritter Jr., H., 1975, Dynamics of mitotic spindle organization and function. In Molecules and Cell Movement., S. Inoue and R.E. Stephens, eds., New York.

Jones-Villeneuve, E.M.V., McBurney, M.W., Rogers, K.A. and Kalnins, V.I., 1982, Retinoic acid induces embryonal carcinoma cells to differentiate into neurons and glial cells. J.Cell Biol. 94: 253-262.

Joshi, H. and Cleveland, D.W., 1989, Differential utilization of beta-tubulin isotypes in differentiating neurites. J. Cell Biol. 109: 663-673.

Keith, C.H., 1990, Neurite elongation is blocked if microtubule polymerization is inhibited in PC 12 cells. Cell Mot. Cytoskel. 17: 95-105.

Khawaja, S., Gundersen, G.G. and Bulinski, J.C., 1988, Enhanced stability of Microtubules enriched in detyrosinated tubulin is not a direct function of detyrosination level. J. Cell Biol. 106: 141-149.

Kilmartin, J.V., Wright, B. and Milstein, C., 1982, Rat monoclonal antitubulin antibodies derived by using a new nonsecreting rat cell line. J. Cell Biol. 93: 576-582.

Kirschner, M.W. and Mitchison, T.J., 1986, Beyond self assembly: from microtubules to morphogenesis. Cell. 45: 329-342.

Klymkowsky, M.W., 1981, Intermediate filaments in 3T3 cells collapse after intracellular injection of a monoclonal anti-intermediate filament antibody. Nature. 291: 249-251.

Klymkowsky, M.W., 1988, Metabolic inhibitors and intermediate filament organization in human fibroblasts. Exp. Cell Res. 174: 282-290.

Klymkowsky, M.W., Bachant, J.B. and Domingo, A., 1989, Functions of intermediate filaments. Cell Mot. Cytoskel. 14: 309-331.

Kreis, T.E., 1987, Microtubules containing detyrosinated tubulin are less dynamic. EMBO J. 6: 141-150.

Kristofferson, D., Mitchison, T. and Kirschner, M., 1986, Direct observation of steady-state microtubule dynamics. J. Cell Biol. 102: 1007-1019.

Kumar, N. and Flavin, M., 1981, Preferential action of a brain detyrosinolating carboxypeptidase on polymerized tubulin. J. Biol. Chem. 256: 7678-7686.

Labarca, C. and Paigen, K., 1980, A simple, rapid, and sensitive DNA assay procedure. Anal. Biochem. 102: 344-352.

Lee, M.K., Rebhun, L.I. and Frankfurter, A., 1990a, Posttranslational modification of class III ß-tubulin. Proc. Natl. Acad. Sci. USA. 87: 7195-7199.

Lee, M.K., Tuttle, J.B., Rebhun, L.I., Cleveland, D.W. and Frankfurter, A., 1990b, The expression and posttranslational modification of a neuron-specific ß-tubulin isotype during chick embryogenesis. Cell Mot. Cytoskel. 17: 118-132.

Lee, M.K., Rebhun, L.I., Luduena, R.F. and Frankfurter, A., 1990c, Carboxy terminal modification of brain ß-tubulin and the effects of brain tubulin heterogeneity on MAP-stimulated assembly. J. Cell Biol. 111: 174a.

Lewis, S.A., Lee, M.G.-S., and Cowan, N.J., 1985, Five mouse tubulin isotypes and their regulated expression during development. J. Cell Biol. 101: 852-861.

L'Hernault, S.W. and Rosenbaum, J.L., 1983, Chlamydomonas α-tubulin is posttranslationally modified in flagella during flagellar assembly. J. Cell Biol. 97: 258-263.

L'Hernault, S.W. and Rosenbaum, J.L., 1985a, Chlamydomonas α-tubulin is posttranslationally modified by acetylation on the ϵ-amino group of a lysine. Biochem. 24: 473-478.

L'Hernault, S.W. and Rosenbaum, J.L., 1985b, Reversal of the posttranslational mofification on Chlamydomonas flagellar α-tubulin occurs during flagellar resorption. J. Cell Biol. 100: 457-462.

Lim, S.-S., Sammak, P.J. and Borisy, G.G., 1989, Progressive and spatially differentiated stability of microtubules in developing neuronal cells. J. Cell Biol. 109: 253-263.

Lim, S.-S., Edson, K.J., Letourneau, P.C. and Borisy, G.G., 1990, A test of microtubule translocation during neurite elongation. J. Cell Biol. 111: 123-130.

Lin, J.J-C. and Feramisco, J.R., 1981, Disruption of the in vivo distribution of the intermediate filaments in fibroblasts through the microinjection of a specific monoclonal antibody. Cell. 24: 185-193.

Lopata, M.S. and Cleveland, D.W., 1987, In vivo microtubules are copolymers of available beta-tubulin isotypes: localization of each of six vertebrate beta-tubulin isotypes using polyclonal antibodies elicited by synthetic peptide antigens. J. Cell Biol. 105: 1707-1720.

Ludueña, R.F., Zimmermann, H.P. and Little, M., 1988, Identification of the phosphorylated ß-tubulin isotype in differentiated neuroblastoma cells. FEBS Lett. 230: 142-

Maccioni, R.B., Rivas, C.I. and Vera, J.C., 1988, Differential interaction of synthetic peptides from the carboxyl-terminal regulatory domain of tubulin with microtubule-associated proteins. EMBO J. 7: 1957-1963.

Margolis, R.L. and Wilson, L., 1978, Opposite end assembly and disassembly of microtubules as steady state in vitro. Cell 13: 1-8.

Maruta, H., Greer, K. and Rosenbaum, J.L., 1986, The acetylation of alpha-tubulin and its relationship to the assembly and disassembly of microtubules. J. Cell Biol. 103: 571-579.

Matus, A., 1988, Microtubule-associated proteins: their potential role in determining neuronal morphology. Ann. Rev. Neurosci. 11: 29-44.

Matus, A., 1990, Microtubule-associated proteins and the determination of neuronal form. J. Physiol. Paris. 84: 134-137.

McBurney, M.W. and Rogers, B.J., 1982, Isolation of male embryonal carcinoma cells and their chromosome replication patterns. Dev. Biol. 89: 503-508.

McNeil, P.L., 1989, Incorporation of macromolecules into living cells. Meth. Cell Biol. 29: 153-173.

McNeil, P.L. and Warder, E., 1987, Glass beads load macromolecules into living cells. J. Cell Sci. 88: 669-678.

Mitchison, T.J., 1989, Mitosis: basic concepts. Curr. Opinion in Cell Biol. 1: 67-74.

Mitchison, T. and Kirschner, M., 1984a, Microtubule assembly nucleated by isolated centrosomes. Nature. 312: 232-237.

Mitchison, T. and Kirschner, M., 1984b, Dynamic instability of microtuble growth. Nature. 312: 237-242.

Mitchison, T. and Kirschner, M.W., 1985, Properties of the kinetochore in vitro. 1. Microtubule nucleation and tubulin binding. J. Cell Biol. 101: 755-765.

Monteiro, M.J. and Cleveland, D.W., 1988, Sequence of chicken cß7 tubulin. Analysis of a complete set of vertebrate ß-tubulin isotypes. J. Mol. Biol. 193: 427-438.

Murofushi, H., 1980, Purification and characterization of tubulin-tyrosine ligase from porcine brain. J. Biochem. 87:979-984.

Noble, M., Lewis, S.A. and Cowan, N.J., 1989, The microtubule binding domain of microtubule associated protein MAP 1B contains a repeated sequence motif unrelated to that of MAP 2 and tau. J. Cell Biol. 109: 3367-3376.

Okabe, S. and Hirokawa, N., 1988, Microtubule dynamics in nerve cells: analysis using microinjection of biotinylated tubulin into PC12 cells. J. Cell Biol. 107: 651-664.

Okabe, S. and Hirokawa, N., 1990, Turnover of fluorescently-labelled tubulin and actin. Nature. 343: 479-481.

Piperno, G. and Fuller, M.T., 1985, Monoclonal antibodies specific for an acetylated form of α-tubulin recognize the antigen in cilia and flagella from a variety of organisms. J. Cell Biol. 101: 2085-2094.

Piperno, G., LeDizet, M. and Chang, X., 1987, Microtubules containing acetylated α-tubulin in mammalian cells in culture. J. Cell Biol. 104: 289-302.

Reinsch, S.S., Mitchison, T.J. and Kirschner, M.W., 1991, Microtubule polymer assembly and transport during axonal elongation. J. Cell Biol. 115: 365-379.

Riederer, B.M., 1990, Some aspects of the neuronal cytoskeleton in development. Eur. J. Morphol. 28: 347-378.

Rudnicki, M.A., Sawtell, N.M., Reuhl, K.R., Berg, R., Craig, J.C., Jardine, K., Lessard, J.L. and McBurney, M.W., 1990, Smooth muscle actin expression during P19 embryonal carcinoma differentiation in cell culture. J. Cell. Physiol. 142: 89-98.

Sammak, P.J. and Borisy, G.G., 1988, Detection of single fluorescent microtubules and methods for determining their dynamics in living cells. Cell Mot. Cytoskel. 10: 237-245.

Sammak, P.J., Gorbsky, G.J. and Borisy, G.G., 1987, Microtubule dynamics in vivo: a test of mechanisms of turnover. J. Cell Biol. 104: 395-405.

Schatten, G., Simerly, C., Asai, D.J., Szöke, E., Cooke, P. and Schatten, H., 1988, Acetylated α-tubulin in microtubules during mouse fertilization and early development. Dev. Biol. 130: 74-86.

Schulze, E. and Kirschner, M., 1986, Microtubule dynamics in interphase cells. J. Cell Biol. 102: 1020-1031.

Schulze, E. and Kirschner, M., 1987, Dynamic and stable populations of microtubules in cells. J. Cell Biol. 104: 277-288.

Schulze, E., Asai, D.J., Bulinski, J.C. and Kirschner, M., 1987, Posttranslational modification and microtubule stability. J. Cell Biol. 105: 2167-2177.

Serrano, L., Diaz-Nido, J., Wandosell, F. and Avila, J., 1987, Tubulin phosphorylation by casein kinase II is similar to that found in vivo . J. Cell Biol. 105: 1731-1739.

Shaw, G. and Hou, Z.C., 1990, Bundling and cross-linking of intermediate filaments of the nervous system. J. Neurosci. Res. 25: 561-568.

Shea, T.B. and Beermann, M.L., 1990, Alterations in dynamics of microtubule assembly during axonal neuritogenesis in NB2a/d1 cells. Cell Biol. Int. Rep. 14: 1093-1098.

Shea, T.B., Beermann, M.L. and Nixon, R.A., 1990, Posttranslational modification of alpha-tubulin by acetylation and detyrosination in NB2a/d1 neuroblastoma cells. Dev. Brain Res. 51: 195-204.

Shea, T.B., Beermann, M.L., Nixon, R.A., 1991a, Sequential requirement for cytoskeletal constituents during axonal initiation, elongation and stabilization. J. Cell Biol. 115: 163a.

Shea, T.B., Beermann, M.L., Nixon, R.A. and Fischer, I., 1991b, Inhibition of neurite outgrowth in neuroblostoma by tau antisense oligonucleotides and intracellular delivery of anti-tau antibodies. J. Cell Biol. 115: 385a.

Shea, T.B., Perrone-Bizzozero, N.I., Beermann, M.L. and Benowitz, L.I., 1991c, Phospholipid-mediated delivery of anti-GAP-43 antibodies into neuroblastoma cells prevents neuritogenesis. J. Neurosci. 11: 1685-1690.

Solomon, F., 1986, Direct identification of microtubule-associated proteins by selective extraction of cultured cells. Meth. Enzymol. 134: 139-147.

Soltys, B.J. and Borisy, G.G., 1985, Polymerization of tubulin in vivo: direct evidence for assembly onto microtubule ends and from centrosomes. J. Cell Biol. 100: 1682-1689.

Sullivan, K.F., Lau, J.T. and Cleveland, D.W., 1985, Apparent gene conversion between beta-tubulin genes yields multiple regulatory pathways for a single beta-tubulin polypeptide isotype. Mol. Cell. Biol. 5: 2454-2465.

Thompson, W.C., 1982, The cyclic tyrosination/detyrosination of α-tubulin. Methods Cell Biol. 24: 235-255.

Tucker, R.P., Binder, L.I., Hemmings, B.A. and Matus, A.I., 1988, The sequential appearance of low- and high-molecular weight forms of MAP 2 in the developing cerebellum. J. Neurosci. 8: 4503-4512.

Villasante, A., Wang, D., Dobner, P., Dolph, P., Lewis., S.A. and Cowan, J.J., 1986, Six mouse alpha-tubulin mRNAs encode five distinct isotypes: testis-specific expression of two sister genes. Mol. Cell. Biol. 6: 2409-2419.

Webster, D.R. and Borisy, G.G., 1989, Microtubules are acetylated in domains which turn over slowly. J. Cell Sci. 92: 57-65.

Webster, D.R., Gundersen, G.G., Bulinski, J.C. and Borisy, G.G., 1987a, Differential turnover of tyrosinated and detyrosinated microtubules. Proc. Natl. Acad. Sci. USA. 84: 9040-9044.

Webster, D.R., Gundersen, G.G., Bulinski, J.C. and Borisy, G.G., 1987b, Assembly and turnover of detyrosinated tubulin in vivo. J. Cell Biol. 105: 265-276.

Webster, D.R., Wehland, J., Weber, K. and Borisy, G.G., 1990, Detyrosination of alpha tubulin does not stabilize microtubules in vivo. J. Cell Biol. 111: 113-122.

Wehland, J., Willingham, M.C. and Sandoval, I.V., 1983, A rat monoclonal antibody reacting specifically with the tyrosylated form of α-tubulin. I. Biochemical characterization, effects on microtubule polymerization in vitro and microtubule polymerization and organization in vivo. J. Cell Biol. 97: 1467-1475.

Weisenberg, R.C., 1972, Microtubule formation in vitro in solutions containing low calcium concentrations. Science. 177: 1104-1105.

Weingarten, M.D., Lockwood, A.H., Hwo, S. and Kirschner, M., 1975, A protein factor essential for microtubule assembly. Proc. Natl. Acad. Sci. USA. 72: 1858-1862.

Winckler, B. and Solomon, F., 1991, A role for microtubule bundles in the morphogenesis of chicken erythrocytes. Proc. Natl. Acad. Sci. USA. 88: 6033-6037.

Zar, J.H., 1984, Biostatistical Analysis. Prentice-Hall, Inc. Englewood Cliffs, New Jersey.